ELECTROKINETIC CAPILLARY

CHROMATOGRAPHY METHODS FOR

SEPARATION AND DETECTION OF

ANILINE AND PHENOL PESTICIDIC

METABOLITES

By

WILLIAM ERIC WALL

Bachelor of Science

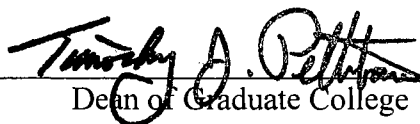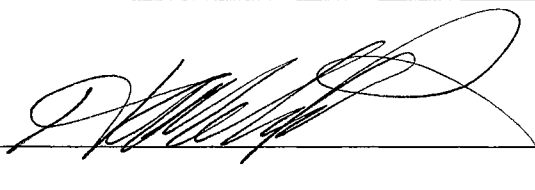Southeastern Oklahoma State University

Durant, Oklahoma

1997

Submitted to the Faculty of the Graduate
College of Oklahoma State University
University in Partial Fulfillment of the
Requirements for the Degree of
DOCTOR OF PHILOSOPHY
May 2003

ELECTROKINETIC CAPILLARY

CHROMATOGRAPHY METHODS FOR

SEPARATION AND DETECTION OF

ANILINE AND PHENOL PESTICIDIC

METABOLITES

Thesis Approved:

_____
Thesis Advisor

_____

_____

_____

_____
Dean of Graduate College

TABLE OF CONTENTS

LIST OF TABLES

LIST OF FIGURES

Figure   Page

Chapter I

Chapter II

LIST OF SYMBOLS AND ABBREVIATIONS

μ_{ep} electrophoretic mobility

μ_{eof} electroosmotic mobility

μ_{app} apparent analyte mobility

$\mu_{ep,mc}$ electrophoretic mobility of the micelle

$\mu_{eff,ep}$ effective electrophoretic mobility

$\mu_{ep,s}$ electrophoretic mobility of the surfactant

$\mu_{ap,s}$ apparent mobility of the surfactant

$\mu_{ep,c}$ electrophoretic mobility of the solute-surfactant complex

$\mu_{ap,c}$ apparent mobility of the solute-surfactant complex

$\Delta\mu$ difference in electrophoretic mobility

$\bar{\mu}$ average apparent electrophoretic mobility of two different adjacent zones

v_{ep} electrophoretic velocity

v_{eof} electroosmotic velocity

v_{app} apparent analyte velocity

l length of capillary from the inlet to the detection point

l_{sweep} length of the sweep zone

l_{inj} injected analyte zone

L total length of the separation capillary

V_i	injection voltage
V	external applied voltage
t_i	injection time
w	amount of sample injected
S_{vol}	volume of sample injected
r	radius of the capillary
C	concentration of the analyte
d	density of the sample solution
g	gravitational acceleration
Δh	height difference between the sample-submerged inlet of the capillary and the outlet of the capillary
η	viscosity of the solution
ΔP	pressure difference across the capillary
E	electric field strength
E_o	electric field strength due to a single buffer
E_1	electric field strength of buffer 1
E_2	electric field strength of buffer 2
F_e	force of ion under influence of electric field
F_d	drag force experienced by an ion
q	particle's net charge
f	translational friction coefficient
f_i	absolute mobility correction factor
f_c	mole fraction of DOSS-solute complex whose electrophoretic mobility is $\mu_{ep,c}$

z	charge number
I	ionic strength
c	molar concentration of ionic running electrolyte
z	zeta potential
κ	Debye-Huckel parameter
t_M	migration time of an analyte
t_o	migration time of an unretained solute
t_{mc}	migration time of the micelle
N	separation efficiency
σ	standard deviation
D	diffusion coefficient of a given solute
α	selectivity
w_i	peak width at inflection point
w_h	peak width at the half-height
w_b	peak width at the base
R_S	resolution
k'	retention factor
σ_T	overall dispersion
σ_{Dif}	dispersion due to diffusion
σ_{Inj}	dispersion due to injection
σ_{Temp}	dispersion due to temperature gradients
σ_{Ads}	dispersion due to adsorption
σ_{Det}	dispersion due to detection

σ_{Ele}	dispersion due to electrodispersion
γ	ratio of resistivities of the low concentration buffer to that of the high concentration buffer
x	fraction of the capillary filled with low resistance buffer
2,4-DiClph	2,4-Dichlorophenol
2,4,5-TriClph	2,4,5-Trichlorophenol
2-Clph	2-Chlorophenol
2-Isopropoxyph	2-Isopropoxyphenol
3,4-DiClAN	3,4-Dichloroaniline
3-Cl-4-MeAN	3-Chloro-4-Methylaniline
3-ClAN	3-ClAN
3-Clph	3-Chlorophenol
3-MeAN	3-Methylaniline
4-BrAN	4-Bromoaniline
4-ClAN	4-Chloroaniline
4-Clph	4-Chlorophenol
4-IsPrAN	4-Isopropylaniline
ACN	acetonitrile
AN	aniline
ANI	anilide
APK	alkyl phenyl ketones
BGE	back ground electrolyte
CAR	carbamate
CE	capillary electrophoresis

CEC	capillary electrochromatography
CGE	capillary gel electrophoresis
CMC	critical micellar concentration
CZE	capillary zone electrophoresis
CIEF	capillary isoelectric focusing
CITP	capillary isotachophoresis
CRA	carbazole-9-N-acetic acid
CTAB	cetyltrimethyl ammonium bromide
Dihydro	2,2-Dimethyl-2,3-dihydrobenzo[b]furan-7-ol
DMAP	4-Dimethylaminopyridine
DOSS	dioctyl sulfosuccinate, sodium salt
EDAC	1-ethyl-3-(3-dimethylaminopropyl) carbodiimide
EKC	electrokinetic capillary chromatography
EOF	electroosmotic flow
FASS	field-amplified sample stacking
FITC	fluorescein isothiocyanate
FMOC	9-fluoroenylmethyl chloroformate
GC	gas chromatography
HPLC	high performance liquid chromatography
LC	liquid chromatography
LIF	laser-induced fluorescence
LOD	limit of detection
LVSS	large-volume sample stacking

MS	mass spectrometry
MECC	micellar electrokinetic capillary chromatography
MEKC	micellar electrokinetic capillary chromatography
Nap	1-Naphthol
NMR	nuclear magnetic resonance
NG	n-nonyl-β-D-glucoside
OG	n-octyl-β-D-glucoside
PentaClph	pentachlorophenol
ph	phenol
PU	phenylurea
SM-EKC	surfactant-mediated electrokinetic capillary chromatography
SDS	sodium dodecyl sulfate

CHAPTER I

SOME BASIC PRINCIPLES OF ELECTROKINETIC CAPILLARY

CHROMATOGRAPHY. SCOPE OF THE STUDY

Introduction and Scope of the Study

Capillary electrophoresis (CE) is a miniaturized separation technique that incorporates high voltage and the subsequent electric current as the driving force for the mass transport. This form of transport results in high separation efficiency and resolution. Furthermore, CE consumes very small sample volumes and reagents and utilizes automated instrumentation, which makes it a powerful tool for environmental, pharmaceutical, and biochemical analyses. Separation in CE is a result of the electrostatic attraction of the charged analytes to the respective electrode of opposite charge under the influence of an applied voltage.

Modifying CE can be easily achieved by adding selectors (i.e., pseudo-stationary phase) into the running electrolyte buffer. In capillary electrochromatography (CEC) and high performance liquid chromatography (HPLC), the stationary phase is immobile, however, in CE the pseudo-stationary phase migrates in a direction corresponding to its net charge and at a different velocity than the running electrolyte. The interaction of the selectors, or pseudo-stationary phases (e.g., micelles, cyclodextrins, polymeric micelles,

etc.) with the analytes of interest alters the mobility of these analytes, and eventually brings about their separation. These pseudo-stationary phases allow the separation of neutral molecules and enhance the separation of charged analytes. A CE separation that consists of a pseudo-stationary phase dissolved in an aqueous or hydro-organic running electrolyte is known as electrokinetic capillary chromatography (EKC). The incorporation of a surfactant in the running electrolyte, which forms a micelle above the critical micellar concentration (CMC) is a technique referred to as micellar electrokinetic capillary chromatography (MECC or MEKC). The use of a surfactant as a pseudo-stationary phase without the formation of a micelle (e.g., surfactants dissolved into high organic content running electrolytes) yields an electrokinetic system that is called in this dissertation surfactant-mediated electrokinetic capillary chromatography (SM-EKC).

In brief, the objectives of this chapter are (i) to inform the reader about the history of CE, (ii) to describe the instrumentation used, (iii) to depict the basic separation principles involved in this technique, and (iv) to discuss the basic principles of on-column preconcentration approaches used in CE. Furthermore, a number of equations and parameters relating to our CE studies will be discussed to give a better understanding of the processes involved in this method.

The scope of this dissertation encompasses the development of novel EKC systems for the separation of pesticidic metabolites and their derivatives at trace levels in real water samples (e.g., lake and tap water). This research was conducted with the aim that other classes of compounds could be potentially used with the methods developed in this dissertation.

Capillary electrophoresis techniques are well known for their high separation efficiencies, however high resolution separation for a multicomponent mixture also requires sufficient selectivity of the technique being employed. In other words, attainment of millions of theoretical plates with a given electrophoretic system is irrelevant for the separation of the mulitcomponent mixture if no selectivity is achieved. Therefore, the importance of introducing and evaluating novel CE systems of unique selectivities and high separation efficiencies for achieving high quality separation (i.e., enhanced peak capacity) is realized in this dissertation. Multicomponent mixtures are often encountered in chemical and biochemical real world analyses. These mixtures require high separation efficiency with ample selectivity, which results in high resolving power. Dilute samples pose another challenge, since high resolving power alone is not always adequate for detection. The separation methodologies incorporated must be able to achieve adequate limits of detection when doing trace analysis studies. The extremely narrow path length (i.e., small capillary diameter) for on-column detection restricts the sensitivity of photometric detectors usually employed in CE (e.g., UV-visible detection). This shortcoming excludes most typical CE techniques for the analysis of dilute samples. To circumvent the detection problems in CE, this dissertation incorporates laser induced fluorescence (LIF) detection of pre-column derivatized solutes to help increase the sensitivity of the detection system. Moreover, this dissertation further addresses the sensitivity issue by offering on-column preconcentration approaches while also introducing selective separation media.

In addition to this introductory chapter, this dissertation contains 3 other chapters that illustrate the derivatization, separation, detection, and trace enrichment approaches

3

developed. Chapter 2 investigates novel MEKC approaches for the separation of derivatized aniline pesticidic metabolites and their detection by LIF. Chapter 3 further elaborates on the detection of these pesticidic metabolites but incorporates a novel SM-EKC separation with an alternate derivatization technique. The incorporation of sodium dioctyl sulfosuccinate (DOSS) as the surfactant allowed the use of high organic content to aid in the separation of the very hydrophobic derivatives. Chapter 4 describes the trace enrichment of phenol pesticidic metabolites and their detection before and after derivatization with yet another fluorescent tag. DOSS surfactant dissolved in a hydro-organic running electrolyte was again employed to aid in the selectivity of the separation system involving the hydrophobic solutes.

Historical Background and Development of Capillary Electrophoresis

Tiselius and co-workers introduced electrophoresis in 1937 as a separation method for macromolecules such as proteins, RNA, and DNA.[1] However, casting the gel, staining, and destaining for the identification of separated solute zones is labor intensive and not very quantitative. Regardless, this method of separation set the stage for developing and investigating more efficient electrophoretic separation systems. A few years later, Strain[2] introduced capillary electrochromatography (CEC) and illustrated the use of electroosmotic flow in chromatography. In 1967, Hjertèn[3] was the first to incorporate glass tubes of 3 mm internal diameters (i.d.) using high electric field strength with on-column UV detection. As interest grew, it was realized that smaller column i.d. would provide more efficient dissipation of heat, which results in less band broadening

4

due to Joule heating. In 1974, Vertanen[4] was able to separate alkali cations with a Pyrex glass tube using potentiometric detection. That same year, Pretorius et al.[5] demonstrated the first true pumping action produced from EOF for use in analytical CEC separation. By 1979, Mikkers et al.[6] accomplished the separation and detection of inorganic and organic compounds with 200 μm PTFE tubing using UV and conductometric detection. Major accomplishments in CE had been made within five decades of its introduction, but inadequate separation efficiencies, large injection volumes, and poor detection sensitivity limited its analytical capabilities.

In 1981, Jorgenson and Lukacs[7] made a major breakthrough concerning these drawbacks of CE. They were able to separate and identify amino acids and peptides using a 75 μm fused-silica capillary with on column fluorescence detection. By applying fluorescence detection instrumentation to a fused-silica capillary of this size, they were able to obtain very high sensitivity and separation efficiency. This accomplishment is greatly known as the start of the modern era of CE and has led to great discoveries involving a variety of techniques and methods now commonly employed in CE.

Once this improved column and instrumentation technology had been proven, more traditional techniques involving gel electrophoresis[8] and isoelectric focusing[9] were soon adapted and investigated in the capillary format. However, in 1984 Terabe[10] and co-workers introduced one of the most widely used techniques in CE known as micellar electrokinetic chromatography (MECC or MEKC). This technique utilizes a micelle as the pseudo-stationary phase that causes differential partitioning of the solutes molecules between the mobile running electrolyte and the micelles. Once a system is tuned and optimized, this partitioning interaction results in a change in the net mobility of the solute

and ultimately results in an enhancement of the overall separation. Sodium dodecyl sulfate (SDS)[11, 12] is one of the most widely used anionic surfactants, which can be used to selectively control the separation of charged molecules as well as neutral compounds. A variety of other pseudo-stationary phases (e.g., cyclodextrins,[13, 14] molecular or polymeric micelles,[15] crown ethers,[16] etc.) have been developed to tune the selectivity of systems as to allow for the separation and determination of chiral compounds. Furthermore, a great deal of investigation has gone into inner-capillary wall modification[17, 18] (e.g., hydrophilic coating) and the development of other stationary mobile phases (monolithic,[19, 20] packed silica bead columns,[21] etc.) for use in CEC, which goes above and beyond typical open tubular capillary column capabilities. The technique of electrophoresis was further advanced in the early 1990's with the introduction of CE on a microchip.[22, 23]

CE has become an extremely versatile tool used in the analytical determination of a wide variety of species ranging from small ions to large biomolecules. CE has been incorporated in the analysis of samples originating from various fields of interest including forensics, pharmaceuticals, environmental, biological, chiral separations, etc.[24] This powerful analytical separation technique has led to a vast number of worldwide meetings concerning CE and CEC, which reflect its great worth and innovation.

Capillary electrophoresis instrumentation is made up of three primary pieces of equipment consisting of a high voltage power supply, a detector, and a data acquisition system as illustrated in figure 1. The high voltage power supply is capable of delivering
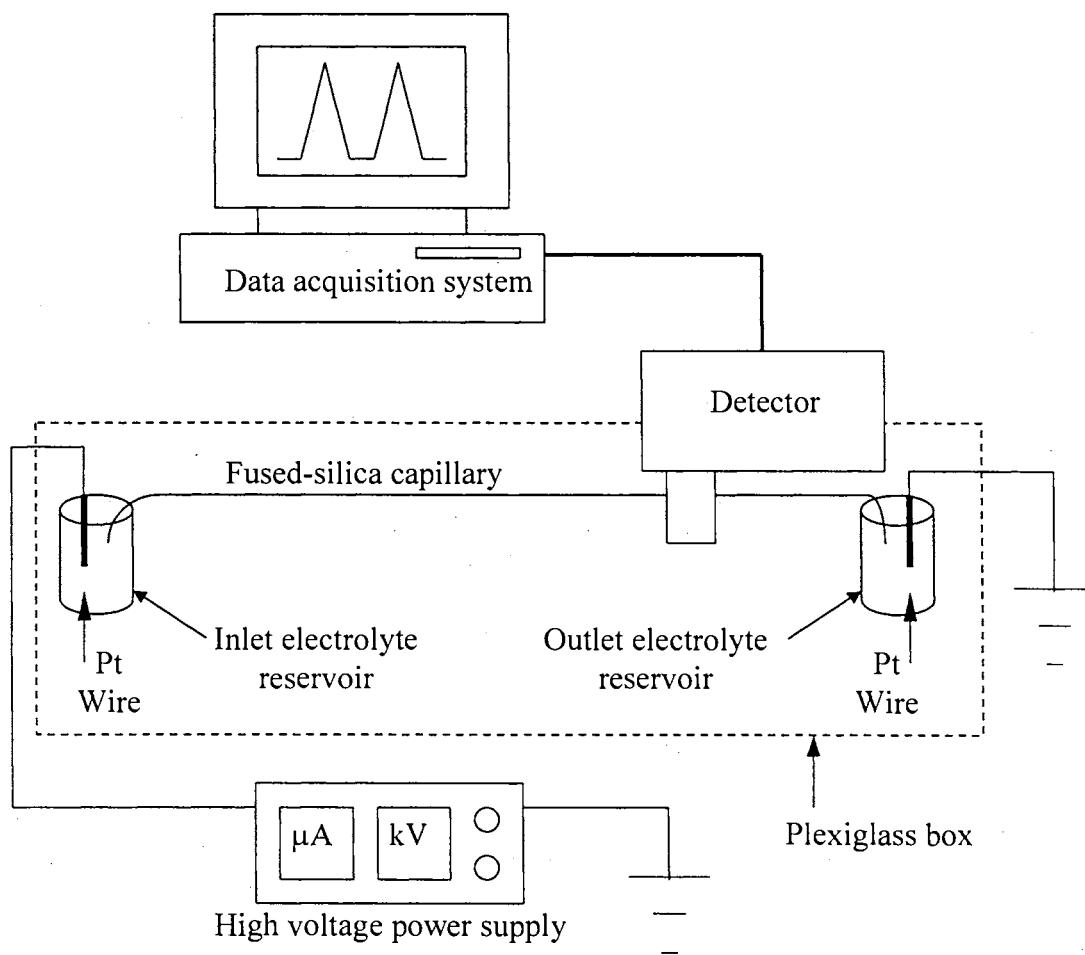
Figure 1. Schematic illustration of a typical manual instrument used for CE.

up to 30 kV. Manual instruments are equipped with plexiglass boxes with safety switches that turn off the voltage upon opening to protect the user from any shock hazard. All automated instruments are also equipped with the same such voltage cut-off switches. The detection is typically carried out on-column by either a UV or fluorescence detector. Both manual and automated systems employ platinum electrodes to provide voltage transfer into the running electrolyte buffer. However, there are many advantageous options that are available with the automated instruments, for example, temperature control, automated sample injection and sampling, and pressurization of the inlet and outlet of the capillary, which reduces bubble formation when performing CEC.

The separation process typically takes place in a fused-silica capillary, which has a polyimide coating that allows more rugged use and overall flexibility. The detection normally takes place on-column through a "window" where the polyimide coating has been removed. This polyimide removal can be done by heating in a flame, electrical wire stripper, or by concentrated sulfuric acid heated at 100 °C, which results in a segment of exposed fused silica that is UV transparent. Overall column length, typically 20 to 80 cm, and internal diameter, typically 10 to 100 μm, can be varied depending on the desired results. The desired results usually depend on the most efficient run time to produce the necessary separation.

Sample Injection

The attainment of reproducible results in CE is very dependent on the mode of sample injection. The two typical injection techniques used in CE are hydrodynamic and electrokinetic and usually depend on the configuration of the instrument. The sample zone length (l_{inj}) when using electrokinetic injection can be described by:

$$l_{inj} = \frac{\left(\mu_{ep} + \mu_{eof}\right)V_i t_i}{L} \qquad (1)$$

where μ_{ep} and μ_{eo} are the electrophoretic and electroosmotic mobility (described by equations (11) and (16) in more detail), respectively. The terms V_i, t_i, and L are the injection voltage, injection time, and capillary length, respectively. The amount of sample injected (w) can be represented mathematically by:[25]

$$w = \pi r^2 l C \qquad (2)$$

where r is the radius of the capillary and C is the concentration. Combining equations (1) and (2) produce an equation for the amount of solute injected as a function of the experimental conditions represented by:

$$w = \frac{\left(\mu_{ep} + \mu_{eof}\right)\pi r^2 V_i t_i C}{L} \qquad (3)$$

Hydrodynamic injection can be further divided into three categories which are head-space pressurization, vacuum injection, or gravity-based sample injection (i.e., siphoning). Manual instruments generally utilize gravity-based injection, which consists of elevating the sample-submerged inlet of the capillary above the outlet end of the capillary. The volume of sample injected (S_{vol}) using gravity-based injection can be mathematically expressed by:[26]

$$S_{vol} = \frac{dg\pi r^4 \Delta h t_i}{8\eta L} \qquad (4)$$

where d is the density of the sample solution, g is the gravitational acceleration, Δh is the height difference between the inlet and outlet ends of the capillary, and η is the viscosity of the solution. Concentration of the sample (C) can then be included in equation (4) to generate an equation in terms of sample injected (w).

9

$$w = \frac{dg\pi r^4 \Delta h C t_i}{8\eta L} \qquad (5)$$

Predominantly, the height difference as well as the time of sample elevation determines the amount of sample that is loaded onto the column. Electrokinetic injection is also utilized by manual and automated instruments and is most dependent on the ionic strength of the sample matrix. However, the amount of solute loaded using electrokinetic injection can be greatly affected by differences in conductivity between the sample matrix and running electrolyte. Furthermore, this conductivity difference can result in a concentration variation between the sample and the actual sample plug that is injected. Although this injection method can hinder analytical quantification, this phenomenon has been exploited as a preconcentration technique. In addition, this technique is popular when dealing with viscous sample matrices as well as with CEC where flow is hindered by the column packing material. Automated instruments are normally equipped to do electrokinetic injections, however hydrodynamic injections are preferred when permissible. Head-space pressurization or vacuum injections are the typical injection methods used with most automated instruments. The amount of analyte injected using pressure can also be calculated mathematically by introducing a term reflecting the pressure difference across the capillary (ΔP):

$$w = \frac{\Delta P \pi r^4 C t_i}{8\eta L} \qquad (6)$$

The injection when using head-space pressurization is a result of the application of a low pressure applied to the inlet vial of the submerged capillary, whereas vacuum injection creates a vacuum on the outlet vial of the submerged capillary. Each technique forces sample matrix to be pushed or pulled, respectively, into the capillary for further analysis.

Detection in CE

Ultraviolet (UV) detection is the most popular detection method with most CE instruments. This is due to its inexpensive cost and versatility, as most analytes absorb in the UV portion of the spectrum. However, detection in CE is a major concern because of the very small path length of the capillary diameter. Because of this, a modification of path length was developed known as the Z-shaped cell, also known as the high sensitivity cell, in which the detection is aligned down a short portion of the long axis of the capillary.[27, 28] However, detection along the long axis of the capillary presents a problem due to increased band broadening and lower efficiencies. A few years later Hewlett-Packard introduced a modified capillary, known as the bubble cell, which is expanded three fold in diameter at the detection window, thus increasing the sensitivity.[29] Laser-induced fluorescence (LIF)[30-34] detection is probably the second most popular form of on-column analyte identification. This detection technique allows the detection of only the fluorescent analytes at a certain excitation wavelength, which proves less versatile than UV detection but allows for much greater sensitivity. Other less commonly used methods of detection include indirect detection techniques,[35-38] amperometry,[39, 40] and conductivity.[41-44] Nuclear magnetic resonance spectroscopy (NMR)[45-48] and more importantly mass spectrometry (MS)[49-53] have been integrated with CE to greatly improve the detection and identification power of CE.

Modes of Separation

Since the development of CE, there have been several variations of separation modes investigated, which focus on different chemical and physical properties of analytes. The various modes are: capillary zone electrophoresis (CZE), micellar

electrokinetic capillary chromatography (MECC or MEKC), surfactant-mediated electrokinetic capillary chromatography (SM-EKC), capillary gel electrophoresis (CGE), capillary isoelectric focusing (CIEF), and capillary isotachophoresis (CITP).

The simplest and most common mode for separation is CZE, which consists of a uniform running electrolyte at constant pH. The separation is dependent on differences in charge-to-mass ratios of the solutes. Anionic and cationic analytes can be separated with this technique; however, all neutral analytes migrate with the EOF and elute at the same time corresponding to the dead volume. There have been a great many separations carried out using CZE with analytes varying from small ions to relatively large biological species (e.g., viruses, bacteria).[54-56]

The MECC separation approach is the most versatile separation method and can be employed to separate ionic and neutral species. Separation in MECC is primarily dependent on the hydrophobic interaction of analytes with the charged micelles with charge-to-mass ratio playing a lesser role. Micelles can only be formed when a surfactant is added above its critical micellar concentration (CMC) and acts as a pseudo-stationary phase that allows the analyte to partition between the mobile phase and the micellar phase. Hydrophobic analytes interact more with the micelles while more hydrophilic analytes interact less. The SM-EKC separation mode behaves in the same manner, however the analytes interact with surfactant monomers, which are usually the result of a hydro-organic running electrolyte buffer that greatly increases the CMC.

The CGE method consists of a capillary that is filled with a porous gel material that is non-mobile and produces no EOF. The separation occurs on the basis of size as the analytes electrophoretically migrate through the gel-filled capillary. The gel acts as

12

an anticonvective medium, which contributes to less band broadening and increased efficiencies. This method is very popular when dealing with large molecular weight solutes and very high theoretical plates (i.e., 30 million per meter[57]) have been reported.

In CIEF, the separation is dependent on the isoelectric point (i.e., pI values) of the analytes. As the solutes electrophoretically migrate through the stationary pH gradient buffer, they become uncharged at the pH zones equaling their pI values. Once the analytes reach their respective zones, they become neutral which results in loss of electrophoretic mobility. The final mobilization step incorporates an electrolyte to induce mobilization of the stationary analytes past the detection window.

Capillary isotachophoresis (CITP) incorporates electrically discontinuous buffer matrices, which results in the separation of the solutes based on their migrations into sharp zones. In short, the sample is injected between a high-mobility leading electrolyte and a low-mobility terminating electrolyte. The analytes concentrate into sample zones between the two electrolytes and migrate at equal velocity towards the detection point.

CE Column Technologies

Fused-silica is by far the most popular capillary material in CE due to its easy column fabrication, electrical resistance, optical transparency, mechanical strength, flexibility, and inexpensive cost. The silanol groups that make up the inner surface of the fused-silica are weakly acidic groups that ionize above a pH of 3.5 resulting in charged silanol (i.e., deprotonated SiO^-) groups, which produce the EOF phenomenon. Cationic analytes present a problem due to the electrostatic interaction with the inner surface of the capillary resulting in peak tailing or extremely large to infinite migration times. A variety of solutions to this problem have been investigated to effectively deal with the

13

analyses of cationic species specifically pH buffer modification (i.e., reducing pH below 3.5) or capillary surface modification by chemical alteration[58-61] or modifier addition[62-64].

Basic Principles of Capillary Electrophoresis

Electrophoretic Migration in the Absence of EOF

Separation using CE involves the movement of charged species through a solution in the presence of an electric field. The cations travel towards the cathode, or negatively charged electrode, while the anions travel toward the anode, or positively charged electrode. In a solution, the conductivity is dependent on the concentration and size of the electrolyte ions, which in turn generate a current from an applied electric field. The overall mobility of the charged solute is also dependent on the charge-to-mass ratio and, to a small extent, the size and three-dimensional shape of the analyte of interest given there is no electroosmotic flow (EOF).

The electric field strength E is a function of the applied voltage V and the capillary length L expressed as:

$$E = \frac{V}{L} \tag{7}$$

An ion experiences a force F_e that is the product of the particle's net charge, q, and the electric field strength represented as:

$$F_e = q \times E \tag{8}$$

Positively charged ions have a positive F_e, which is a reflection of the force that is pushing them in the direction of the negative electrode, whereas the anions are being

14

forced in the opposite direction reflecting a negative F_e. There is another force, however acting on the particles known as the drag force. The drag force is opposite to that of the electrical force experienced and acts to slow the acceleration due to the electrical force. The drag force is a result of the medium interaction with the ionic particle as it migrates through the surrounding running electrolyte. The drag force F_d is directly proportional to the ion's electrophoretic velocity v_{ep}, and is given by:

$$F_d = -f \times v_{ep} \tag{9}$$

where f is the translational friction coefficient. For small spherical ionic particles Stoke's Law can represent f:

$$f = 6\pi\eta r \tag{10}$$

where viscosity of the running electrolyte is η and the radius of the particles migrating through this medium is r. As seen in equations (9) and (10), drag force also known as the frictional drag is directly proportional to the electrophoretic velocity, viscosity of the running electrolyte, and the radius of the particle. Given a charged particle in an electrolyte solution, the application of an electric field will accelerate this species to a limiting velocity as a result of the opposing frictional drag. A balance is achieved between the accelerating electrical force and the opposing frictional drag and a steady state velocity is attained. The sum of these two forces is equal to zero under these conditions and the limiting velocity, or electrophoretic velocity v_{ep}, is achieved. This velocity can be derived from equations (8) and (9) and is represented as follows:

$$v_{ep} = \frac{qE}{f} \tag{11}$$

15

An expression for the electrophoretic mobility (μ_{ep}) can be obtained from equations (10) and (5) given the definition. The expression of this mobility is electrophoretic velocity of the charged particle per unit field strength as follows:

$$\mu_{ep} = \frac{v_{ep}}{E} = \frac{q}{6\pi\eta r} \tag{12}$$

Assuming there is no electroosmotic flow, equation (12) reflects the dependence of μ_{ep} on the net charge of the particle (pK_a) and it's three-dimensional size and shape as well as the viscosity and temperature of the medium.

The absolute electrophoretic mobility μ_o can be extrapolated given an infinitely dilute solution at a given temperature. This is a constant parameter, which is characteristic for a given charged species. Deviations from the absolute mobility can be accounted for in a correction factor, arbitrarily represented as f_i. The actual electrophoretic mobility can then be related to the absolute electrophoretic mobility expressed as:

$$\mu_{app} = f_i \times \mu_{ep} \tag{13}$$

This correction factor in equation (13) was derived for organic anions as a function of the charge number z and ionic strength I of the running electrolyte as follows:

$$f_i = \exp(-0.77\sqrt{zI}) \tag{14}$$

where the ionic strength is:

$$I = \tfrac{1}{2}\sum_{}^{k} cz^2 \tag{15}$$

16

where c is the molar concentration of the ionic running electrolyte buffer. It should be noted that there are limitations to these equations and should be restricted to relatively low concentration ranges and charge numbers. Equation (15) should be considered empirical for an ionic strength in the range between 10^{-1} and 10^{-3} M.

Electroosmotic Flow in Open Tubes

One of the most fundamental concepts of CE is the bulk flow of the running electrolyte as a result of the overall surface charge on the interior of the capillary wall. Fused-silica capillaries are the most popular and widely used due to the well-known silanol (SiOH) chemistry of the inner surface of the capillary. Under slightly acidic to basic conditions, the inner wall of the capillary is lined with negatively charged silanol groups (i.e., deprotonated silanol, SiO$^-$). As illustrated in figure 2, the negatively charged inner wall will attract positively charged cations to the surface and repel negative anions. Furthermore, the solid phase/liquid phase interface along the capillary wall will result in a potential gradient inside the capillary due to the charge distribution. The positively charged region directly contacting the inner surface of the capillary is called the compact region, which is tightly bound and immobile. The next region, moving away from the inner wall and towards the center of the capillary, is the diffuse region made up of a more overall positive charge. This region is the primary mobilization constituent produced when an electric field is applied. The cations migrate towards the negatively charged electrode, which produces a bulk transfer resulting in a constant electroosmotic flow.

a.

b.
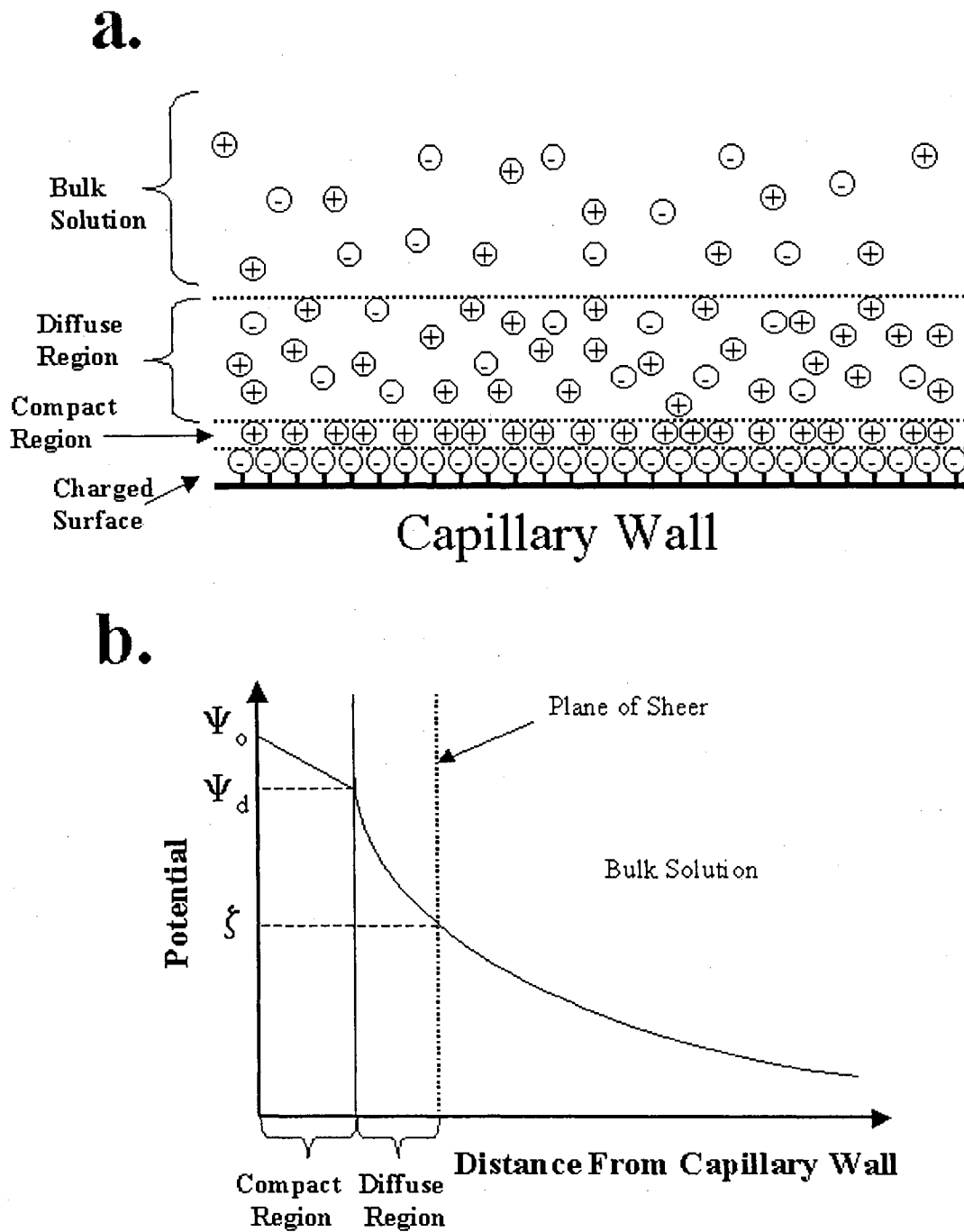
Figure 2. Illustration of (a) the electric double-layer regions and (b) the electric double-layer potential gradient as a function of the relative distance from the capillary wall.

18

The innermost region is considered the bulk solution and is electrically neutral relative to the other two regions. It is important to note that this process is not disregarding electroneutrality; however there is a heterogeneous charge distribution that is the primary reason for electroosmotic flow.

Figure 2 represents the electric potential (ψ) as a function of the distance from the inner capillary wall. The electric potential at the surface of the capillary wall (ψ_o) is the greatest and linearly decreases out to the diffuse region. The potential at the compact-diffuse region interface is represented as ψ_d. From the diffuse region through the bulk solution there is an exponential decay in the electric potential. The zeta potential (ζ) is found at the boundary of the diffuse region and the bulk solution, also known as the plane of sheer. It is obvious from Fig. 2 that the potential drastically decreases as you progress inward from the inner surface of the capillary. The zeta potential is considered characteristic of the movement of solution at the plane of sheer. The diffuse region of the electric double layer containing solvated cations is responsible for the migration of the bulk solution towards the negatively charged electrode. The mathematical expressions for the EOF in terms of velocity (v_{eof}) or mobility (μ_{eof}) are:[65]

$$v_{eof} = \frac{\varepsilon \zeta}{4 \pi \eta} E \qquad (16)$$

or

$$\mu_{eof} = \frac{\varepsilon \zeta}{4 \pi \eta} \qquad (17)$$

where ε is the dielectric constant. The zeta potential is dependent of the surface charge on the capillary wall and therefore dependent on pH. At more basic conditions the silanol

groups on the surface of the capillary wall are more deprotonated, which causes a greater

EOF than at acidic conditions where the silanol groups are predominately protonated.

Increased ionic strength causes compression in the electric double layer that reduces the

zeta potential and decreases the EOF. The opposite holds true for a relative decrease in

the ionic strength. The zeta potential is directly proportional to the surface charge density

(ρ) and the thickness of the double layer (δ) and is expressed as:[66]

$$\zeta = \frac{4\pi\delta\rho}{\varepsilon} \tag{18}$$

or given by the Helmholtz equation:[67]

$$\zeta = \frac{4\pi\eta\mu_{eof}}{\varepsilon} \tag{19}$$

The dependence of the zeta potential on ionic strength is reflected by the thickness of the

electric double layer δ, which is inversely proportional to the Debye-Huckel parameter

(κ). Applying modern electrolyte theory to equation (18) will produce the mathematical

dependence expressed as:

$$\zeta = \frac{4\pi\rho}{\kappa\varepsilon} \propto \frac{1}{\sqrt{I}} \tag{20}$$

Since the surface charge is strongly pH dependent and ζ is directly proportional to the

surface charge, the influence of pH on EOF is realized. More silanol groups are ionized

with a more alkaline pH causing a relative increase in EOF, whereas the opposite holds

true for a more acidic pH. In addition, ζ is inversely proportional to I resulting in a

decrease in ζ with increasing ionic strength, which will contribute to a decrease in EOF.

A beneficial characteristic of EOF is the flat flow profile generated by the electrical pumping action. Mechanical pumping results in a laminar or parabolic flow profile as used in many other chromatographic methods. Figure 3 demonstrates the consequential peak shape distribution for both flow profile phenomena.

a. Electroosmotic Flow Profile

b. Laminar Flow profile
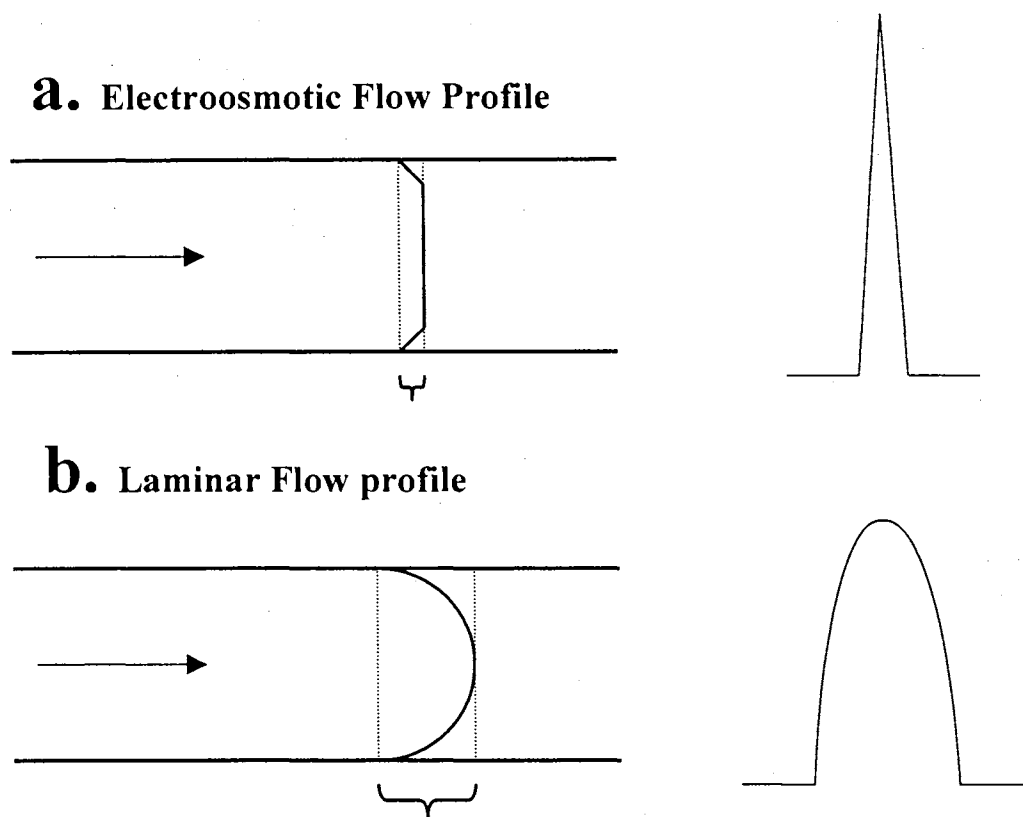
Figure 3. A diagram of flow profiles and their consequential peak shape. (a) EOF plug profile resulting from electrical driving force resulting in sharper peak shape as illustrated on the right. (b) Laminar plug profile seen when a mechanical pump is used resulting in a relatively broader peak distribution.

Apparent Mobility and Migration Time

The apparent mobility (μ_{app}) is what is actually measured in CE, and is the sum of the electrophoretic and electroosmotic mobilities. The μ_{ep} can be measured from the migration time and is expressed by:

$$\mu_{app} = \mu_{ep} + \mu_{eof} = \frac{lL}{t_M V} \qquad (21)$$

where l is the length of the capillary to the detector (cm), L is the total length of the capillary (cm), t_M is the observed migration time, and V is the applied voltage. Furthermore, the apparent velocity (v_{app}) of a given solute is related to mobility and can be described by:

$$v_{app} = v_{ep} + v_{eof} = (\mu_{ep} + \mu_{eof})\frac{V}{L} \qquad (22)$$

Likewise, the μ_{eof} can be described as a function of the column parameters, the voltage, and the migration time of a neutral solute, t_o:

$$\mu_{eof} = \frac{lL}{t_o V} \qquad (23)$$

Rearrangement of equation (21) with substitution of equation (23) will give the mathematical expression for μ_{ep} as:

$$\mu_{ep} = \mu_{app} - \mu_{eof} = \frac{lL}{V}\left(\frac{1}{t_M} - \frac{1}{t_o}\right) \qquad (24)$$

22

The "sign" (i.e., negative or positive) of μ_{ep} is dependent on the direction of ion movement, which corresponds to the charge of the ion. An anion will have a negative μ_{ep} whereas a cation will have a positive value.

Separation Efficiency

The incorporation of a capillary with an electrically driven flow results in much higher separation efficiencies as compared to typical liquid chromatography (LC) methods. The absence of a stationary phase in CE eliminates band broadening due to mass transfer between the mobile phase and the stationary phase. The flat flow profile seen in CE is advantageous over the laminar flow profile, which leads to radial velocity gradients due to frictional forces between the mobile phase and the column walls. Dispersion due to eddy diffusion and stagnant mobile phase is unimportant in CE. Furthermore, any convection related dispersion from joule heating is minimal because of the effective dissipation of heat through the capillary walls, contrary to most other electrophoresis techniques (i.e., gel electrophoresis).

The number of theoretical plates (N) in CE expresses the separation efficiency, which is simply shown by:

$$N = \left(\frac{l}{\sigma}\right)^2 \tag{25}$$

where σ is the standard deviation of the peak, given in unit length. Under ideal conditions the only contributor to solute-zone broadening can be considered to be longitudinal diffusion (along the length of the capillary). Therefore, the efficiency can be

23

correlated to molecular diffusion as in chromatography and can be described by Einstein's equation:

$$\sigma^2 = 2Dt_M = \frac{2DlL}{u_{ep}V} \tag{26}$$

where D is the diffusion coefficient of the solute. By substituting equation (26) into equation (25), the direct relationships of separation efficiency can be realized as:

$$N = \frac{\mu_{ep}Vl}{2DL} = \frac{\mu_{ep}El}{2D} \tag{27}$$

Efficiency is directly proportional to field strength resulting in less dispersion at relatively higher voltage and shorter column length. N is inversely proportional to D indicating that larger molecules with lower diffusion coefficients will have higher efficiencies. In fact, theoretical plate counts of several million can be obtained for nucleotides, proteins, and other large biomolecules.[68] Given a typical electropherogram, the theoretical plate number can be calculated from the following equation:

$$N = 4\left(\frac{t_M}{w_i}\right)^2 = 5.54\left(\frac{t_M}{w_h}\right)^2 = 16\left(\frac{t_M}{w_b}\right)^2 \tag{28}$$

where w_i, w_h, and w_b are peak widths at the respective inflection point, half-height, and peak base.

Resolution and Selectivity

The selectivity, α, can be described as related to mobility by the expression:

$$\alpha = \frac{\Delta\mu_{ep}}{\mu} = \frac{\Delta\mu_{ep}}{\mu_{ep} + \mu_{eof}} \tag{29}$$

Resolution (R_S) is mostly stated as:

$$R_S = \frac{2(t_2 - t_1)}{w_1 - w_2} = \frac{t_2 - t_1}{4\sigma} \qquad (30)$$

where t is migration time, w is baseline peak width (in time), and σ is the standard deviation. The subscripts 1 and 2 refer to the two different solutes of interest. Separation in CE is primarily driven by separation efficiency (i.e., sharp solute zones) in which small differences in solute mobility (<0.05% in some cases[69]) are usually enough for complete resolution. The resolution of two solutes can be described in terms of efficiency as:

$$R_S = \left(\frac{1}{4}\right)\sqrt{N}\left(\frac{\Delta\mu}{\overline{\mu}}\right) \qquad (31)$$

where $\Delta\mu$ is the difference in electrophoretic mobility and $\overline{\mu}$ is the average apparent electrophoretic mobility of the two different adjacent zones. Furthermore, velocity or time^{-1} may be substituted for mobility to give a more simple equation when calculating resolution from a given electropherogram. The substitution of equation (27) into equation (31) yields a theoretical equation for the resolution as related to electroosmotic flow and is expressed as:

$$R_S = \left(\frac{1}{4\sqrt{2}}\right)\Delta\mu\left(\frac{V}{D(\overline{\mu} + \mu_{eof})}\right)^{1/2} \qquad (32)$$

Efficiency is found to increase linearly with applied voltage, however, resolution is related to voltage by a square root relationship. That is to say, voltage must be quadrupled to double the resolution. It is obvious from equation (32) that infinite resolution will be achieved when $\overline{\mu}$ and μ_{eof} are equal and opposite; however, the

analysis time will also approach infinity. Therefore, the overall operational parameters must be optimized as to achieve an adequate resolution within a reasonable analysis time.

Retention Factor and Resolution in MECC

The retention factor (k') accounts for the amount of interaction of a given solute with the stationary phase. In the case of micelles used in CE, k' can be modified as to account for the presence of the micellar pseudo-stationary phase in a given running electrolyte.

$$k' = \frac{t_R - t_o}{t_o \left(1 - \frac{t_R}{t_{mc}}\right)} \tag{33}$$

The terms t_R, t_o, and t_{mc} are the retention time of the neutral solute, the time of a non-retained neutral solute (i.e., EOF marker), and the time of the micelle respectively, as observed from an electropherogram. As t_{mc} approaches infinity (i.e., the overall velocity of the micelle approaches zero), equation (33) simplifies to give the classical retention factor expression used in liquid chromatography. Figure 4 illustrates a typical separation of a two neutral solutes using MECC. The resolution between two solute zones in MECC is expressed by:[67]

$$R_s = \frac{\sqrt{N}}{4} \left(\frac{\alpha - 1}{\alpha}\right) \left(\frac{k_2'}{1 + k_2'}\right) \left(\frac{1 - \frac{t_o}{t_{mc}}}{1 + \left(\frac{t_o}{t_{mc}}\right) k_1'}\right) \tag{34}$$

26

a.

Detection
Point

Injection
Point

↓

↓

↑   ↑   ↑   ↑

Unretained   Neutral   Neutral
Solute   Solute 1   Solute 2   Micelle

b.

t_o t_{R1} t_{R2} t_{mc}

Time
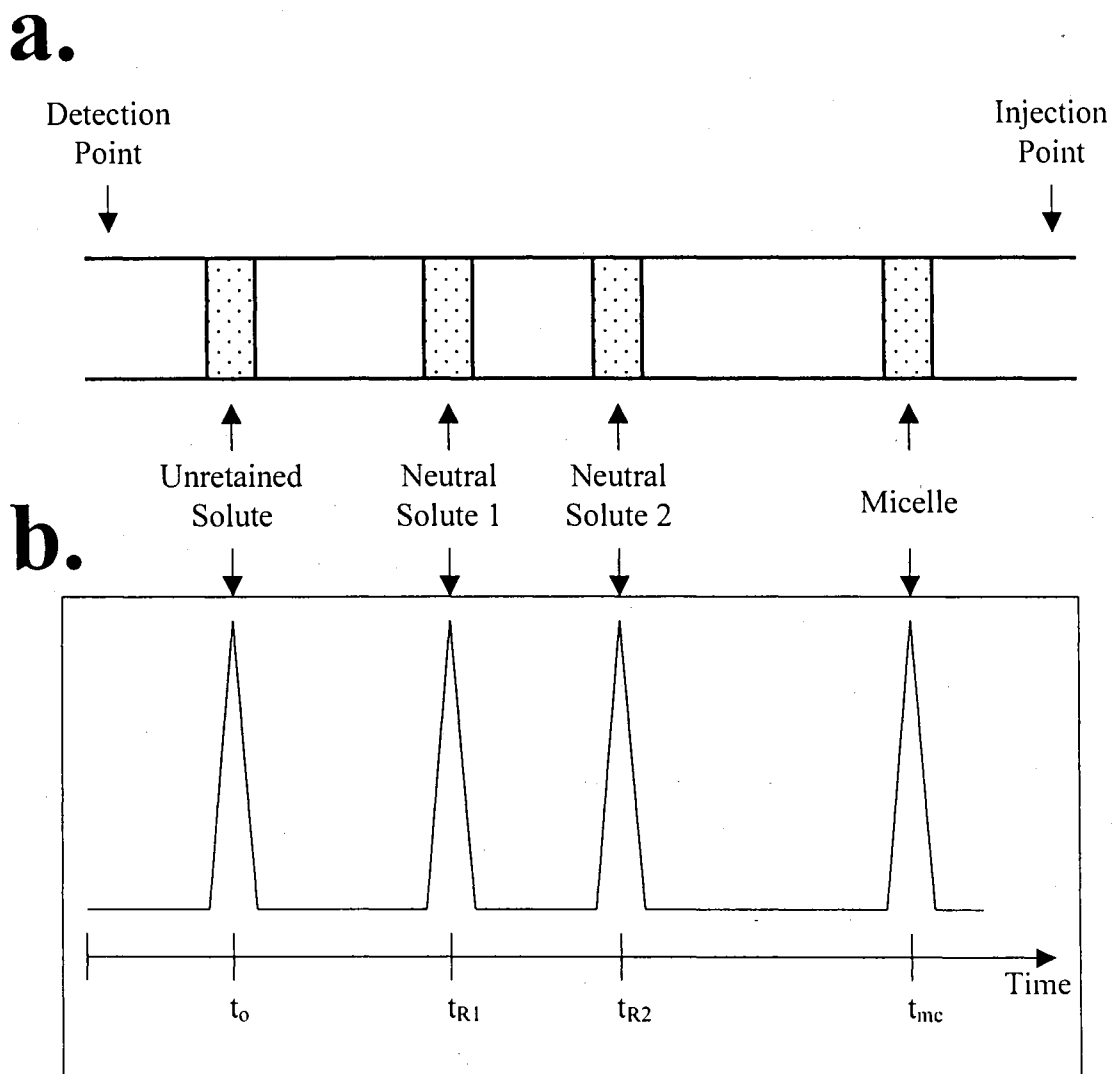
Figure 4. Illustration of a double component analysis using MECC. (a) The on-column separation of all the components and (b) the resulting electropherogram using MECC.

where α is the separation factor ($\alpha = k'_2/k'_1$). The major factors contributing to the

optimization of resolution are α and the elution range parameter, t_o/t_{mc}. These two

27

factors can most easily be manipulated by varying the composition (e.g., pH, ionic strength, organic modifier, "class I" modifier[70], etc.) of the running electrolyte. This, in turn, will alter the hydrophobicity of the micelle, the surface charge density of the capillary wall, the surface charge density of the micelle surface, etc.

As stated in equation (30), the value of resolution simplifies to give an equation that is applicable for all electrophoretic and chromatographic methods.

Factors Affecting Separation Efficiency

Equation (26) describes the calculated dispersion, however, this equation is based on the assumption that longitudinal (i.e., molecular) diffusion is the only contributor to band broadening. In fact, a number of contributors such as Joule heating (i.e., temperature gradients), injection plug length, and analyte interactions with the capillary affect the overall efficiency. These phenomena are usually minute, however, a better description of the overall dispersion (σ^2_T) is:[69]

$$\sigma_T^2 = \sigma_{Dif}^2 + \sigma_{Inj}^2 + \sigma_{Temp}^2 + \sigma_{Ads}^2 + \sigma_{Det}^2 + \sigma_{Ele}^2 \tag{35}$$

The subscripts are diffusion, injection, temperature gradients, adsorption, detection, and electrodispersion, respectively. The domination of any of these diffusion terms will invalidate equation (27), and theoretical efficiency limits will be unattainable.

On-line Preconcentration Methods for Capillary Electrophoresis

Basic Principles Involved in On-line Preconcentration

A steady-state overall velocity of a charged particle is a result of the electrophoretic velocity of the charged particle being co- or counter-directional to the

EOF of the bulk solution. According to equation (11), the electrophoretic velocity v_{ep} is directly proportional to the electric field strength, E, which was defined in equation (7). When considering a capillary containing two buffers that vary in resistivities (i.e., ionic strength) the field strengths are defined as:[71]

$$E_1 = \frac{\gamma E_o}{\gamma x + (1-x)} \tag{36}$$

and

$$E_2 = \frac{E_o}{\gamma x + (1-x)} \tag{37}$$

where E_o, E_1, and E_2 are the field strengths of only buffer 1 or 2, the overall field strength of buffer 1 and the overall field strength of buffer 2, respectively. The term γ is the ratio of the resistivities of the low concentration buffer to that of the high and the fraction of the capillary filled with low resistance buffer is denoted by x. The results of this effect are unfavorable when dealing with sample injections of relatively high salt concentrations. These analytes will migrate slowly through the low resistance, high conductivity sample injection matrix until they reach the running electrolyte buffer (i.e., background electrolyte (BGE)) where they accelerate and, in turn, result in band broadening. However, the alternate scenario with a high ionic strength BGE and low ionic strength sample injection has proven very useful and advantageous. This phenomenon is responsible for on-line sample concentration involving techniques using polarity switching, matrix switching, and the acid/base titration of a sample zone. Furthermore, practically all on-column preconcentration methods take advantage of the differences in velocity between high ionic and low ionic strength buffer boundaries. Due to this trend, a large sample volume consisting of relatively low analyte concentration can

be introduced into the capillary column. The overall analyte band will be gradually narrowed to produce a concentrated zone resulting in larger peak height.

Field-Amplified Sample Stacking

Field-amplified sample stacking (FASS) is based on the principle that ions travel at a relatively higher velocity in a low ionic strength buffer and slow down dramatically at the boundary of the high ionic strength buffer (Osborn et. al.[71] have written a recent review). Furthermore, the velocity of the analyte decreases so dramatically that a narrow zone of stacking occurs at the buffer interface as described in figure 5. The drawback to FASS is the differences in EOF caused by the two different ionic strength buffers, creating laminar flow, which contributes to band broadening of the sample zone.[72, 73] Another disadvantage is the requirement of careful current monitoring up to 95 to 99% of the original value. This factor can contribute to reproducibility problems of peak height and loss of analyte, which can adversely affect quantitative determinations. The injection of a high viscosity plug (i.e., ethylene glycol) prior to the injection of a water plug before the loading of the sample matrix has been incorporated to combat this problem. This modification has shown to slow the electrophoretic mobility of the analyte into the BGE.[74, 75] Furthermore, the utilization of organic by Shihabi in the sample matrix has proven to increase the signal-to-noise ratio.[76] Zhang has reported improvements on limit of detection of up to 1000 fold using such preconcentration techniques.[77]

Figure 5. Illustration of field enhanced injection of cationic analyte dissolved in low ionic strength buffer with high ionic strength BGE. (a) A water plug is hydrodynamically injected. (b) Application of positive potential results in fast migration of cations through the high field strength buffer towards the detection end of the capillary also initiating an EOF towards the outlet.

Field-amplified sample stacking (FASS) has been widely incorporated in the analysis of DNA fragments,[78] pharmaceuticals in serum,[79, 80] drugs of abuse.[81, 82] Furthermore, these techniques have reached widespread use in protein and peptide analysis[83] as well as environmental analysis.[84-86] Nonaqueous FASS CE methods[87, 88] have also been employed in addition to nonaqueous chiral separations.[89]

Large-Volume Sample Stacking

Large-volume sample stacking (LVSS) is another variation of FASS using anionic analytes.[71] The analytes are dissolved in water and hydrodynamically introduced into a large portion of the capillary. Negative polarity is applied first which results in an EOF of the bulk BGE towards the injection end of the capillary. However, the anionic analytes migrate at a high velocity towards the detection end of the capillary up to the high ionic

31

strength BGE. All cationic and neutral species exit the injection end of the capillary by either their electrophoretic mobility or the EOF. The current is monitored in a similar fashion as in FASS up to 95-99% of the original value at which time a positive polarity is applied and the EOF is reversed forcing the narrow zone towards detection. Figure 6 illustrates the basic steps involved in the stacking process.

This technique has been utilized in the analysis of drugs,[90, 91] chemicals of environmental concern,[92, 93] and phenols.[94, 95] A modification of this method has been used to incorporate the detection of cationic analytes.[96, 97] This variation requires the use of an EOF modifier (e.g., cetyltrimethyl ammonium bromide (CTAB)) to reverse or suppress the EOF under negative polarity conditions. In the case of CTAB, the sample is initially dissolved in water and a negative polarity is applied resulting in an EOF that forces the sample plug out of the column. However, BGE containing CTAB is pulled into the capillary and coats the surface causing a reversal in the direction of the EOF.[71]

FASS Using MEKC for the Preconcentration of Neutral Analytes

Micellar electrokinetic capillary chromatography methods for preconcentration were developed to improve the detectability of neutral analytes. This procedure consists of hydrodynamically loading a sample dissolved in a low ionic strength micellar solution into a capillary. A high ionic strength BGE is incorporated to create the stacking boundary. Negative polarity is applied which results in stacking of the anionic micelles towards the detection end of the plug. However, the EOF forces the flow in the direction of the capillary inlet. Once a current of 95-99% of its original value has been achieved,
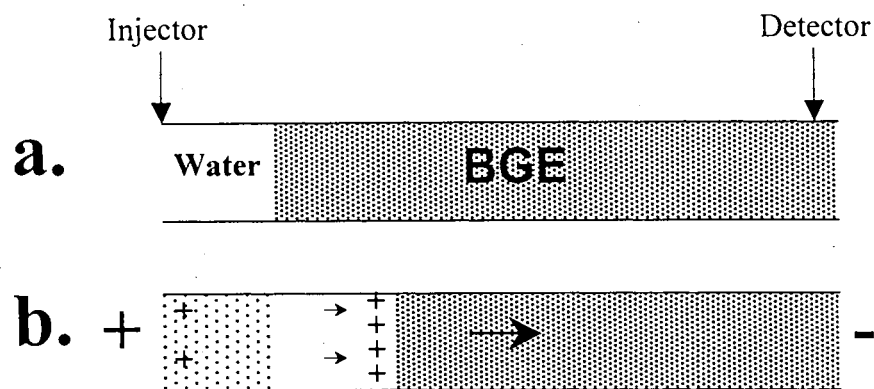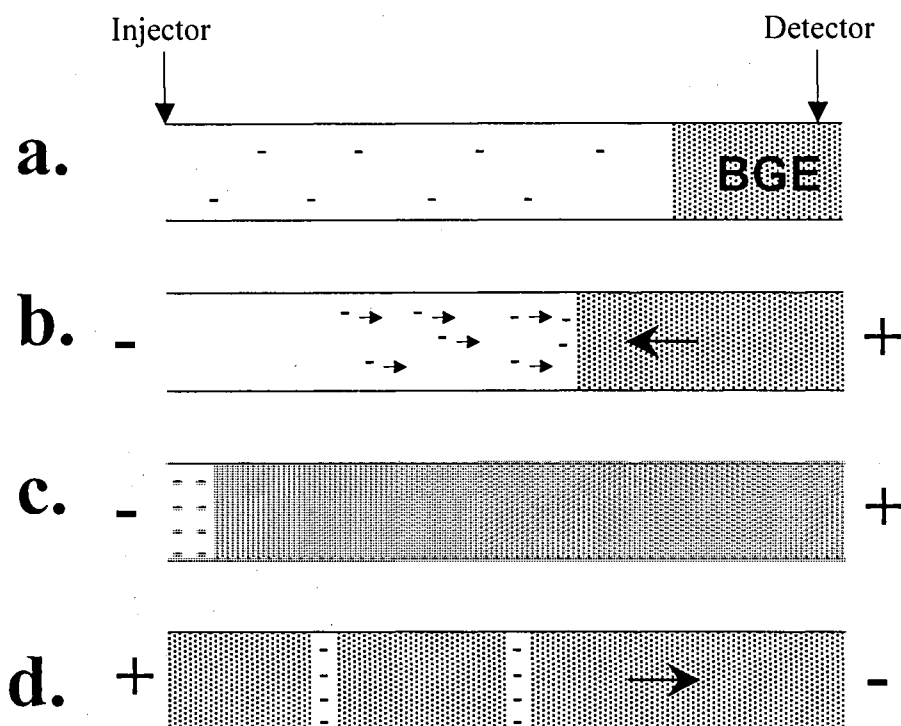
Figure 6. Illustration of LVSS of anionic analyte dissolved in low ionic strength buffer with high ionic strength BGE. (a) Sample is hydrodynamically injected at relatively low concentration. (b) Application of negative potential results in fast migration of anions through the high field strength buffer towards the detection end of the capillary also initiating an EOF towards the inlet. (c) Voltage is terminated when current has reached 95-99% of its original value leaving a concentrated zone of analyte at the buffer boundary. (d) Positive potential is then applied which results in EOF and migration of the narrow zone(s) towards the detector.

the polarity is switched and the resulting EOF forces the narrow zone towards the end of the capillary. In this case, the anionic micelles race towards the capillary inlet and stack at the BGE boundary. The net EOF force is greater than the electrophoretic mobility of the micelles so the narrow band is then forced in the opposite direction (i.e., towards the detector). The parameters (e.g., pH, micelle concentration, % organic, injection time) involved when incorporating these techniques have been thoroughly

studied.[98-101] Modifications of this technique incorporating an injected water plug have been studied to improve the overall stacking method when using reverse migrating micelles.[102, 103] The incorporation of high salt concentrations in the sample matrix has also been investigated which will have a great impact on the preconcentration of biological samples.[104-106]

Sweeping Using MEKC for the Preconcentration of Neutral Analytes

Sweeping is a preconcentration technique that incorporates micelles as the neutral analyte "carrier". A sample is hydrodynamically injected into the column and consists of the analyte and the BGE except without any surfactant. A negative potential is applied at low pH, which suppresses EOF. The column is then placed in buffer containing BGE with anionic micelles that migrate towards the detection end of the capillary. The analytes partition (i.e., interact) with the micelles and are swept along with them. Figure 7 illustrates the basic configuration of the procedure. The success of this phenomenon is dependent on the analytes' affinity for the micelle.[71] The relationship between the length of the sweep zone (l_{sweep}) and the length of the injected analyte zone (l_{inj}) is given by:[107]

$$l_{sweep} = l_{inj}\left(\frac{1}{1+k'}\right)$$

(38)

where k' is the retention factor given by equation (33).

Sweeping methods have improved sensitivity of up to 5000 fold resulting in a huge increase in the use of this preconcentration technique.[107] Quirino and Terabe have hybridized the stacking and sweeping techniques to approach million-fold sensitivity increase of cations.[108] Other hybridizations and combinations of this preconcentration method have been utilized including liquid-liquid extractions [109] and anion stacking.[110]

Injector   Detector

a.   a   b   a   b   a
                b   a   b

l_{inj}

b. _   ******
           ******b   a   b   a   +
           ******
           ******b   a   a   b
           Anionic micelle migration under
               suppressed EOF conditions ⟶

c. _   ***************b**********a
           ***************b**********a   +
           ***************b**********a
           ***************b**********a
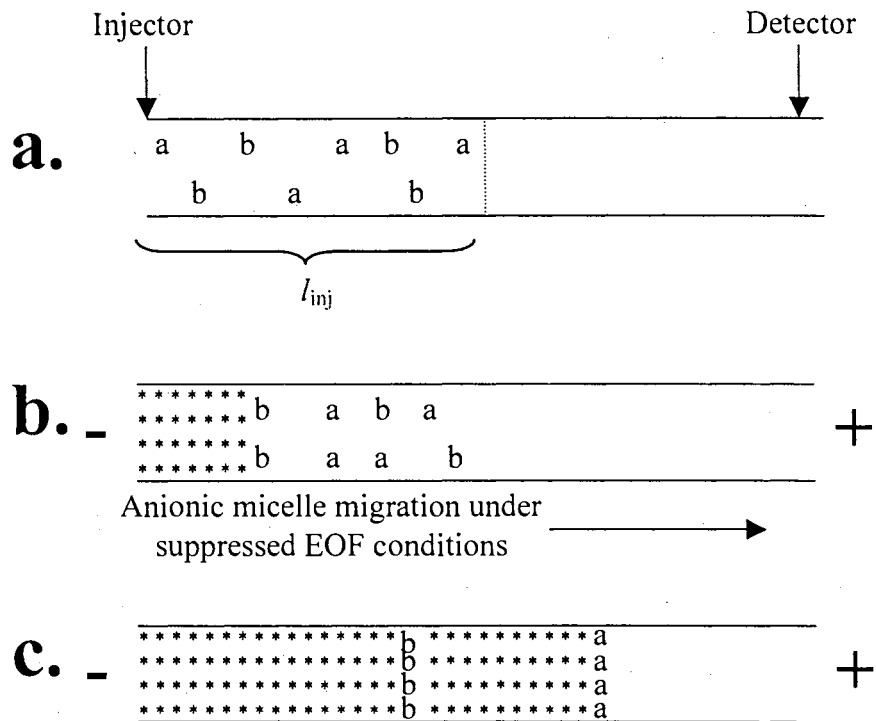
Figure 7. Sweeping method for preconcentration of neutral solutes ("a" and "b"), with anionic micelle (*). (a) The sample dissolved in low pH (i.e., suppressed EOF) BGE without surfactant is hydrodynamically injected into the column. (b) The capillary inlet is placed in the same BGE only containing anionic micelles, which migrate towards the outlet of the capillary upon application of a negative potential. (c) Sweeping is a result of the interaction of the solute with the micelle resulting in a narrow zones of concentrated analyte.

Conclusions

Chapter I has outlined the scope of this dissertation and presented some of the basic principles relevant to the research involved in the chapters to come. In addition, this chapter demonstrates the high resolving power of CE, which can be readily exploited in

the separation and quantitation of a wide variety of species. Furthermore, the physical instrumentation, separation methods, and detection approaches have been overviewed to reveal the adaptability and versatility of the CE techniques.

References

1. Tiselius, A., *Trans. Faraday Soc.* **1937**, *33*, 524-531.

2. Strain, H.H., *J. Am. Chem. Soc.* **1939**, *61*, 1292-1293.

3. Hjertèn, S., *Chromatogr. Rev.* **1967**, *9*, 122-219.

4. Vertanen, R., *Acta. Polytech. Scand.* **1974**, *123*, 1-67.

5. Pretorius, V.; Hopkins, B.J.; Schieke, J.D., *J. Chromatogr.* **1974**, *99*, 23-30.

6. Mikkers, F.E.P.; Everaerts, F.M.; Verheggen, P.E.M., *J. Chromatogr.* **1979**, *169*, 11-20.

7. Jorgenson, J.; Lukacs, K.D., *Anal. Chem.* **1981**, *53*, 1298-1302.

8. Hjertèn, S., *J. Chromatogr.* **1983**, *270*, 1-6.

9. Hjertèn, S.; Zhu, M.D., *J. Chromatogr.* **1985**, *346*, 265-270.

10. Terabe, S.; Otsuka, K.; Ichikama, K.; Tsuchiya, A.; Ando, T., *Anal. Chem.* **1984**, *56*, 111-113.

11. Takagi, T., *Electrophoresis* **1997**, *18*, 2239-2242.

12. Terabe, S.; Ichikama, K.; Ando, T., *J. Chromatogr.* **1985**, *332*, 211-217.

13. Fanali, S.; Kilar, F., *J. Cap. Elect.* **1994**, *1*, 72-78.

14. Vescina, M.C.; Fermier, A.M.; Guo, Y., *J. Chromatogr. A* **2002**, *973*, 187-196.

15. Shamsi, S.A.; Palmer, C.P.; Warner, I.M., *Anal. Chem.* **2001**, *73*, 140A-149A.

16. Chiou, C.-S.; Shih, J.-S., *Anal. Chim. Acta* **1998**, *360*, 69-76.

17. Horvath, J.; Dolnik, V., *Electrophoresis* **2001**, *22*, 644-655.

18. Liu, C.-Y., *Electrophoresis* **2001**, *22*, 612-628.

19.   Lammerhofer, M.; Svec, F.; Frechet, J.M.J.; Lindner, W., *Trends Anal. Chem.* **2000**, *19*, 676-698.

20.   Schweitz, L.; Andersson, L.I.; Nilsson, S., *J. Chromatogr. A* **1998**, *817*, 5-13.

21.   Colon, L.A.; Reynolds, K.J.; Alicea-Maldonaldo, R.; Fermier, A.M., *Electrophoresis* **1997**, *18*, 2162-2174.

22.   Yang, Q.; Hidajat, K.; Li, S.F., *J. Chromatogr. Sci.* **1997**, *35*, 358-373.

23.   Bruin, G.J., *Electrophoresis* **2002**, *21*, 3931-3951.

24.   Isaaq, H.J., *J. Liq. Chrom. & Rel. Technol.* **2002**, *25*, 1153-1170.

25.   Huang, X.; Coleman, W.; Zare, R., *J. Chromatogr.* **1989**, *480*, 95-110.

26.   Wallingord, R.A.; Ewing, A.G., *Adv. Chromatogr.* **1990**, *29*, 1-.

27.   Moring, S.E.; Reel, R.T.; van Soest, R.E., *Electrophoresis* **1993**, *14*, 3454-3459.

28.   *Agilent Technologies On-Line, Peak No. 1* **1998**.

29.   Heiger, D.N.; Kaltenbach, P.; Sievert, H.-J., *Electrophoresis* **1994**, *15*, 1234-1247.

30.   Molina, M.; Manuel, S., *Electrophoresis* **2002**, *23*, 2333-2340.

31.   Ren, J.; Fang, N.; Wu, D., *Anal. Chim. Acta* **2002**, *470*, 129-135.

32.   Somsen, G.W.; Welten, H.T.; Mulder, F.P.; Swart, C.W.; Kema, I.P.; de Jong, G.J., *J. Chromatogr. B* **2002**, *775*, 17-29.

33.   Viskari, P.J.; Colyer, C.L., *J. Chromatogr. A* **2002**, *972*, 269-276.

34.   Wall, W.E.; Chan, K.; El Rassi, Z., *Electrophoresis* **2001**, *22*, 2320-2326.

35.   Chen, Y.; Xu, Y., *J. Liq. Chrom. & Rel. Technol.* **2002**, *25*, 843-855.

36.   Schoftner, R.; Pfeifer, A.; Buchberger, W., *J. Sep. Sci.* **2002**, *25*, 507-513.

37.   Siren, H.; Vantsi, S., *J. Chromatogr. A* **2002**, *957*, 17-26.

38. Zunic, G.; Jelic-Ivanovic, Z.; Colic, M.; Spasic, S., *J. Chromatogr. B* **2002**, *772*, 19-33.

39. Wang, J.; Chatrathi, M.P.; Tian, B., *Anal. Chim. Acta* **2000**, *416*, 9-14.

40. Wang, J.; Chatrathi, M.P.; Madhu, P.; Tian, B.; Polsky, R., *Electrophoresis* **2000**, *12*, 691-694.

41. Baltussen, E.; Guijt, R.M.; Steen, G.B.; Laugere, F.; Baltussen, S., *Electrophoresis* **2002**, *23*, 2888-2893.

42. Castro, R.; Moreno, M.V.; Natera, R.; Garcia-Rowe, F.; Hernandez, M.J.; Barroso, C.G., *Chromatographia* **2002**, *56*, 57-61.

43. Kuban, P.; Karlberg, B.; Kuban, P.; Kuban, V., *J. Chromatogr. A* **2002**, *964*, 227-241.

44. Wang, J.; Pumera, M.; Collins, G.; Opekar, F.; Jelinek, I., *Analyst* **2002**, *127*, 719-723.

45. Koide, T.; Ueno, K., *J. Chromatogr. A* **2001**, *923*, 229-239.

46. Schewitz, J.; Pusecker, K.; Gfrorer, P.; Gotz, U.; Tseng, L.-H.; Albert, K.; Bayer, E., *Chromatographia* **1999**, *50*, 333-337.

47. Wedig, M.; Laug, S.; Christians, T.; Thunhorst, M.; Holzgrabe, U., *J. Pharm & Biomed. Anal.* **2001**, *27*, 531-540.

48. Suss, F.; Kahle, C.; Holzgrabe, U.; Scriba, G.K., *Electrophoresis* **2002**, *23*, 1301-1307.

49. Meyer, T.; Waidelich, D.; Frahm, A.W., *Electrophoresis* **2002**, *23*, 1053-1062.

50. Deterding, L.J.; Cutalo, J.M.; Khaledi, M.G.; Tomer, K.B., *Electrophoresis* **2002**, *23*, 2296-2305.

51. Huikko, K.; Kotiaho, T.; Kostiainen, R., *Rapid. Comm. in MS* **2002**, *16*, 1562-1568.

52. Prange, A.; Schaumloeffel, D., *Anal. & Bioanal. Chem.* **2002**, *373*, 441-453.

53. Tanaka, Y., *Sepu* **2002**, *20*, 317-327.

54. Ebersole, R.C.; McCormick, R.M., *Biotechnology* **1993**, *11*, 1278-1282.

55. Armstrong, D.W.; Schulte, G.; Shchneiderheinze, J.M.; Westenberg, D.J., *Anal. Chem.* **1999**, *71*, 5465-5469.

56. Shintani, T.; Yamada, K.; Torimura, M., *J. Chromatogr. A* **2002**, *210*, 245-249.

57. Cohen, A.S.; Karger, B.L., *J. Chromatogr.* **1987**, *397*, 409-417.

58. Matyska, M.T.; Pesek, J.J.; Boysen, R.I.; Hearn, M.T., *J. Chromatogr. A* **2001**, *924*, 211-221.

59. Pesek, J.J.; Matyska, M.T.; Sentelles, S.; Galceran, M.T.; Chiari, M.; Pirri, G., *Electrophoresis* **2002**, *23*, 2982-2989.

60. Pesek, J.J.; Matyska, M.T.; Tran, H., *J. of Sep. Sci.* **2001**, *24*, 729-735.

61. Riepe, H.-G.; Loreti, V.; Garcia-Sanchez, R.; Camara, C.; Bettmer, J., *Fres. J. Anal. Chem.* **2001**, *370*, 488-491.

62. Fujimoto, C., *Electrophoresis* **2002**, *23*, 2929-2937.

63. Konig, S.; Welsch, T., *J. Chromatogr. A* **2000**, *894*, 79-88.

64. Pullen, P.E.; Pesek, J.J.; Matyska, M.T.; Frommer, J., *Anal. Chem.* **2000**, *72*, 2751-2757.

65. Rice, C.L.; Whitehead, R., *J. Phys. Chem* **1965**, *69*, 4017-4024.

66. Adamson, A., *Physical Chemistry of Surfaces*. **1967**, New York: Interscience.

67.   Li, S.F.Y., *Capillary Electrophoresis: Principles, Practice, and Applications.*

        1992, Amsterdam: Elsevier.

68.   Altria, K.D., *Capillary Electrophoresis Guidebook.* Methods in Molecular

        Biology. Vol. 52. **1996**, Totowa, N.J.: Humana Press.

69.   Heiger, D.N., *High Performance Capillary Electrophoresis-An introduction.*

        1992: Hewlitt-Packard Company.

70.   Wall, W.E.; Allen, D.J.; Denson, K.D.; Love, G.I.; Smith, J.T., *Electrophoresis*

        1999, *20*, 2390-2399.

71.   Osbourn, D.M.; Weiss, D.J.; Lunte, C.E., *Electrophoresis* **2000**, *21*, 2768-2779.

72.   Camilleri, P., *Capillary Electrophoresis: Theory and Practice.* 2nd ed, ed.

        Camilleri, P. **1998**, Boca Raton: CRC Press.

73.   Chien, R.-L.; Helmer, J.C., *Anal. Chem.* **1991**, *63*, 1354-1361.

74.   Chien, R.-L.; Burgi, D.S., *J. Chromatogr.* **1991**, *559*, 141-152.

75.   Zhang, C.-X.; Thormann, W., *Anal. Chem.* **1998**, *70*, 540-548.

76.   Shihabi, Z.K., *J. Chromatogr. A* **1999**, *853*, 3-6.

77.   Zhang, C.-X.; Thormann, W., *Anal. Chem.* **1996**, *68*, 2523-2532.

78.   Tan, W.G.; Tyrell, D.L.J.; Dovichi, N.J., *J. Chromatogr. A* **1999**, *853*, 309-319.

79.   Zhang, C.-X.; Aebi, Y.; Thormann, W., *Clin. Chem* **1996**, *42*, 1805-1811.

80.   Perez-Ruiz, T.; Martinez-Lozano, C.; Sanz, A.; Bravo, E., *Chromatographia*

        2002, *56*, 63-67.

81.   Tagliaro, F.; Manetto, G.; Crivellente, F.; Scarcella, D.; Marigo, M., *Foresn. Sci.*

        Int. **1998**, *92*, 201-211.

82.   Wey, A.B.; Zhang, C.-X.; Thormann, W., *J. Chromatogr. A* **1999**, *853*, 95-106.

83.   Stroink, T.; Paarlberg, E.; Waterval, J.C.M.; Bult, A.; Underberg, W.J.M., *Electrophoresis* **2001**, *22*, 2374-2383.

84.   Fung, Y.-S.; Mak, J.L.L., *Electrophoresis* **2001**, *22*, 2260-2269.

85.   Zhu, L.; Lee, H.K., *Anal. Chem.* **2001**, *73*, 3065-3072.

86.   Tegeler, T.J.; El Rassi, Z., *J. AOAC Int.* **1999**, *82*, 1542-1548.

87.   Morales, S.; Cela, R., *Electrophoresis* **2002**, *23*, 408-413.

88.   Morales, S.; Cela, R., *J. Chromatogr. A* **1999**, *846*, 401-411.

89.   Wang, F.; Khaledi, M.G., *J. Chromatogr. B* **1999**, *731*, 187-197.

90.   Harland, G.B.; McGrath, G.; McClean, S.; Smyth, W.F., *Anal. Commun.* **1997**, *34*, 9-11.

91.   Lai, C.C.; Kelley, J.A. in *224th ACS National Meeting.* **2002**. Boston, MA: American Chemical Society.

92.   Cooper, P.A.; Jessop, K.M.; Moffatt, F., *Electrophoresis* **2000**, *21*, 1574-1579.

93.   Hissner, F.; Daus, B.; Mattusch, J.; Heinig, K., *J. Chromatogr. A* **1999**, *1999*, 497-502.

94.   Wall, W.E.; Li, J.; El Rassi, Z., *J. Sep. Sci.* **2002**, *25*, 1-6, *(In Press)*.

95.   Martinez, D.; Borrull, F.; Calull, M., *J. Chromatogr. A* **1997**, *788*, 185-193.

96.   Quirino, J.P.; Terabe, S., *Electrophoresis* **2000**, *21*, 355-359.

97.   Baryla, N.E.; Lucy, C.A., *Electrophoresis* **2001**, *22*, 52-58.

98.   Quirino, J.P.; Terabe, S., *Anal. Chem.* **1998**, *70*, 149-157.

99.   Palmer, J.; Munro, N.J.; Landers, J.P., *Anal. Chem.* **1999**, *71*, 1679-1687.

100.   Palmer, J.; Burgi, D.S.; Landers, J.P., *Anal. Chem.* **2002**, *74*, 632-638.

101.   Kim, J.-B.; Otsuka, K.; Terabe, S., *J. Chromatogr. A* **2001**, *912*, 343-352.

102. Quirino, J.P.; Otsuka, K.; Terabe, S., *J. Chromatogr. B* **1998**, *714*, 29-38.

103. Otsuka, K.; Hayashibara, H.; Yamauchi, S.; Quirino, J.P.; Terabe, S., *J. Chromatogr. A* **1999**, *853*, 413-420.

104. Palmer, J.; Landers, J.P., *Anal. Chem.* **2000**, *72*, 1941-1943.

105. Molina, M.; Silva, M., *Electrophoresis* **2000**, *21*, 3625-3633.

106. Quirino, J.P.; Terabe, S.; Bocek, P., *Anal. Chem.* **2000**, *72*, 1934-1940.

107. Quirino, J.P.; Terabe, S., *Science* **1998**, *282*, 465-468.

108. Quirino, J.P.; Terabe, S., *Anal. Chem.* **2000**, *72*, 1023-1030.

109. Takagai, Y.; Igarashi, S., *Anal. Bioanal. Chem.* **2002**, *373*, 87-92.

110. Kim, J.-B.; Otsuka, K.; Terabe, S., *J. Chromatogr. A* **2001**, *932*, 129-137.

CHAPTER II

MICELLAR ELECTROKINETIC CAPILLARY CHROMATOGRAPHY OF ANILINE

PESTICIDIC METABOLITES DERIVATIZED WITH FLUORESCEIN

ISOTHIOCYANATE AND THEIR DETECTION IN REAL

WORLD WATER AT LOW LEVELS BY LASER-

INDUCED FLUORESCENCE*

Introduction

Capillary electrophoresis is increasingly employed in the separation and detection

of pesticides.[1, 2] However, its application to the separation of the transformation products

of pesticides (or metabolites) is rather scarce.[3-6] This is despite the fact that most

pesticides undergo transformation in the environment through various degradation

processes including hydrolysis, photolysis, oxidation, biodegradation, etc. producing the

so-called metabolites. Most often the metabolites are highly resistant in water and soils,

and therefore their residues as well as their mobility or sorption in soils are very

important problems. Furthermore, the metabolites of pesticides are even more toxic than

their parent compounds.[7, 8] This explains the initiative of the National Pesticides Survey,

in a joint project between EPA's Office of Drinking Water and the Office of Pesticide

Programs to include many pesticides and their metabolites in their monitoring programs.[9, 10] This report is concerned with the CE of anilines, which are widespread environmental

pollutants, owing to their relatively high water solubilities.[11, 12] They can be present in the

aquatic environment as a result of industrial discharges from industrial processes using substituted anilines as reagents for the synthesis of pharmaceuticals and dyes.[13] As shown in Table 1, they also occur as the metabolites of widely used pesticides such as phenylureas, carbamates and anilides.[13] Anilines are more toxic than the parent pesticides.

Thus far, and to the best of our knowledge, little work has been done on the CE of anilines[14-16] and virtually no sensitive detection schemes have been reported yet. Therefore, it is the aim of this article to describe a precolumn derivatization scheme based on the fluorescent labeling of anilines with fluorescein isothiocyanate (FITC) and their subsequent separation by CE with laser-induced fluorescence (LIF) detection. The CE separation system of the FITC-aniline derivatives described in the present work is based on micellar electrokinetic capillary chromatography (MECC) with glycosidic surfactants in the presence of borate electrolytes, thus leading to the formation of in situ charged micelles. In situ charged micelles, which were introduced and characterized recently in our laboratories, refer to micelles consisting of glycosidic surfactants complexed with borate anions. [17-22] In situ charged micelles allow the manipulation of the migration time window and in turn resolution and peak capacity with the pH and amount of borate in the running electrolyte.

Experimental

Instrument

A Beckman P/ACE system 5510 (Fullerton, CA, USA) was used for all experiments. It was equipped with a Beckman Laser Module 488, which consists of a 3 mW, 488 nm air-cooled argon-ion laser. A Beckman diode array detector was used for UV absorbance detection. P/ACE station software was used for data acquisition. An emission band-pass filter of 520 nm ± 2 nm, purchased from Corion (Holliston, MA, USA) was used for the LIF detection of the FITC derivatives. The experiments were

TABLE 1.

STRUCTURES, ABBREVIATIONS, pKa VALUES AND PARENT PESTICIDES OF THE ANILINES. PU, PHENYLUREA HERBICIDES; CAR, CARBAMATE INSECTICIDES; ANI, ANILIDE PESTICIDES
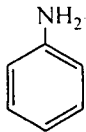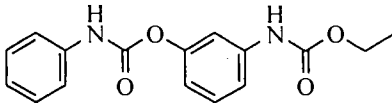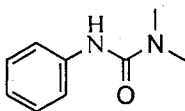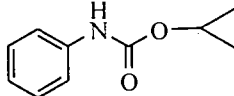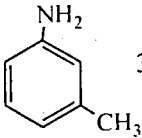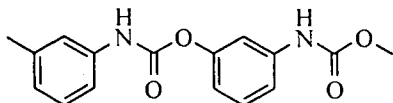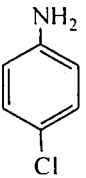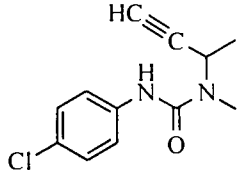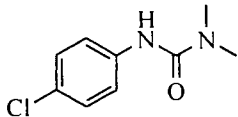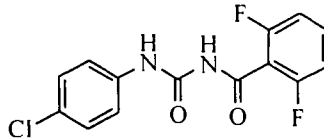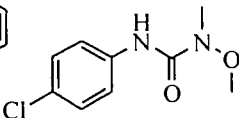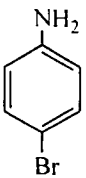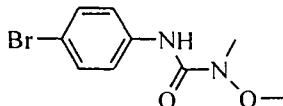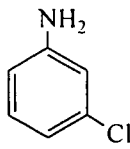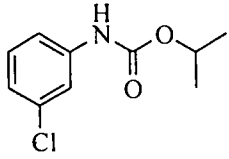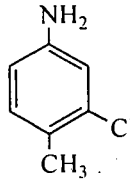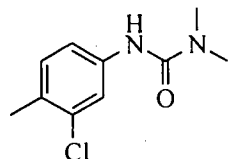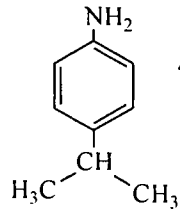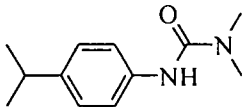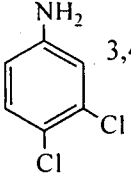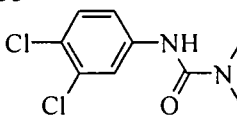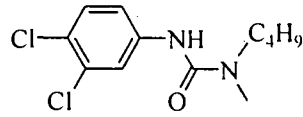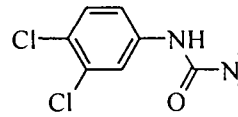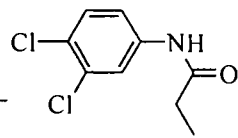
Structure	Name	Abbreviation	pK_a	Parent pesticides
(aniline structure, NH₂)	Aniline	AN	4.70[a] 4.60[b] 4.66[c]	Desmedipham (CAR); Fenuron (PU); Propham (CAR)
(3-methylaniline structure, NH₂, CH₃)	3-Methylaniline	3-MeAN	4.71[a] 4.69[b] 4.91[c]	Phenmedipham (CAR)
(4-chloroaniline structure, NH₂, Cl)	4-Chloroaniline	4-ClAN	3.52[a] 3.98[b] 4.06[c]	Buturon (PU); Monuron (PU); Diflubenzuron (PU); Monolinuron (PU)
(4-bromoaniline structure, NH₂, Br)	4-Bromoaniline	4-BrAN	3.88[a] 3.58[c]	Metobromuron (PU)

46

TABLE 1. CONTINUED

Structure	Name	Abbreviation	pKₐ	Parent pesticides
	3-Chloroaniline	3-ClAN	3.52^a 3.46^b 3.94^c	Chlorpropham (CAR)
	3-Chloro-4-methylaniline	3-Cl-4-MeAN	4.05^a	Chlortoluron (PU)
	4-Isopropylaniline	4-IsPrAN	5.0^d	Isoproturon (PU)
	3,4-Dichloroaniline	3,4-DiClAN	3.33^c	Diuron (PU) Neburon (PU) Linuron (PU) Propanil (ANI)

pKₐ values are taken from: a) Ref. [32]; b) Ref. [33]; c) Ref. [34]; d) Ref. [32]

carried out using fused-silica capillaries obtained from Polymicro Technologies (Phoenix, AZ, USA). The dimensions of the capillaries were 50 cm to the detection window and 57 cm total length, with 50 µm internal diameter and 365 µm outer diameter. In all experiments, the temperature was held constant at 20 °C by the instrument's

thermostating system. Samples were pressure-injected at 0.034 bar (*i.e.*, 3.5 kPa) for various lengths of time. Between runs, the capillary was rinsed with distilled water, 1.0 M KOH, distilled water, and running electrolyte for 2, 6, 4, and 3 min, respectively.

Reagents and Materials

The following anilines, 4-chloroaniline (4-ClAN, 98% purity), 4-bromoaniline (4-BrAN, 97% purity), 3,4-dichloroaniline (3,4-DiClAN, 98% purity), 3-chloroaniline (3-ClAN, 99% purity), 3-chloro-4-methylaniline (3-Cl-4-MeAN, >99% purity) and 4-isopropylaniline (4-IsPrAN, 99% purity) were purchased from Aldrich (Milwaukee, WI). 3-Methylaniline (3-MeAN, >99% purity) was purchased from Fluka (Ronkonkoma, NY, USA), and aniline (AN, >99% purity) was obtained from Fisher (Fairlawn, NJ, USA) along with the HPLC grade acetone and boric acid. For structures, abbreviations, pKa values and the parent pesticides of anilines, see Table 1. The derivatizing agent FITC (90% purity by HPLC) was purchased from Sigma (St. Louis, MO, USA). Sodium hydroxide and potassium hydroxide were purchased from EM Science (Cherry Hill, NJ, USA). Monobasic sodium phosphate was obtained from Mallinckrodt (Paris, KY, USA). The surfactants *n*-octyl-β-D-glucoside (OG) and *n*-nonyl-β-D-glucoside (NG) were purchased from Anatrace (Maumee, OH, USA).

Precolumn Derivatization

The aniline pesticidic metabolites were tagged with FITC as follows. The analytes were first dissolved in HPLC grade acetone at a concentration of 1.0×10^{-2} M. An aliquot of this solution was then diluted to a final concentration of 1.0×10^{-4} M with 20 mM borate dissolved in deionized water, pH 9.5. 40 μL of 2.5×10^{-3} M FITC dissolved in HPLC grade acetone were then added to a 960 μL aliquot of the 1.0×10^{-4} M analyte in an amber vial. This brings it up to a 1:1 mole ratio for analyte to FITC in the reaction mixture. The reaction was stirred overnight (at least 9 hrs) at room temperature. These

48

samples were subsequently diluted and used for sample injections for the electropherograms generated under the various operating conditions. This derivatization was also used for determining the LOD by successive dilution. Fresh derivatives were prepared weekly due to the formation of side and degradation products.

The precolumn derivatization of the anilines with FITC at the LOD was carried out using three different water systems including tap water, lake water, and deionized water. The aniline pesticidic metabolites (AN, 3-MeAN and 3-ClAN) were initially made up to be 1×10^{-2} M in acetone. The tap water and the lake water were filtered through 0.2 μm filters, from Scientific Resources (Eatontown, NJ, USA), before using them to prepare the 20 mM sodium borate at pH of 9.5. These solutions were then used for the final dilution of the 1×10^{-2} M analytes to 8.9×10^{-9} M. 1.2 μL of 2.5×10^{-3} M FITC dissolved in acetone was then pipetted into a 999 μL aliquot of the 8.9×10^{-9} M analytes in an amber vial to achieve 100:1 mole ratio of FITC to solute in the reaction mixture. The reaction proceeded overnight at room temperature with constant stirring.

Results and Discussion

Derivatized and underivatized anilines were separated by capillary electrophoresis over a wide range of conditions in order to determine the optimal conditions for separation and detection. As native species (i.e., underivatized anilines), the anilines are weak bases, which eventually electrophorese and separate at low pH as protonated species by capillary zone electrophoresis (CZE). However, the most challenging part of their CE is their detection at low levels. This required their derivatization with a fluorescent tags such as FITC. The FITC derivatives were then separated by MECC using in situ charged glycosidic surfactants complexed with borate anions under various conditions including pH, borate concentration and surfactant concentration. The two glycosidic surfactants utilized were OG and NG.

CZE of Underivatized Anilines

Figure 1 is a typical electropherogram of underivatized anilines obtained by CZE

with a running electrolyte of 50 mM sodium phosphate, pH 2.5, at an applied voltage of
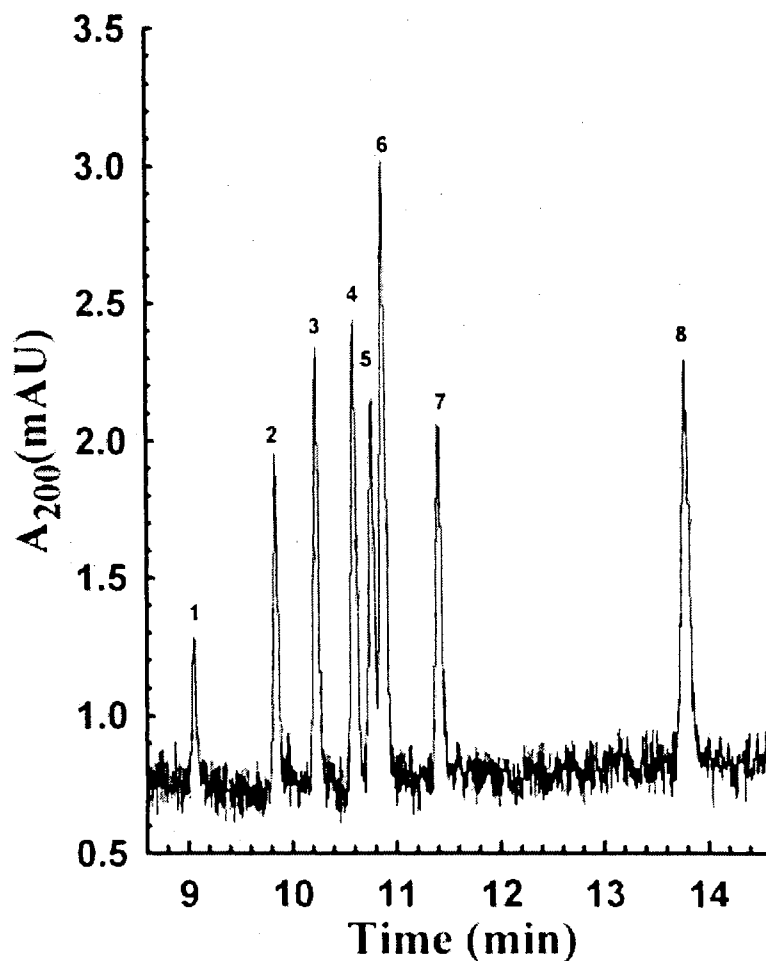
Figure 1. Electropherogram of underivatized anilines. Conditions: capillary column, 50 cm / 57 cm x 50 μm i.d.; running electrolyte, 50 mM phosphate, pH 2.5; voltage, 18 kV; column temperature, 20 °C. Underivatized analytes: 1, AN; 2, 3-MeAN; 3, 4-ClAN; 4, 4-BrAN; 5, 3-ClAN; 6, 3-Cl-4-MeAN; 7, 4-IsPrAN; 8, 3,4-DiClAN.

50

18 kV. These anilines are weak bases with pK_a values in the range 3.33 to 5.0, see Table 1. At pH 2.5, they exist at different degrees of protonation with AN (pK_a = 4.60-4.70), 3-MeAN (pK_a = 4.69-4.91) and 4-IsPrAN (pK_a = 5.0) almost fully protonated. Also, at pH 2.5 the electroosmotic flow (EOF) is negligible since the silanol groups of the fused-silica surface are fully protonated. As expected, the anilines migrated in the order of decreasing charge-to-mass ratio with the highest AN migrating first and the lowest 3,4-DiClAN migrating last. Although they are well separated, the limit of detection (LOD) of these analytes is quite high ($\sim 10^{-5}$ M) in the UV at 200 nm, see Table 2. Thus, precolumn derivatization is needed to allow their detection at low levels.

TABLE 2.

LOD OF SOME REPRESENTATIVE UNDERIVATIZED ANILINES BY UV AT 200 nm AND OF THEIR FITC DERIVATIVES BY LIF DETECTION.

Solute	LOD (M)	
	Underivatized solutes (UV detection)	FITC derivatized solutes (LIF detection)
3-MeAN	2.0×10^{-5}	8.7×10^{-10}
3-Cl-4MeAN	8.0×10^{-6}	3.1×10^{-10}
4-IsPrAN	4.0×10^{-5}	4.2×10^{-10}
3-ClAN	9.0×10^{-6}	4.4×10^{-10}
3,4-DiClAN	1.0×10^{-5}	3.9×10^{-10}

51

FITC Derivatization—Percent Conversion, Limits of Detection and Derivatization of Trace Amounts in Real Waters

Figure 2 illustrates the reaction scheme for the FITC derivatization of anilines, which involves the formation of a stable thiourea bond between the isothiocyanate group of the FITC tag and the amino group of the aniline analyte.[23] The FITC derivatization was performed at four different mole ratios of tag to analyte, namely 1:1, 3:1, 7:1 and 10:1 in order to examine the % analyte conversion as a function of excess tag in the
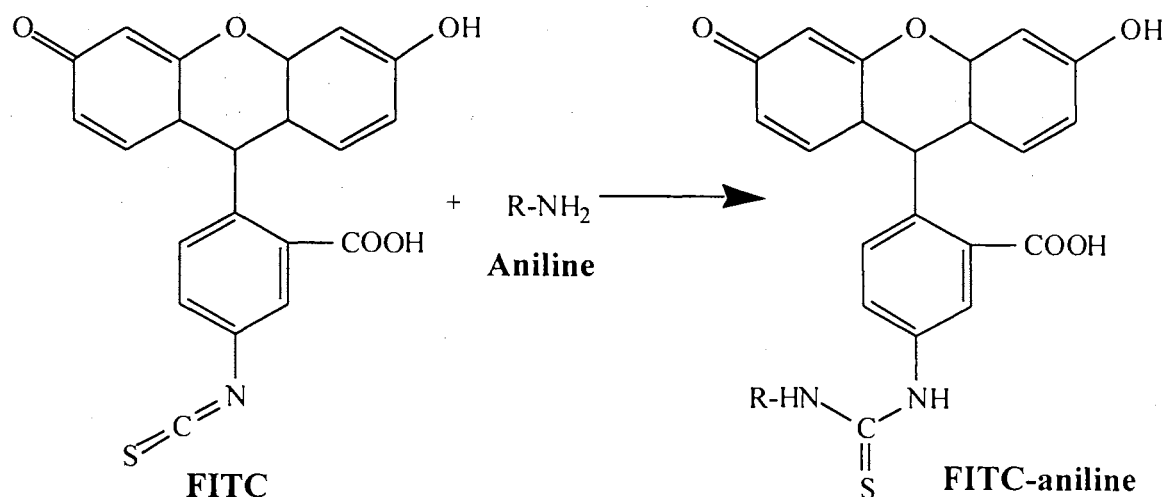
Figure 2. FITC derivatization of an amine such as an aniline.

reaction mixture. The results obtained are presented in Fig. 3 for five different and representative anilines, namely 3-MeAN, 3-ClAN, 3-Cl-4-MeAN, 4-IsPrAN and 3,4-DiClAN. As expected, the higher the mole ratio the larger the % conversion. While the alkyl substituted anilines (e.g., 4-IsPrAN and 3-MeAN) approached complete conversion at 10:1 mole ratio, the halogen substituted anilines lagged behind in terms of % conversion, and especially the disubstituted 3,4-DiClAN. This may be explained by the

52
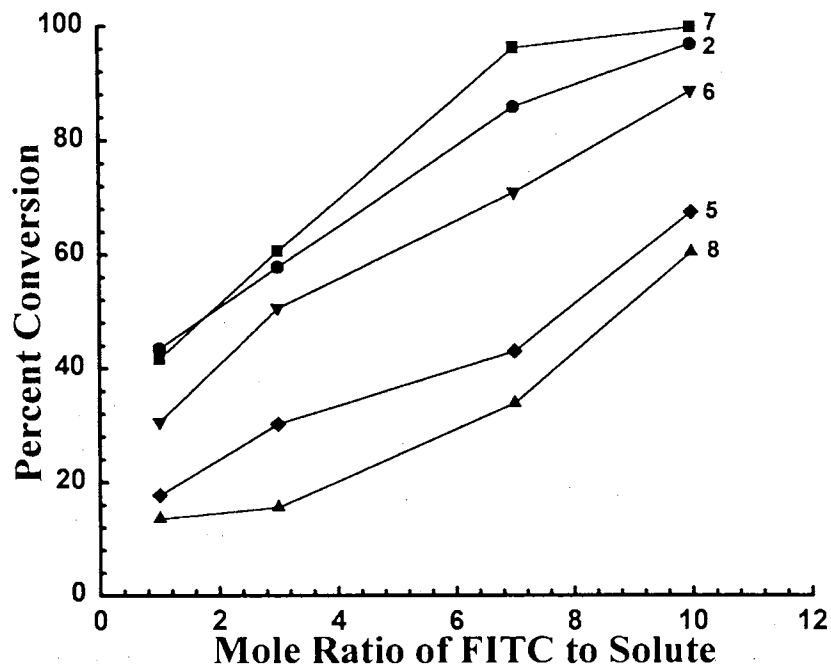
Figure 3. Plots of the percent conversion of analyte to the FITC derivative. Conditions as in Fig. 1. Analytes: 2, FITC-3-MeAN; 5, FITC-3-ClAN; 6, FITC-3-Cl-4-MeAN; 7, FITC-4-IsPrAN; 8, FITC 3,4-DiClAN.

inductive electron-withdrawing effect of chlorine, which is caused by its relatively high electronegativity. This inductive effect makes the nitrogen less nucleophilic and consequently less reactive toward electrophiles.[24] On the other hand, alkyl groups are classified as activating groups because of their electron repelling effect, which makes the nitrogen of aniline more nucleophilic thus promoting electrophilic attack.[24] This trend is substantiated by the behavior of 3-Cl-4-MeAN, which shows a lesser conversion than the alkyl substituted anilines (e.g., 3-MeAN, 4-IsPrAN) but a higher conversion than the strictly halogenated aniline (i.e., 3,4-DiClAN). The % conversion of a given aniline solute to its FITC derivative was determined by CZE analysis (as in the preceding

section) of two aliquots of the given aniline at the same solute concentration where one of the underivatized aliquot to the peak area of the analyte obtained on the electropherogram of the derivatized aliquot permitted the determination of the % of remaining underivatized analyte and in turn the % conversion.

The measurement of percent conversion was essential for the determination of the exact LOD of the FITC-aniline derivatives. As can be seen in Table 2, the FITC derivatization allowed the sensitive LIF detection of anilines and yielded LODs in the 10^{-10} M level. The LOD values were measured from successive dilution of a derivatization reaction involving 1:1 mole ratio of tag to analyte. The concentration of analytes in the most diluted reaction mixture were 1.0×10^{-9}, 2.0×10^{-9}, 1.0×10^{-9}, 2.5×10^{-9} and 2.8×10^{-9} M for 4-IsPrAN, 3-MeAN, 3-Cl-4-MeAN, 3-ClAN and 3,4-DiClAN, respectively. The LODs reported in Table 2 were obtained by multiplying the analyte concentration in the most dilute mixture by the % conversion. The LODs correspond roughly to 5 orders of magnitude lower than in the UV of underivatized anilines. The LOD was approximated when a signal-to-noise ratio of 3 to 1 was achieved. LIF detection lowered the LOD by 20,000 fold for 3,4-DiClAN to as much as 95,000 fold for 4-IsPrAN.

Our interest was to demonstrate the feasibility of derivatization at trace levels, namely at the LOD. In addition, our interest was also to be able to perform the derivatization at the LOD level in real water such as tap and lake water. As stated above the LOD as reported directly to the concentration of underivatized analytes was on the order of 1.0 to 2.8×10^{-9} M. By spiking the various waters with three different anilines at 8.9×10^{-9} M, which is about 3 times more concentrated than the LOD, the derivatization was readily achieved when the mole ratio of FITC to analyte was set at 100:1, see Fig. 4. For details of the derivatization at very near the LOD (i.e., 8.9×10^{-9} M in underivatized analyte) in deionized water, and in real water, see experimental section. It should be mentioned that using a very large excess of FITC (100 times more than the analyte) when derivatizing at the LOD concentration level, the amount of FITC degradation and side
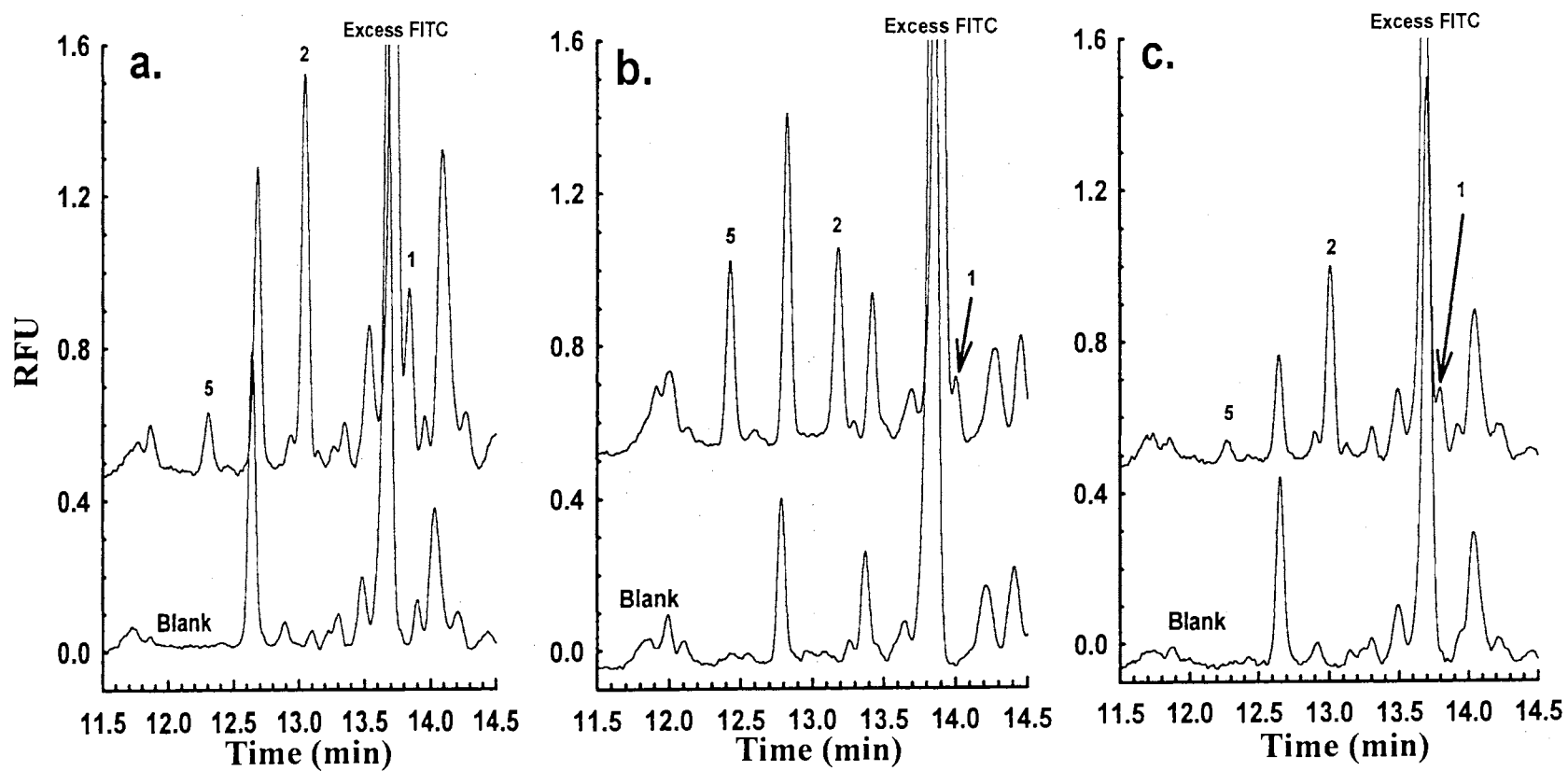
Figure 4. Electropherograms of FITC derivatization of 3 anilines at 8.9 x 10^{-9} M in deionized water (a), tap water (b) and lake water (c) matrices. Running electrolyte, 400 mM borate titrated to pH 9.0 with sodium hydroxide containing 40 mM OG; applied voltage, 25 kV. Other conditions as in Fig. 1. Analytes: 1, FITC-AN; 2, FITC-3-MeAN; 5, FITC-3-ClAN.

products increased, see Fig. 4. Lau and co-workers describe the possible degradation and side products for FITC derivatization.[25] It should be mentioned that the purity of FITC is 90% by HPLC as certified by the supplier. In other words, some of the peaks in the electropherograms shown in Fig. 4 could be simply those of the impurities of the FITC tag. The major peak in Fig. 4 eluting at ca. 13.7 to 13.8 min is that of excess FITC. The derivatization in deionized water produced the strongest signal for FITC-3-MeAN and for FITC-AN (Fig. 4a). The derivatization done in tap water gave the overall strongest signal from 3-ClAN (Fig. 4b). The derivatization did prove to be successful at 8.9×10^{-9} M with the lake water matrix, however the signal exhibited by FITC-3-ClAN was relatively weak (Fig. 4c). As shown in Fig. 4, the derivatization can be achieved directly in real water without extensive sample clean up. The real water samples were only cleaned from microparticles by filtration through 0.2 μm filters. The tap and lake water gave more or less the same blank signal as that of deionized water.

MECC of FITC Derivatives

In a recent article by He et al.[26] on the precolumn derivatization of peptides with FITC and subsequent separation by capillary electrochromatography in a microfabricated system, it was reported that FITC-peptide derivatives yielded higher fluorescence at alkaline pH than at acidic pH. This finding provided the rationale to evaluate the in situ charged micelles, which are based on the complexation of glycosidic surfactants with borate at alkaline pH, in the separation of FITC-aniline derivatives. As stated in the introduction, in situ charged micelles were recently introduced from our laboratory[17-21, 27, 28], and proved useful in the MECC of a wide range of species.[29-31]

Figure 5 shows the separation of the FITC-aniline derivatives at alkaline pH in the presence or absence of OG. The electropherogram in Fig. 5a was obtained with a running

Figure 5. Electropherograms of FITC tagged anilines. Running electrolytes, 300 mM boric acid titrated with NaOH to pH 10.0 (a) and containing 25 mM OG in (b) 30 mM OG in (c) and 40 mM OG in (d); applied voltage, 25 kV. Other conditions as in Fig. 1. Analytes: 1, FITC-AN; 2, FITC-3-MeAN; 3, FITC-4-ClAN; 4, FITC-4-BrAN; 5, FITC-3-ClAN; 6, FITC-3-Cl-4-MeAN; 7, FITC-4-IsPrAN; 8, FITC-3,4-DiClAN.

electrolyte consisting of 300 mM sodium borate, pH 10.0, while the electropherograms in

Fig. 5b, c and d were obtained with electrolytes consisting again of 300 mM sodium

borate, pH 10.0, but at 3 different OG concentrations. In the absence of OG (Fig. 5a), the FITC-aniline derivatives eluted in the order of alkyl substituted anilines, aniline and halogen substituted anilines, indicating that the dissociation of the weak phenolic acid group of the FITC moiety increases in the order of alkyl substituted anilines < aniline < halogen substituted anilines. This order of phenolic group ionization can be attributed to the induction effect of halogens. In fact, 3,4-DiClAN eluted last. Upon adding 25 mM OG to the running electrolyte (Fig. 5b), a significant change in the migration order was observed and an improvement in the overall separation was obtained. This is despite the fact that 25 mM OG is about the critical micellar concentration (CMC) of the surfactant in pure water, and therefore the amount of micellized surfactant concentration is negligible. This may indicate that the monomeric OG-borate complex associated with the various FITC-aniline derivatives. The migration order of the FITC-anilines in the presence of OG-borate surfactant is the result of the interplay of nonpolar association and electrostatic repulsion between analyte and surfactant molecules of same electric charges. Increasing the OG concentration to 30 and 40 mM as in Fig. 5c and 5d brought about the realization of MECC separation systems, and further change in migration order was observed. As can be seen in Fig. 5, increasing the OG concentration from 25 to 30 mM brought about dramatic changes in selectivity (compare Fig. 5b to 5c) and this selectivity did not undergo significant change as the OG concentration was increased from 30 to 40 mM (compare Fig. 5c to 5d).

Similar trends were observed with the NG surfactant, see Fig. 6. At 8 mM NG in the running electrolyte, which is very near the surfactant's CMC (CMC = 6.5 mM in pure water), the migration profile of the FITC derivatives was very close to that obtained with 25 mM OG with a noticeable difference in the migration time: the derivatives migrate faster in the presence of NG than OG. At 8 mM NG, the micellized surfactant concentration is about 1.5 mM while at 25 mM OG, the micellized surfactant concentration is negligible. The presence of 1.5 mM surfactant in the form of NG-borate
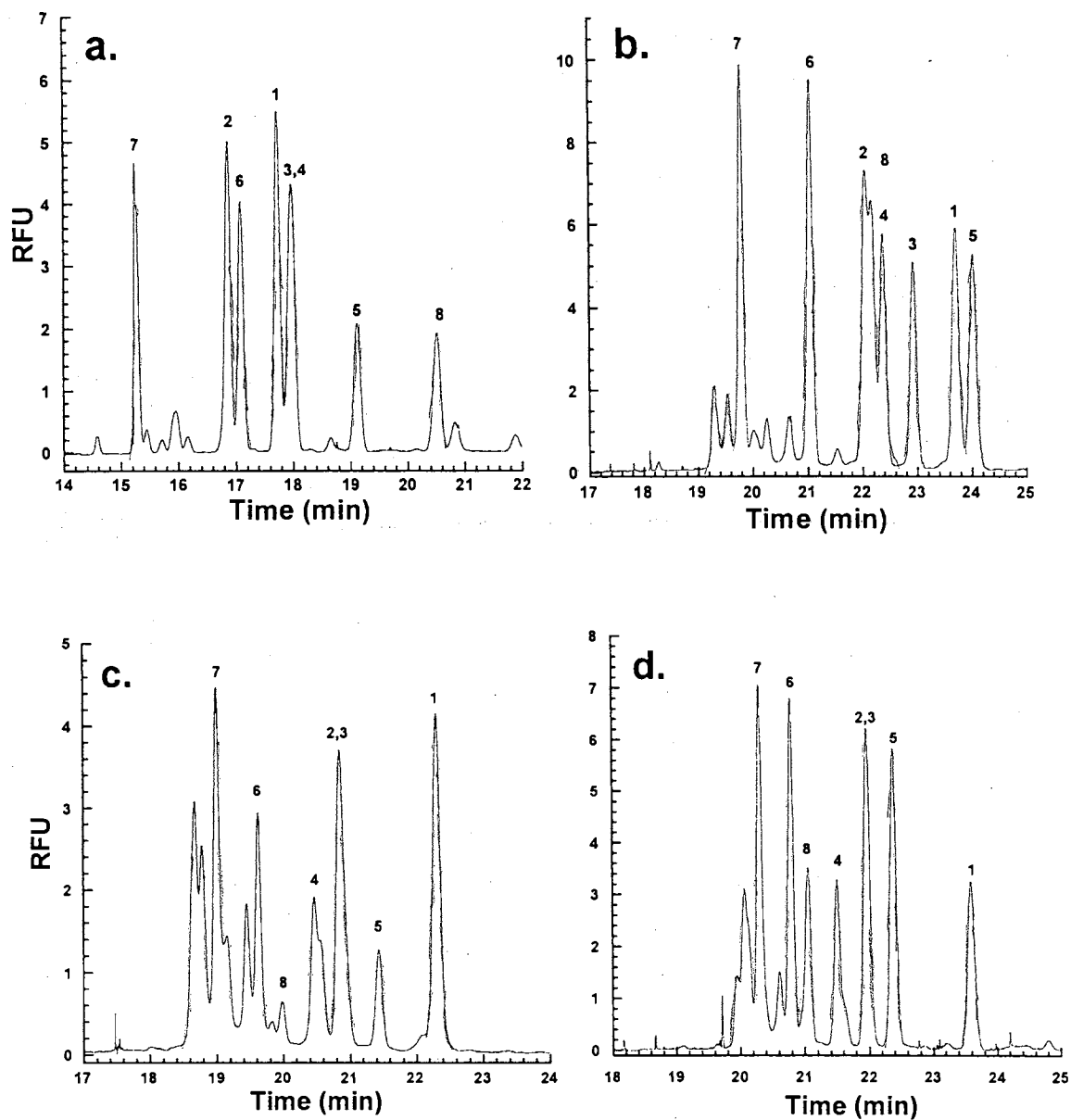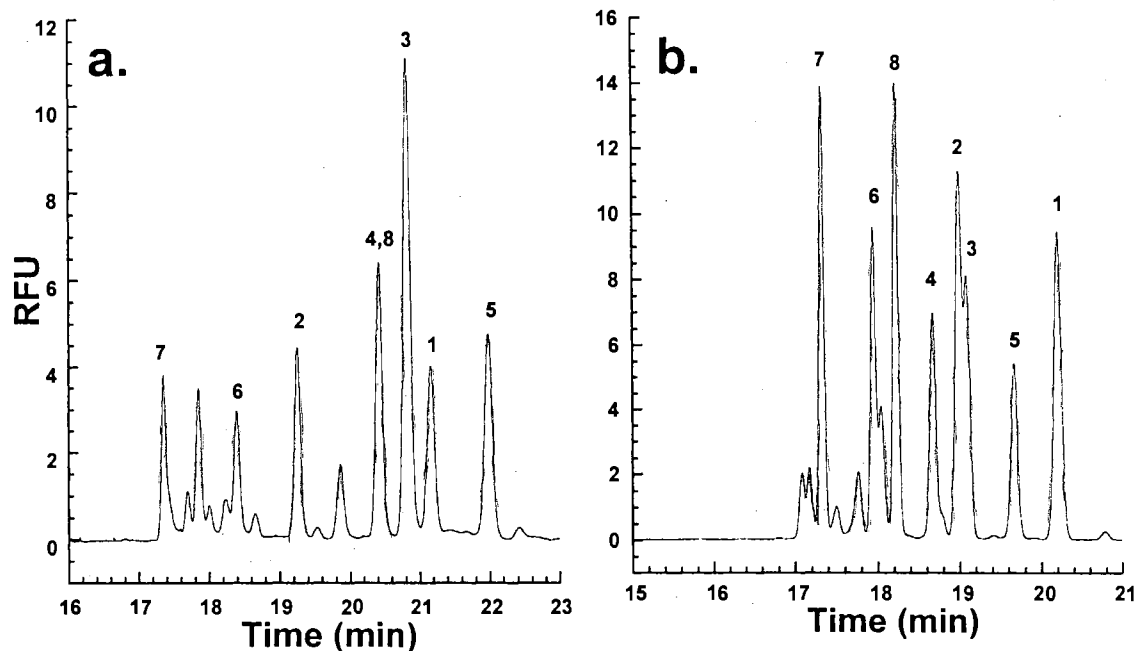
Figure 6. Electropherograms of FITC tagged anilines. Running electrolytes, 300 mM boric acid titrated with NaOH to pH 10.0 and containing 8 mM NG in (a) and 15 mM NG in (b); applied voltage, 25 kV. Other conditions as in Fig. 1 and peak assignments as in Fig. 5.

micelles may explain the faster migration obtained with 8 mM NG. Increasing the NG concentration from 8 to 15 mM resulted in dramatic change in the selectivity as when the OG surfactant concentration was increased from 25 to 40 mM, and the migration profile at 15 mM NG was about the same as that obtained with 40 mM OG. But, again the derivatives migrate faster with NG than with OG indicating stronger interaction with the NG-borate micelle than with the OG-borate micelle despite the fact that the micellized surfactant concentration with 40 mM OG is 15 mM versus 8.5 mM in the case of 15 mM NG. This may be attributed to the presence of one extra methylene group in the alkyl tail of NG.

59
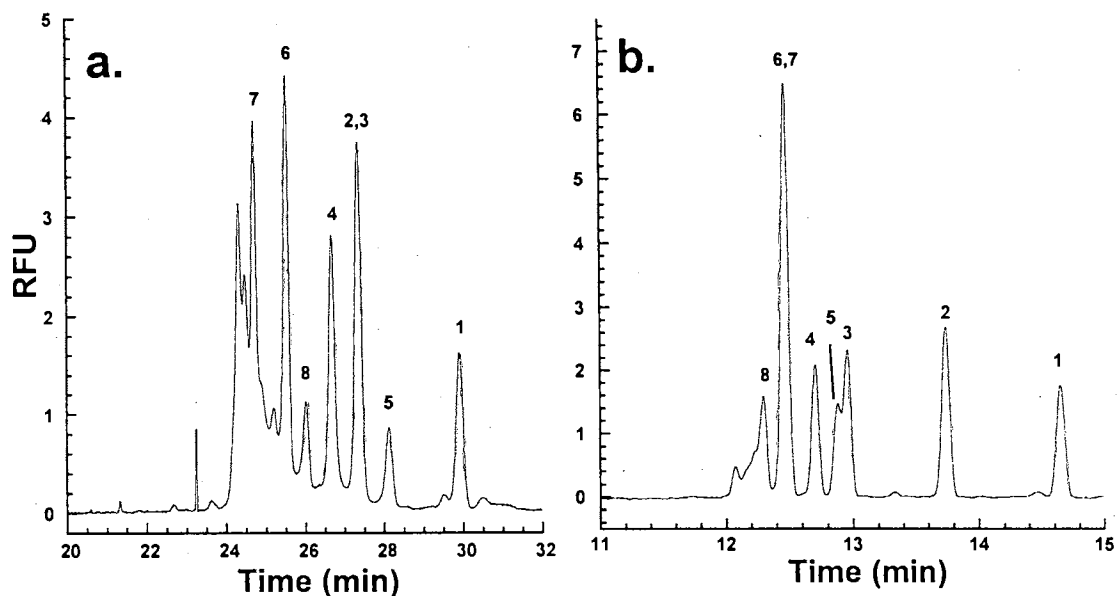
Figure 7. Electropherograms of FITC tagged anilines. Running electrolytes, 400 mM boric acid titrated with NaOH to pH 10.0 in (a) and pH 9.0 in (b) and containing 40 mM OG; applied voltage, 25 kV. Other conditions as in Fig. 1 and peak assignments as in Fig. 5.

Increasing the borate concentration at constant OG concentration and constant pH resulted only in a longer migration time for the FITC-aniline derivatives (compare Fig. 5d to Fig. 7a) without causing a significant change in selectivity. This is because at elevated borate concentration the surface charge density of the OG-borate micelle increases due to increasing OG-borate complexation. Also, increasing the borate concentration corresponds to increasing the ionic strength thus causing an increase in the electrolyte viscosity and a decrease in the thickness of the electric double layer with a net result of decreasing the EOF. On the other hand, decreasing the pH of the running electrolyte resulted in faster migration time for the FITC derivatives with dramatic change in selectivity (compare Fig. 7a to Fig. 7b) as manifested by changes in migration order of

the FITC-aniline derivatives.   As expected, decreasing the pH yields a decrease in the OG-borate complex formation and in turn the surface charge density of the in situ charged micelle.   Also, the weak phenolic acid group of the FITC-aniline derivatives may be less dissociated at pH 9.0 than at pH 10.0. The two combined effects would explain the speeding of the migration as the pH is decreased.   Furthermore, these two effects explain the change in the migration order as a result of change in the degree of association/repulsion between solutes and OG-borate micelles as the pH was changed. In all cases, AN-FITC seems to be the least interactive with the micelle, thus migrating slower than those interacting strongly with the micelle such as 3,4-DiClAN-FITC, 4-IsPrAN-FITC and 3-Cl-4-MeAN-FITC.

Conclusions

We have demonstrated the FITC precolumn derivatization of aniline pesticidic metabolites in deionized and real waters at the LOD concentration level. Besides filtration from microparticles, the derivatization in real waters spiked with trace amounts of anilines did not require extensive sample clean-up. The fluorescent signals of the FITC derivatives were not affected by possible interferents in the water samples due to the selectivity of the precolumn derivatization and the LIF detection. The matrices of the waters used in this study (i.e., tap and lake water) showed minor effects on the extent of solute derivatization with FITC at the LOD level.   These results are encouraging and should be regarded as a solid precedent for other precolumn derivatization in real waters and subsequent separation and detection by CE-LIF. The in situ charged micelles used in the CE separation of the FITC-aniline derivatives yielded unique selectivity and afforded the sensitive detection at alkaline pH.

References

1. Karcher, A.; El Rassi, Z., *Electrophoresis* **1999**, *20*, 3280-3296.

2. El Rassi, Z., *Electrophoresis* **1997**, *18*, 2465-2481.

3. Aga, D.S.; Heberle, S.; Rentsch, D.; Han, R.; Mueller, S.R., *Environ. Sci. Technol.* **1999**, *33*, 3462-3468.

4. Kubilius, D.T.; Rodney, J., *J. Chromatogr. A* **1998**, *793*, 349-355.

5. Stutz, H.; Pitterschatscher, K.; Malissa Jr., H., *Mikrochim. Acta* **1998**, *128*, 107-117.

6. Karcher, A.; El Rassi, Z., *Electrophoresis* **2000**, *21*, 2043-2050.

7. De Bertrand, N.; Barcelo, D., *Anal. Chim. Acta* **1991**, *254*, 235-244. ·

8. Fielding, M.; Barcelo, D.; Helweg, A.; Galasi, S.; Torstenson, L.; Van Zoonen, P.; Wolter, R.; Angeletti, G., *Pesticides in Ground Drinking Water.* **1992**, Brussels: Commission of the European Communities. 136.

9. Munch, D.J.; Frebis, C.P., *Environ. Sci. Technol.* **1992**, *26*, 921-925.

10. Munch, D.J.; Graves, R.L.; Maxey, R.A.; Engel, T.M., *Environ. Sci. Technol.* **1990**, *24*, 1446-1462.

11. Feng, L.; Wang, L.-S.; Zhao, Y.-H.; Song, B., *Chemosphere* **1996**, *32*, 1575-1583.

12. van Gestel, C.A.M.; Adema, D.M.M.; Driven-van Breman, E.M., *Water, Air, Soil Pollut.* **1996**, *88*, 119-132.

13. Hatrik, S.; Tekel, J., *J. Chromatogr. A* **1996**, *733*, 217-233.

14. Hilmi, A.; Luong, J.H.T.; Nguyen, A.-L., *Chemosphere* **1998**, *36*, 3137-3147.

15. Li, J.; Fritz, J.S., *J. Chromatogr. A* **1999**, *840*, 269-279.

16. Brimley, W.C.; Jones, W.J., *J. Chromatogr. A* **1994**, *680*, 163-173.

17. Cai, J.; El Rassi, Z., *J. Chromatogr. A* **1992**, *608*, 31-45.

18. Smith, J.T.; El Rassi, Z., *J. Chromatogr. A* **1994**, *685*, 131-143.

19. Smith, J.T.; El Rassi, Z., *Electrophoresis* **1994**, *15*, 1248-1259.

20. Smith, J.T.; El Rassi, Z., *J. Microcol. Sep.* **1994**, *6*, 127-138.

21. Smith, J.T.; Nashabeh, W.; El Rassi, Z., *Anal. Chem.* **1994**, *66*, 1119-1133.

22. Smith, J.T.; El Rassi, Z., *J. Capil. Elect.* **1994**, *1*, 136-143.

23. Lunn, G.; Hellwig, L.C., *Handbook of Derivatization Reactions for HPLC*. **1998**, New York: John Wiley & Sons.

24. Baker, A.D.; Engel, R., *Organic Chemistry*. **1999**, St. Paul: West Publishing.

25. Lau, S.K.; Zaccardo, F.; Little, M.; Banks, P., *J. Chromatogr. A* **1998**, *809*, 203-210.

26. He, B.; Ji, J.; Regnier, R.E., *J. Chromatogr. A* **1999**, *853*, 257-262.

27. Mechref, Y.; El Rassi, Z., *J. Chromatogr. A* **1996**, *724*, 285-296.

28. Mechref, Y.; Smith, J.T.; El Rassi, Z., *J. Chromatogr. A* **1995**, *18*, 3769-3786.

29. Karcher, A.; El Rassi, Z., *J. Liq. Chromatogr. Rel. Technol.* **1998**, *21*, 1411-1432.

30. Karcher, A.; Melouk, H.A.; El Rassi, Z., *J. Agric. Food Chem.* **1999**, *47*, 4267-4274.

31. Tegeler, T.; El Rassi, Z., *J. AOAC* **1999**, *82*, 1542-1549.

32. Perrin, D.D.; Dempsy, B.; Serjeant, E.P., *pKa Prediction for Organic Acids and Bases*. **1981**, London: Chapman and Hall.

33. Chollet, M.; Legouin, B.; Burgot, J.L., *J. Chem. Soc. Perkin Trans.* **1998**, *2*, 2227-2231.

34. Hanai, T.; Koizumi, K.; Kinoshita, T., *J. Liq. Chromatogr. Rel. Technol.* **2000**, *23*, 363-385.

CHAPTER III

SURFACTANT-MEDIATED ELECTROKINETIC CAPILLARY CHROMATOGRAPHY OF ANILINE PESTICIDIC METABOLITES DERIVATIZED WITH 9-FLUORENYLMETHYL CHLOROFORMATE AND THEIR DETECTION BY LASER-INDUCED FLUORESCENCE*

Introduction

Amino compounds such as anilines can be converted to fluorescent derivatives through a variety of precolumn derivatization reactions; for recent reviews on the derivatization of amino compounds for CE analysis see References 1 and 2. In order to complement our contribution to the CE analysis of anilines, which are very important environmental pollutants (see preceding chapter, Ref. 3), it was imperative to consider another fluorescent tag that will confer the anilines different characteristics in terms of separation and detection by CE. In the preceding chapter, the anilines were derivatized with fluorescein isothiocyanate (FITC), which converted the analytes into acidic compounds, thus allowing their separation over a wide range of electrolyte composition by capillary zone electrophoresis (CZE) as well as by micellar electrokinetic capillary chromatography (MECC). In addition, the FITC-anilines were readily detected by laser-

induced fluorescence (LIF) at the 10^{-10} M level when excited with an argon ion laser at 488 nm. However, the FITC derivatization requires relatively long reaction time and yields degradation and side products.[4] In the present chapter, the anilines were derivatized with 9-fluorenylmethyl chloroformate (FMOC) to yield the fluorescent FMOC-anilines. The advantages of FMOC derivatization include very short reaction time (1 min or less), high yield (i.e., reaction goes to near completion) and simplicity.[1,2,5,6] These features should promote automation and consequently facilitate the analysis of a large number of samples in reasonably short time. In addition, the FMOC derivatization yields neutral derivatives of relatively strong hydrophobic characters, which should allow the use of hydro-organic electrolyte systems and in turn different selectivity. In fact, and as will be shown below, the FMOC-anilines derivatives were best electrophoresed when a surfactant-mediated electrokinetic capillary chromatography (SM-EKC) system was used. The SM-EKC system is based on sodium dioctyl sulfosuccinate (DOSS)/acetonitrile (ACN) mixtures in buffered electrolytes originally introduced by Shi and Fritz in 1995 for the separation of neutral polyaromatic compounds.[7] This SM-EKC system was further characterized with alkylphenylketone homologous series as typical models of neutral solutes.

<div align="center">

Description of the Surfactant-Mediated Electrokinetic
Capillary Chromatography System

</div>

The SM-EKC system illustrated in Fig. 1a consists of electrolytes based on the DOSS surfactant at various ACN content (see Fig. 1b for structure of DOSS). The accurate chemical name of DOSS is in fact sodium di-2-ethylhexyl sulfosuccinate. At the ACN concentration used in this study (20% or greater), it is well established that micelle formation is inhibited and consequently the DOSS surfactant dissolves primarily as monomers.[8] The inhibitory effect of ACN on micellization is based on the reduction
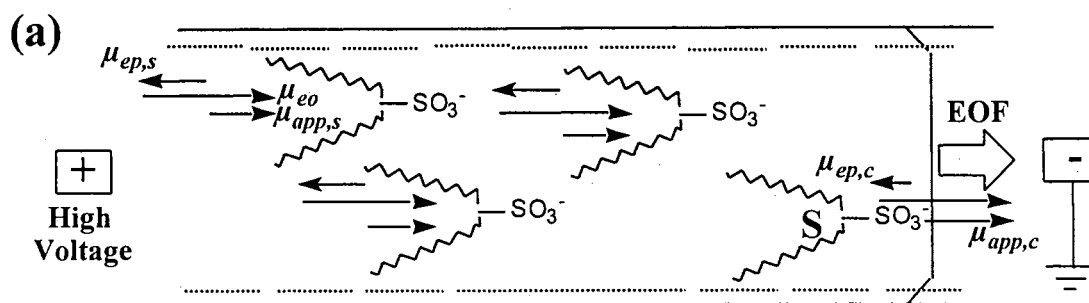
$\mu_{ep,s}$: electrophoretic mobility of the surfactant; μ_{eo}: electroosmotic mobility; $\mu_{app,s}$: apparent mobility of the surfactant; $\mu_{ep,c}$: electrophoretic mobility of the solute-surfactant complex; $\mu_{app,c}$: apparent mobility of the solute-surfactant complex; S: solute
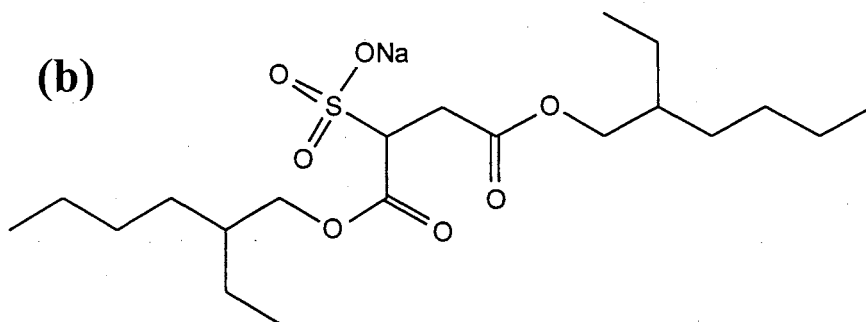
Figure 1. (a) Schematic illustration of the separation principles in the SM-EKC system under investigation. (b) Structure of the DOSS surfactant.

of the dielectric constant of the aqueous phase by the organic solvent which would cause increased mutual repulsion of the ionic heads in the micelle, thus opposing micellization. The FMOC-anilines are quite hydrophobic compounds of low water solubility requiring such electrolyte systems to allow their separation by capillary electrophoresis. While the organic modifier is to permit the solubilization of the FMOC-anilines, the DOSS is to associate with these solutes and to impart them with the charge necessary for their differential migration and eventually separation. This is shown in the following equation:

$$\mu_{eff,ep} = f_c \mu_{ep,c} \qquad (1)$$

where $\mu_{eff,ep}$ is the effective electrophoretic mobility of the solute and f_c is the mole fraction of DOSS-solute complex whose electrophoretic mobility is $\mu_{ep,c}$. The neutral FMOC-aniline (or any other neutral solute) will acquire the electrophoretic mobility of the complex when f_c approaches 1, i.e., when the solute associates intimately with the DOSS surfactant. Thus, the stronger the association of the solute with the DOSS surfactant the higher the effective electrophoretic mobility of the solute and vice versa.

The DOSS surfactant belongs to the branched type of surfactants where the polar head group occupies a central position in the hydrophobic chain which in this case is made up of two 2-ethylhexyl branches, see Fig. 1b. In general, the critical micellar concentration (CMC) of a branched surfactant is higher than the CMC of an unbranched surfactant (i.e., all carbon atoms are in the same tail) having the same number of carbon atoms.[8] In fact, in pure water, DOSS has a relatively high CMC of 2.5 mM at room temperature[9] when compared to the CMC of sodium hexadecyl sulfonate ($C_{16}H_{33}SO_3^-$ Na^+), which is 0.7 mM in pure water at 50 °C.[8] The DOSS surfactant yielded cloudy solutions when dissolved in aqueous electrolyte solutions such as the ones used in the present study (i.e., 8 mM sodium borate, pH 8.5) at concentrations higher than 2.5 mM. Thus was the necessity of adding an organic modifier, e.g., ACN to allow the inclusion in the running electrolyte of a useful DOSS concentration for achieving the separation of FMOC-anilines.

<div align="center">Materials and Methods</div>

Reagents and Materials

See Chapter II for the model aniline analyte purchases (see Table 1 of Chapter I for structures). The alkyl phenyl ketones, acetophenone, propiophenone, butyrophenone, valerophenone, hexanophenone and heptanophenone were also purchased from Aldrich. The DOSS was also purchased from Aldrich. HPLC grade ACN and boric acid were obtained from Fisher (Fairlawn, NJ, USA). The derivatizing agent FMOC was purchased

from Sigma Chemical Co. (St. Louis, MO, USA). Sodium hydroxide, potassium hydroxide, and sodium borate were obtained from EM Science (Cherry Hill, NJ, USA).

CE Instruments

For UV absorbance detection instrumentation see Chapter II. Between runs, the capillary was rinsed with distilled water, 1.0 M KOH, distilled water, and running electrolyte for 4, 6, 4, and 3 min, respectively. LIF measurements were performed in Dr. H. Issaq laboratories at NCI-Frederick Cancer Research and Development Center, Frederick, MD, USA. LIF excitation was provided by a solid-state UV laser operating at 266 nm (NanoUV-266, Uniphase, San Jose, CA, USA). A 5 mm diameter best-form lens was used to focus the laser beam onto the separation capillary. Fluorescence was collected at a 90° angle from the excitation beam with a UV-grade, 10X microscope objective (Carl Zeiss, Thornwood, NY, USA). The collected emission was detected by a photomultiplier tube (PMT, Oriol, Stratford, CT, USA). A 310 nm-band pass filter was used to reduce fluorescence background. The PMT current was monitored by a picoammeter (Keithley, Cleveland, Ohio, USA) and its voltage output was displayed on a PC computer via an A/D interfacing module (Beckman Instruments, Fullerton, CA, USA). CE was performed with a Crystal 310 CE module (ATI/Unicam, Boston, MA, USA). Separation was carried out at room temperature and 18 kV with 50 μm x 60 cm (57 cm to detector) fused-silica capillary (Polymicro Technologies, Phoenix, AZ, USA). Samples were injected by pressure (30 mbar) for 6 s. The separation buffer consisted of 50 mM DOSS, 8 mM sodium borate (pH 8.5) and 40% ACN (v/v) for the LIF study.

Precolumn Derivatization

The aniline pesticidic metabolites were tagged by dissolving the analytes at a concentration of 1.0×10^{-2} M in HPLC grade ACN. A 150 μL aliquot of each of these analyte solutions was then pipetted into 350 μL of ACN and 500 μL of 10 mM FMOC also dissolved in ACN. This brought the final concentration of analyte to 1.5 mM and the

derivatizing agent to 5 mM. After brief stirring for a few minutes, these samples were subsequently diluted and used for further sample injections for the electropherograms generated under the various operating conditions. This derivatization was also used for determining the LOD by successive dilution.

FMOC derivatization in lake water spiked with anilines (namely, AN, 3-MeAN and 3-ClAN) at a concentration at the level of the UV absorbance limit of detection was carried out as follows. Lake water was first buffered with 5 mM sodium borate, pH 9.5. The buffered water was then mixed with ACN at 1:1 ratio (v/v) to allow the dissolution of FMOC at relatively large excess in the reaction mixture and consequently secure the rapid derivatization of the dilute analytes. The water/ACN (1:1 v/v) was spiked with anilines at 5.0×10^{-6} M by diluting a 50 μL aliquot of 1.0×10^{-2} M analytes dissolved in HPLC grade ACN in a 100 mL volumetric flask with the lake water/ACN (1:1). A 1-mL sample of this spiked water solution was then pipetted into an amber vial to which 60 μl of 50 mM FMOC were then added. This brings the final concentration of each analyte to 4.7×10^{-6} M and the mole ratio of tag to analyte to 100 to 1. This large FMOC excess was necessary to promote the reaction of tag with the given analyte to form the corresponding FMOC derivative.

Results and Discussion

MECC of FMOC-anilines

As a starting point in separating the neutral FMOC-anilines, the in situ charged micellar system based on glycosidic surfactant-borate complex, which was described in the preceding chapter for the separation of FITC-anilines,[3] was first evaluated in the separation of FMOC-anilines. The OG-borate micellar system did not resolve the FMOC-anilines and the analytes coeluted toward the migration time of the micelle. This fact excluded any attempt to evaluating SDS in separating the FMOC-anilines. Previously, we have shown that the in situ OG-borate micelle provided more equitable
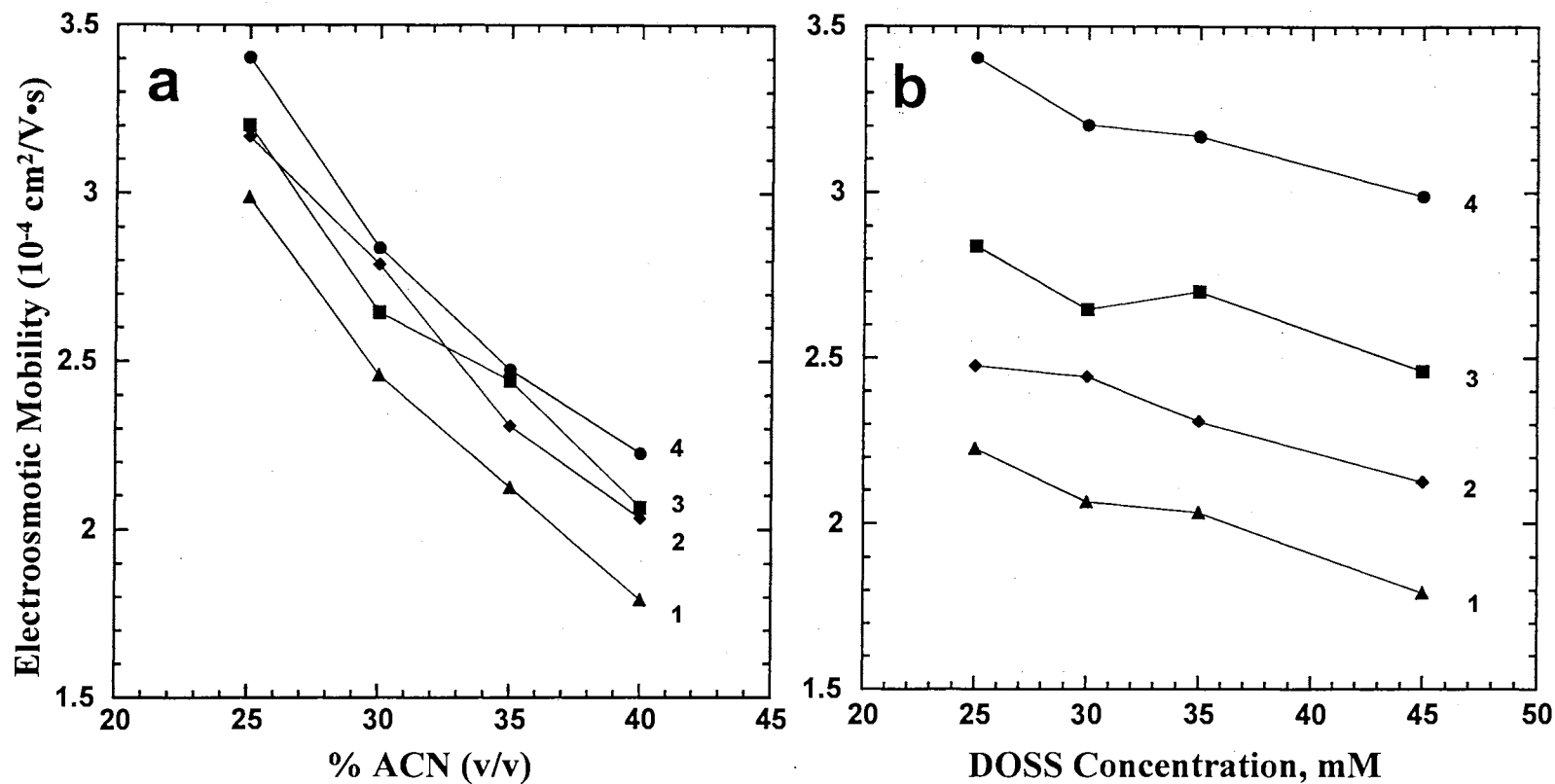
Figure 2. (a) Plots of electroosmotic mobility versus %ACN (v/v) and (b) versus DOSS concentration in the running electrolyte. Capillary, fused-silica, 50 cm/57 cm x 50 μm I.D.; electrolytes: (a) 45 mM DOSS (curve 1), 35 mM DOSS (curve 2), 30 mM DOSS (curve 3) and 25 mM DOSS (curve 4) at various %ACN (v/v); (b) 40% ACN (curve 1), 35 % ACN (curve 2), 30% ACN (curve 3) and 25% ACN (curve 4) at various DOSS concentration; background buffer, 8 mM sodium borate, pH 8.5; running voltage, 18 kV.

partitioning of solutes between the aqueous phase and the micellar phase than that encountered with the traditional SDS micellar system.[10]

Unlike the FITC-aniline derivatives (see preceding chapter), the FMOC-aniline analytes are neutral compounds of relatively strong hydrophobic character, thus requiring the incorporation of charged monomeric hydrophobic selectors in the running electrolyte to bring about their differential migration in CE. In fact, and as will be shown below, the FMOC-anilines were separated by SM-EKC, namely in the presence of DOSS and ACN as the organic modifier (see Description of the SM-EKC System, pp 65-67). The amount of DOSS and % ACN were varied in order to determine the optimum separation conditions.

Evaluation of the DOSS/ACN Electrolyte Systems

The SM-EKC system under investigation was characterized at various DOSS concentration and ACN content with the FMOC-anilines as well as with alkyl phenyl ketone homologous series as typical models of neutral solutes. At a given surfactant concentration, e.g., at 25, 30, 35 or 45 mM DOSS, increasing the % ACN in the running electrolyte in the range studied decreased the magnitude of EOF, see Fig. 2a. Also, at a fixed % ACN in the running electrolyte, increasing the surfactant concentration yielded a decrease in the magnitude of the EOF. This is illustrated in Fig 2 b. These findings corroborate those reported earlier by Shi and Fritz.[7] While increasing the organic modifier content of the running electrolyte brings about a decrease in its dielectric constant, increasing the DOSS concentration yields an increase in electrolyte's viscosity and ionic strength. Thus, the net result of increasing the organic content or DOSS concentration in the running electrolyte is a decrease in the magnitude of EOF. Therefore, these two components are the major players in terms of manipulating speed and quality of separation with the DOSS/ACN electrolyte systems.
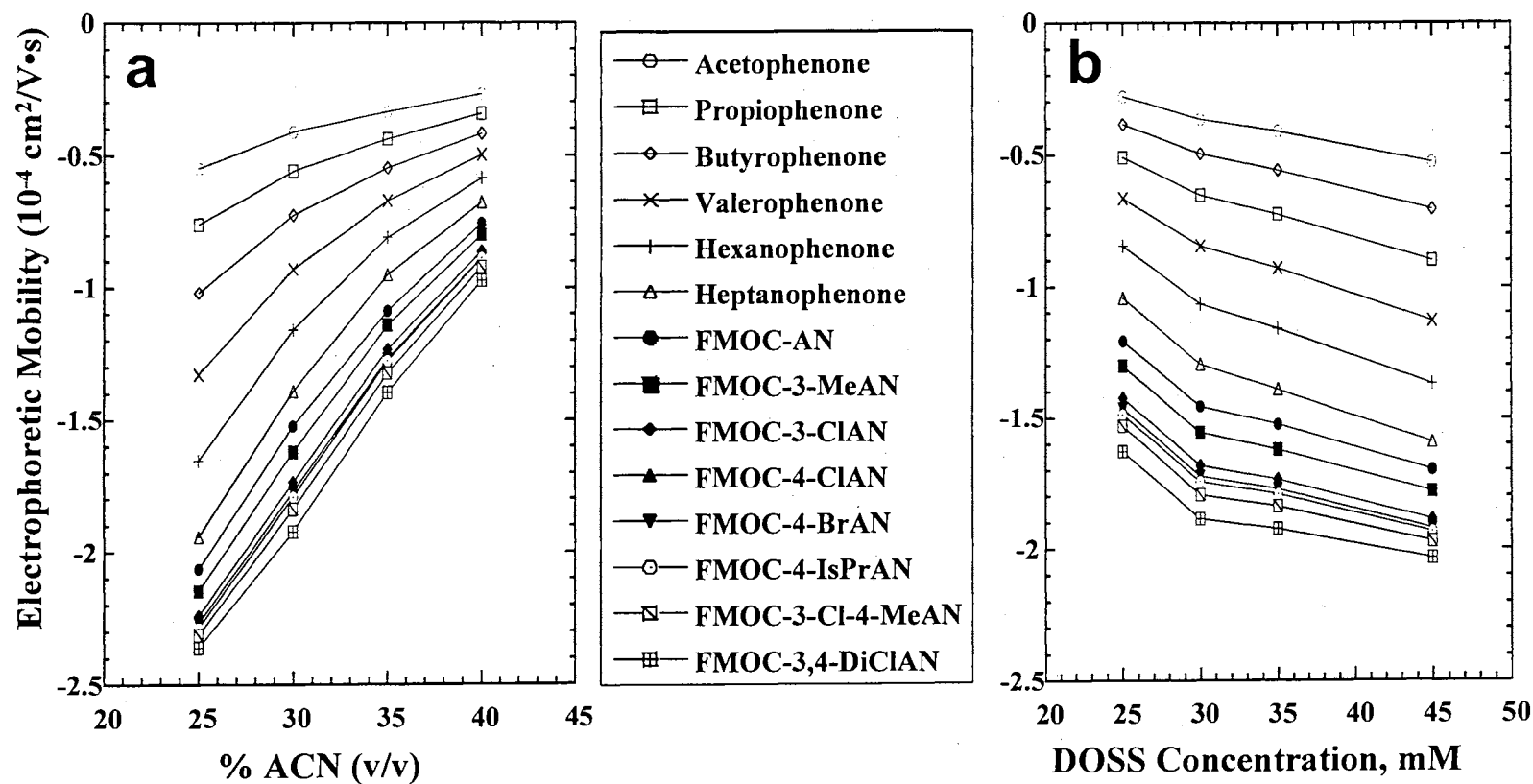
Figure 3. (a) Plots of solute's effective electrophoretic mobility versus %ACN (v/v) and (b) versus DOSS concentration in the running electrolytes. Electrolytes: (a) 35 mM DOSS in 8 mM sodium borate, pH 8.5, at various %ACN (v/v); (b) 30% ACN (v/v) in 8 mM sodium borate, pH 8.5, at various DOSS concentration. Other conditions are the same as in Fig. 2.

As pointed out earlier (Description of SM-EKC System, pp 65-67), neutral solutes acquire an electrophoretic mobility, the so-called effective electrophoretic mobility, due to its association with the charged surfactant. At a given surfactant concentration, increasing the % ACN in the running electrolyte yielded a decrease in the effective electrophoretic mobility of each solute, see Fig 3a. This is due to decreasing solute-surfactant association and in turn f_c, see eq 1. On the other hand, at a given % ACN in the running electrolyte, increasing the DOSS concentration resulted in increasing the effective electrophoretic mobility of the solute as a result of increasing f_c, see Fig 3b and eqn 1.

Figure 4 illustrates the electropherograms of FMOC-anilines and alkyl phenyl ketones obtained with 35 mM DOSS and 40, 30 or 25% (v/v) ACN. At 40% (v/v) ACN, the FMOC derivatives of 4-ClAN, 4-BrAN and 4-IsPrAN coeluted, and the analysis time was below 26 min, see Fig. 4a. Decreasing the ACN content to 30 and 25% allowed the separation of FMOC-4-IsPrAN from the FMOC derivatives of 4-ClAN and 4-BrAN which still coalesced into a single peak. This is at the expense of a slightly longer analysis time of about 31 and 33 min at 30 and 25% (v/v) ACN, respectively. Although at constant DOSS concentration, the EOF increases with decreasing % ACN in the running electrolyte, the solute-DOSS association increases thus leading to a higher effective electrophoretic mobility of the solute, which then explains the increase in analysis time at lower % ACN in the running electrolyte. In all cases and as expected, the order of elution (i.e., selectivity) of FMOC-anilines with the DOSS/ACN electrolyte systems is significantly different from that observed for the FITC-anilines with OG-borate micellar systems.

Figure 5 shows the electropherograms of FMOC-anilines and alkyl phenyl ketones at 30% ACN (v/v) and 25, 30 or 45 mM DOSS in the running electrolyte. Increasing the DOSS concentration from 25 to 45 mM did not bring about the separation

Figure 4. Electropherograms of alkyl phenyl ketones and FMOC-anilines. Electrolytes: 35 mM DOSS in 8 mM sodium borate, pH 8.5, at (a) 40% ACN, (b) 30% ACN and (c) 25% ACN; column temperature, 20 °C. Other conditions as in Fig. 2. Analytes: 1, acetophenone; 2, propiophenone; 3, butyrophenone; 4, excess FMOC; 5, valerophenone; 6, hexanophenone; 7, heptanophenone; 8, FMOC-AN; 9, FMOC-3-MeAN; 10, FMOC-3-ClAN; 11, FMOC-4-ClAN; 12, FMOC-4-BrAN; 13, 4-IsPrAN; 14, FMOC-3-Cl-4-MeAN; 15, FMOC-3,4-DiClAN.

of FMOC-4-ClAN and FMOC-4-BrAN but increased the analysis time substantially by almost three fold, see Fig. 5.

FMOC Derivatization-Percent Conversion, Limits of Detection and Derivatization of Anilines at Low Concentrations in Lake Water

As with secondary and primary amino compounds,[11,12] the derivatization of anilines with FMOC yields stable carbamates. Other important properties of the FMOC-aniline derivatives are their relatively much higher UV absorbance and short labeling time when compared to FITC-aniline derivatives. In fact, FITC-anilines exhibited no absorbance signal in the UV even when injected from 10^{-2} M samples. As described in the Experimental, the FMOC derivatization was performed at a 3:1 mole ratio of tag to analyte, and the conversion was found to be highly quantitative at greater than 98%. The percent conversion of a given aniline solute to its FMOC derivative was determined by CZE as described in the case of FITC-anilines in the preceding chapter[3] using a running electrolyte of 50 mM sodium phosphate, pH 2.5, and an applied voltage of 18 kV.

As can be seen in Table 1, the FMOC derivatization of anilines allowed a more sensitive UV absorbance detection of the analytes and yielded LOD's in the 10^{-6} M level which is about 5 to 25 folds lower than the LOD's of underivatized anilines. The LOD achieved by LIF detection varied from 2.2 x 10^{-7} M for FMOC-3-Cl-4-MeAN to as low as 5.7 x 10^{-8} M for FMOC-AN. The LOD's obtained by LIF are about 330- to 2700-fold lower than the LOD's obtained by UV for underivatized anilines. In all cases, the LOD was approximated when a signal-to-noise ratio of 3 to 1 was achieved. As reported in Table 1, the LOD of FMOC-anilines by UV absorbance detection at 214 nm was on the order of 10^{-6} M as was obtained by successive dilution. By spiking the lake water with three different anilines (AN, 3-MeAN and 3-ClAN) at 4.7 x 10^{-6} M, which is about three times more concentrated than the LOD, the derivatization was readily achieved when the mole ratio of FMOC to analyte was set at 100:1, see Fig. 6. For details of the derivatization at very near the LOD (i.e., 4.7 x 10^{-6} M analyte) in lake water, see the
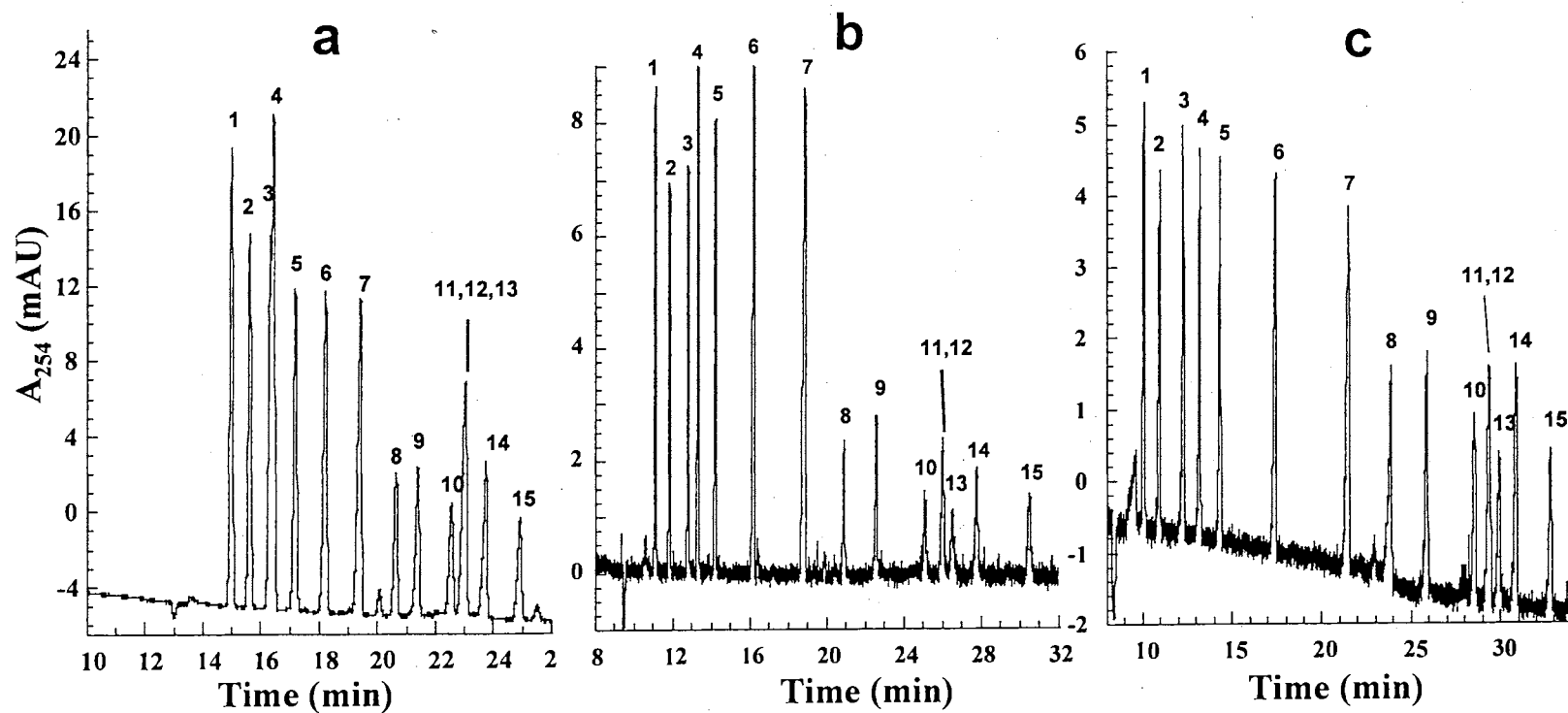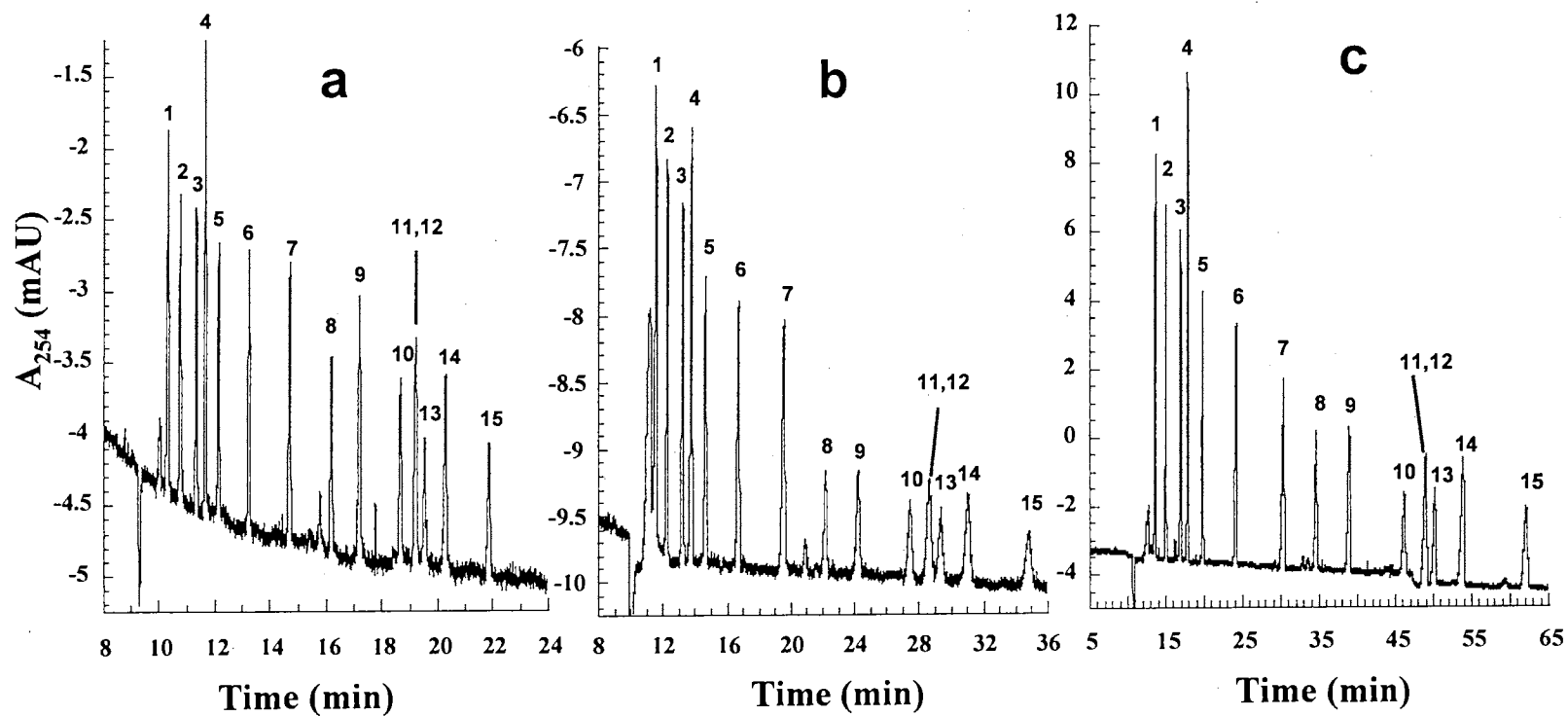
75

Figure 5. Electropherograms of alkyl phenyl ketones and FMOC-anilines. Electrolytes: 8 mM sodium borate, pH 8.5, at 30% ACN (v/v) and containing (a) 25 mM DOSS, (b) 30 mM DOSS and (c) 45 mM DOSS. column temperature, 20 °C. Other conditions as in Fig. 2. Analytes as in Fig 4.

TABLE 1.

LIMIT OF DETECTION OF DERIVATIZED AND UNDERIVATIZED
ANILINES BY UV ABSORBANCE AND LIF

Solute	LOD (M) of underivatized anilines	LOD (M) of FMOC-anilines	
	UV at 200 nm	UV at 214 nm	LIF
AN	NM	NM	5.7×10^{-8}
3-MeAN	2.0×10^{-5}	1.1×10^{-6}	7.4×10^{-8}
3-Cl-4-MeAN	8.0×10^{-6}	1.0×10^{-6}	2.2×10^{-7}
4-IsPrAN	4.0×10^{-5}	1.6×10^{-6}	NM
3-ClAN	9.0×10^{-6}	1.7×10^{-6}	2.7×10^{-7}
3,4-DiClAN	1.0×10^{-5}	1.2×10^{-6}	4.9×10^{-7}

NM = Not measured

experimental section. As shown in Fig. 6, the derivatization can be achieved directly in real world water matrices without extensive sample clean-up. The lake water sample was only cleaned from microparticles by filtration through 0.2 μm filters. Returning to Table 1, the LOD of FMOC-anilines by LIF was on the order of 10^{-7} to 10^{-8} M. Similar to the UV absorbance results, the FMOC derivatization was also readily achieved at near LOD ($\approx 5 \times 10^{-7}$ M).
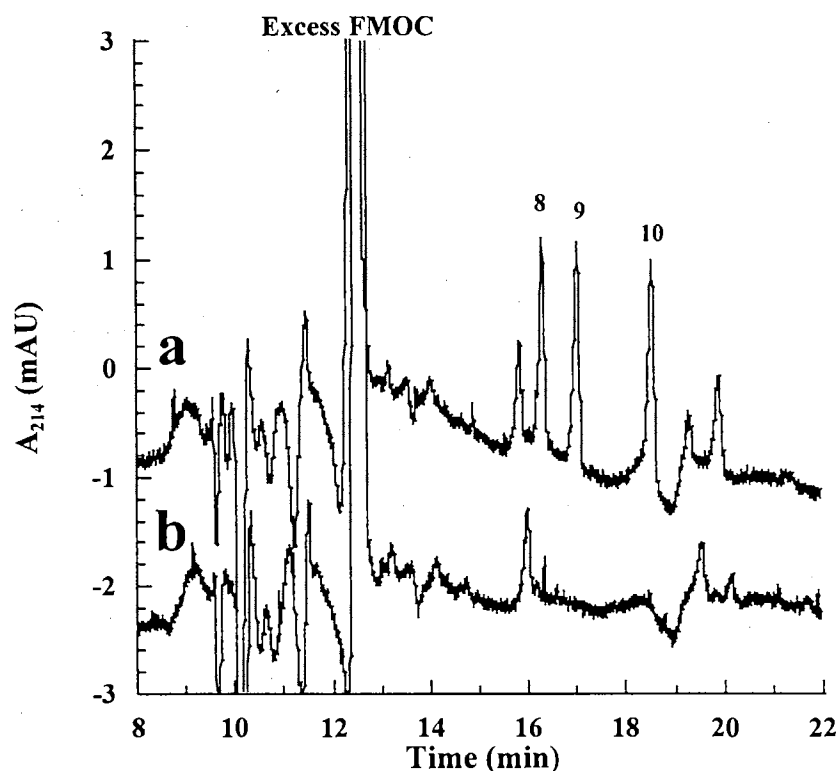
Figure 6. (a) Electropherograms of FMOC derivatization of 3 anilines at 4.7 x 10^{-6} M in lake water matrix, (b) blank. Electrolyte: 35 mM DOSS in 8 mM sodium borate, pH 8.5, at 40% (v/v) ACN; applied voltage, 25 kV; column temperature, 20 °C. Other conditions as in Fig. 2. Analytes: 8, FMOC-AN; 9, FMOC-3-MeAN; 10, FMOC-3-ClAN.

Conclusions

The derivatization of aniline pesticidic metabolites with FMOC was readily achieved in real water (e.g., lake water) at near LOD without extensive sample clean-up requiring only the removal of microparticles by microfiltration of the water. This was facilitated by the selectivity of the FMOC labeling. Furthermore, SM-EKC utilizing DOSS/ACN electrolyte systems proved once more to be very useful in the separation of

78

hydrophobic compounds such as the FMOC-anilines. Hydrophobic compounds are very difficult to separate in plain aqueous MECC due to their strong association with the micelles.

References

1. Waterval, J.C.P.; Lingeman, H.; Bult, A. Underberg, W.J.M., *Electrophoresis* **2000**, *21*, 4029-4045.

2. Bardelmeijer, H.A.; Waterval, J.C.M.; Lingeman, H.; van't Hof, R.; Bult, A. Underberg, W.J.M., *Electrophoresis* **1997**, *18*, 2214-2227.

3. Wall, W; El Rassi, Z., *Electrophoresis* **2001**, *22*, 2318-2325

4. Lau, S.K.; Zaccardo, F.; Little, M.; Banks, P., *J. Chromatogr. A* **1998**, *809*, 203-210.

5. Chan, K.C.; Janini, G.M.; Muschik, G.M.; Issaq, H.J., *J. Chromatogr.* **1993**, *653*, 93-97.

6. Chan, K.C.; Janini, G.M.; Muschik, G.M.; Issaq, H.J., *J. Chromatogr.* **1993**, *622*, 269-273.

7. Shi, Y.; Fritz, J.S., *Anal. Chem.* **1995**, *67*, 3023-3027.

8. Rosen, M., *Surfactants and Interfacial Phenomena*, Wiley, New York, **1989**.

9. Williams, E.F.; Woodberry, N.T.; Dixon, J.K., *J. Colloid Sci.* **1957**, *12*, 452-459.

10. Cai, J.; El Rassi, Z., *J. Chromatogr.* **1992**, *608*, 31-45.

11. Einarsson, S.; Josefsson, B.; Lagerkvist, S., *J. Chromatogr.* **1983**, *282*, 609-618.

CHAPTER IV

CAPILLARY ELECTROPHORESIS OF DERIVATIZED AND UNDERIVATIZED

PHENOL PESTICIDIC METABOLITES. PRECONCENTRATION AND LASER-

INDUCED FLUORESCENCE DETECTION OF DILUTE SAMPLES

Introduction

This chapter is concerned with the CE separation of some substituted phenols, and more specifically the phenol pesticidic metabolites shown in Table 1, which lists typical parent pesticides for the phenols under investigation. The analysis of substituted phenols is of importance to environmental regulatory agencies as these materials pose significant human and environmental hazards. Some of these phenols, e.g., phenol (ph), 2-chlorophenol (2-Clph), 2,4-dichlorophenol (2,4-DiClph), 2,4,5-trichlorophenol (2,4,5-TriClph) and pentachlorophenol (PentaClph), are on the United States Environmental Protection Agency (USEPA) list of priority pollutants[1] because they are highly toxic even at low concentrations.

Gas chromatography (GC)[2-4] and to a larger extent high performance liquid chromatography (HPLC)[4-7] have found wide use in the analyses of phenols in water. Usually, the analysis of phenols by GC is complicated by the polarity of some of these solutes and their low vapor pressure, thus necessitating sample derivatization to enhance

TABLE 1.

STRUCTURES, ABBREVIATIONS, pKa VALUES AND PARENT
HERBICIDES OF THE PHENOLS
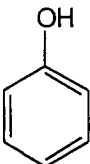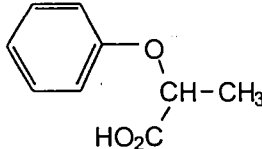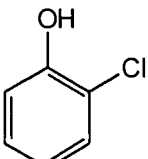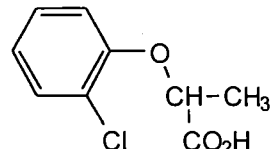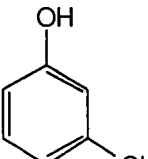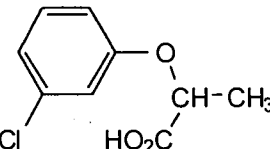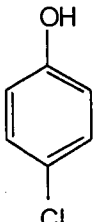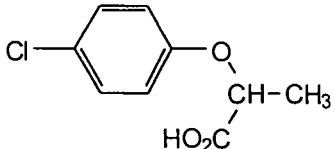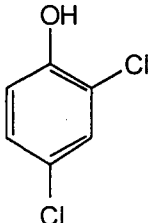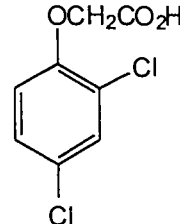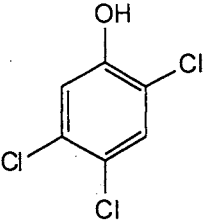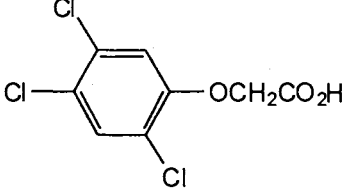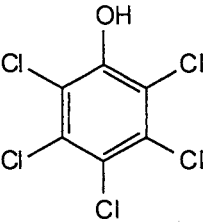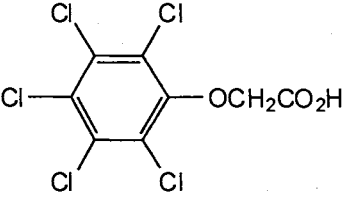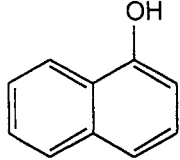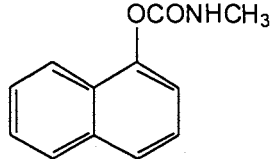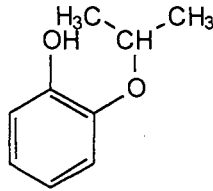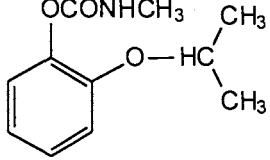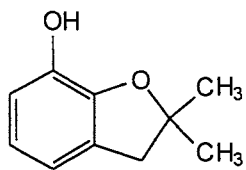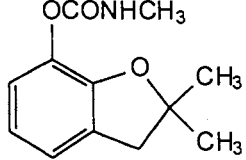
Structure	Name	Abbreviation	pKa	Parent Herbicides
	Phenol	ph	9.99	 2-Phenoxypropionic acid
	2-chlorophenol	2-Clph	8.55	 2-(2-chlorophenoxy)propionic acid
	3-chlorophenol	3-Clph	9.10	 2-(3-chlorophenoxy)propionic acid
	4-chlorophenol	4-Clph	9.43	 2-(4-chlorophenoxy)propionic acid
	2,4-dichlrophenol	2,4-DiClph	7.85	 (2,4-dichlorophenoxy)acetic acid (2,4-D

TABLE 1 CONTINUED

Structure	Name	Abbreviation	pKa	Parent Herbicides
	2,4,5-trichlorophenol	2,4,5-TriClph	7.37	(2,4,5-trichlorophenoxy)acetic acid (2,4,5-T)
	Pentachlorophenol	PentaClph	4.50	(Pentachlorophenoxy)acetic acid
	1-Napthol	Nap	9.30	Carbaryl
	2-Isopropoxyphenol	2-Isopropoxyph	**	Baygon
	2,2-dimethyl-2,3-dihydrobenzo[b]furan-7-ol	Dihydro	**	Bendiocarb

pK$_a$ are from Refs [1, 36]

**No pK$_a$ values were found in the literature for these two phenols. However, it is safe to state that they are relatively much weaker acids than the other listed phenols because they migrated first in CZE

83

volatility and detectability. This is usually a time consuming process requiring extensive sample preparation and manipulation with possible sample loss. HPLC methods are usually based on reversed-phase chromatography with either isocratic or gradient elution. Although HPLC has been shown to provide relatively low limit of detection in the range 1 to 20 ng injected onto the column with post-column derivatization,[5] the inherent limited resolving power of HPLC imposes extensive optimization which often involves complex procedures or numerous experiments, especially gradient elution.

More recently, capillary electrophoresis (CE) has been applied for the analysis of phenols of environmental interest.[1, 8-16] The recent interest in CE is not surprising since CE offers high resolving power and unique selectivity, which make CE a good alternative tool for phenols that are not directly amenable to GC or are not separated by HPLC. However, most of the CE studies involving phenols have either used standard phenols as model solutes to evaluate fundamental retention and migration issues as well as system evaluation in micellar electrokinetic capillary chromatography (MECC).[1, 8, 12-14, 17] and in capillary zone electrophoresis (CZE).[18] The main reason for which most studies demonstrated standard phenol separations and not real samples is the limited sensitivity of UV detectors (> mg/L, i.e., ~ 10^{-4} to 10^{-5} M). To use CE for the analysis of phenols in real waters in which pollutants exist at μg/L levels (i.e., 10^{-8} to 10^{-9} M levels), improved detection systems and sample enrichment methods should be implemented. Thus far, only a few attempts have addressed the detection of phenol pesticidic metabolites in real water at low levels.[9, 11, 15, 19] In these investigations, the reported limits of detection (LOD) were 2.2 x 10^{-7} to 2.8 x 10^{-8} M by UV absorbance detection at 214 nm in CZE using an off-line solid phase extraction step,[9] 10^{-6} to 10^{-7} M range in CZE using indirect laser-induced fluorescence detection (LIF) in the presence of 1 mM fluorescein as the fluorescing background electrolyte, and about 10^{-6} M for p-chlorophenol using an on-column amperometric detection after CZE separation.[15] While amperometric detection

provides one to two orders of magnitude decrease in LOD as compared to that in UV, electrochemical (EC) detection is rather tedious requiring sophisticated instrumental set-ups which involve electrical decoupling of the CE and the EC electrode and physical alignment of the EC electrode with the capillary inlet to ensure optimum and reproducible measurements.[20] Also, indirect LIF detection, which ensures 1 to 2 orders of magnitude lower LOD than UV absorbance detection, has some drawbacks such as (i) predominance of interferences (i.e., absence of specificity) due to the fact that the detection results from the fluorescing property of the background electrolyte and not the optical property of the analyte and (ii) compromising between optimum peak resolution and satisfactory detection sensitivity.[21] Although off-line preconcentration such as solid-phase extraction prior to CE separation usually enrich samples by at least a 1000 fold thus allowing the detection of dilute samples,[22] on-line preconcentration is usually preferred because the later does not lead to sample loss.

The originality of the present chapter resides in three aspects: (i) implementation of field-amplified sample stacking (FASS) for on-column pre-concentration of dilute phenol samples to allow trace analysis of underivatized phenols in the UV, (ii) introduction of a pre-column derivatization with a fluorescent tag to facilitate the detection of phenols by LIF after CEC separation and (iii) the evaluation of surfactant mediated electrokinetic capillary chromatography (SM-EKC).

Materials and Methods

Reagents and Materials

The aromatic phenols (for structures see Table 1), 4-chlorophenol (4-Clph, 99+% purity), 3-chlorophenol (3-Clph, 98% purity), 2-chlorophenol (2-Clph, 99+% purity), 2,4-dichlorophenol (2,4-DiClph, 99% purity), 2,4,5-trichlorophenol (2,4,5-TriClph, >98%

purity), 2-isopropoxyphenol (2-Ispropoxyph, 97% purity), pentachlorophenol (PentaClph, 98% purity) and 2,2-dimethyl-2,3-dihydrobenzo[b]furan-7-ol (Dihydro, 99% purity) were purchased from Aldrich (Milwaukee, WI, U.S.A.). Phenol (ph, >95% purity) was obtained from J.T. Baker (Phillipsburg, NJ, U.S.A.) and 1-Napthol (Nap, >95% purity) was purchased from Eastman (Rochester, NY, U.S.A.) HPLC grade acetonitrile (ACN) was obtained from Fisher (Fairlawn, NJ, U.S.A.). The derivatizing agent carbazole-9-N-acetic acid (CRA) was prepared in our laboratory[23] according to the previous procedures (Fig.1a).[24] 4-Dimethylaminopyridine (DMAP) and 1-ethyl-3-(3-dimethylaminopropyl) carbodiimide (EDAC) were purchased from Sigma (St. Louis, MO) Sodium hydroxide, potassium hydroxide, and sodium borate were purchased from EM Science (Cherry Hill, NJ, U.S.A.). The surfactant DOSS was also purchased from Aldrich. Structure of the surfactant, DOSS, is shown in Fig. 1, Chapter 3.
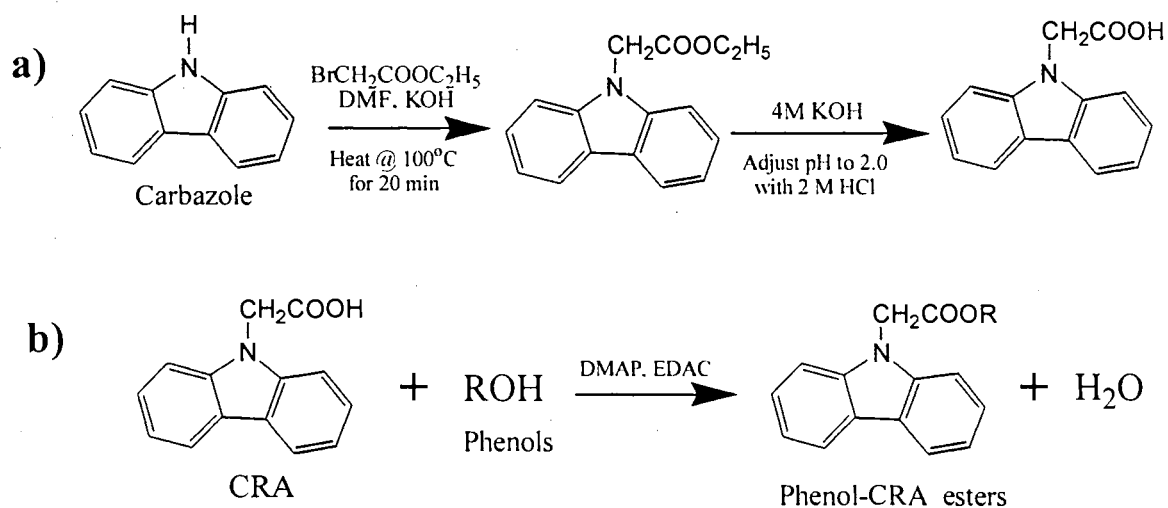
Figure 1. Reaction scheme for the synthesis of (a) CRA and the derivatization scheme for the synthesis of the (b) CRA-phenol derivatives.

CE Instruments

A Beckman P/ACE system 5510 (Fullerton, CA, U.S.A.) was used for all experiments. It was equipped with an Omnichrome (Chino, CA, U.S.A.) Model 3056-8M He-Cd laser multimode, 8 mW at 325 nm and a data handling system comprised of an IBM personal computer and P/ACE station software. A Beckman diode array detector was used for all UV detection. P/ACE station software was used for data acquisition. An emission band-pass filter of 380 nm $\pm$ 2 nm, purchased from Corion (Holliston, MA, U.S.A.) was used for the LIF detection of the CRA derivatives. The experiments were carried out using fused-silica capillaries obtained from Polymicro Technologies (Phoenix, AZ, U.S.A.). The dimensions of the capillaries were 50 cm to the detection window and 57 cm total length, with 50 μm internal diameter and 365 μm outer diameter. In all experiments, the temperature was held constant at 25 °C by the instrument's thermostating system. Samples were pressure-injected at 0.034 bar (*i.e.*, 3.5 kPa) for various lengths of time. When using a surfactant containing running buffer, the capillary was rinsed between runs with buffer without surfactant, distilled water, 1.0 M KOH, distilled water, buffer without surfactant and running buffer for 1, 1, 3, 1, and 3 min, respectively. When using borate-running buffer, the capillary was rinsed between runs with 1.0 M KOH for 5 minutes at the beginning of the day and was simply rinsed with running buffer between runs.

Procedures

Precolumn Derivatization

Enough of the aromatic phenol pesticidic metabolites were weighed out into a 2 dram amber vial to make a final concentration of 1.00×10^{-2} M in 1.00 mL of "solvent". 500 µL of ACN was pipeted along with 200 mL of 0.5 M DMAP, 100 µL of 0.65 M EDAC and 200 µL of 0.25 M CRA. A small amount of heat was necessary to help dissolve the CRA and EDAC stock solutions. This brought the final concentration of analyte to 10 mM and the derivatizing agent to 50 mM. As described in the literature, the DMAP was used as a base catalyst and the EDAC was used to promote coupling.[25] The reaction was left stirring overnight at 60 °C in a dri-bath while stirring. These samples were subsequently diluted and used further for sample injections for the electropherograms generated under the various operating conditions. This derivatization was also used for determining the LOD by successive dilution. Fresh derivatives were prepared bi-weekly to prevent degradation of the derivatives.

Results and Discussion

CE of Underivatized Phenols

CZE

As native species (i.e., underivatized phenols), the phenols are weak acids (see Table 1 for pK_a), which eventually electrophorese and separate at moderately high pH as
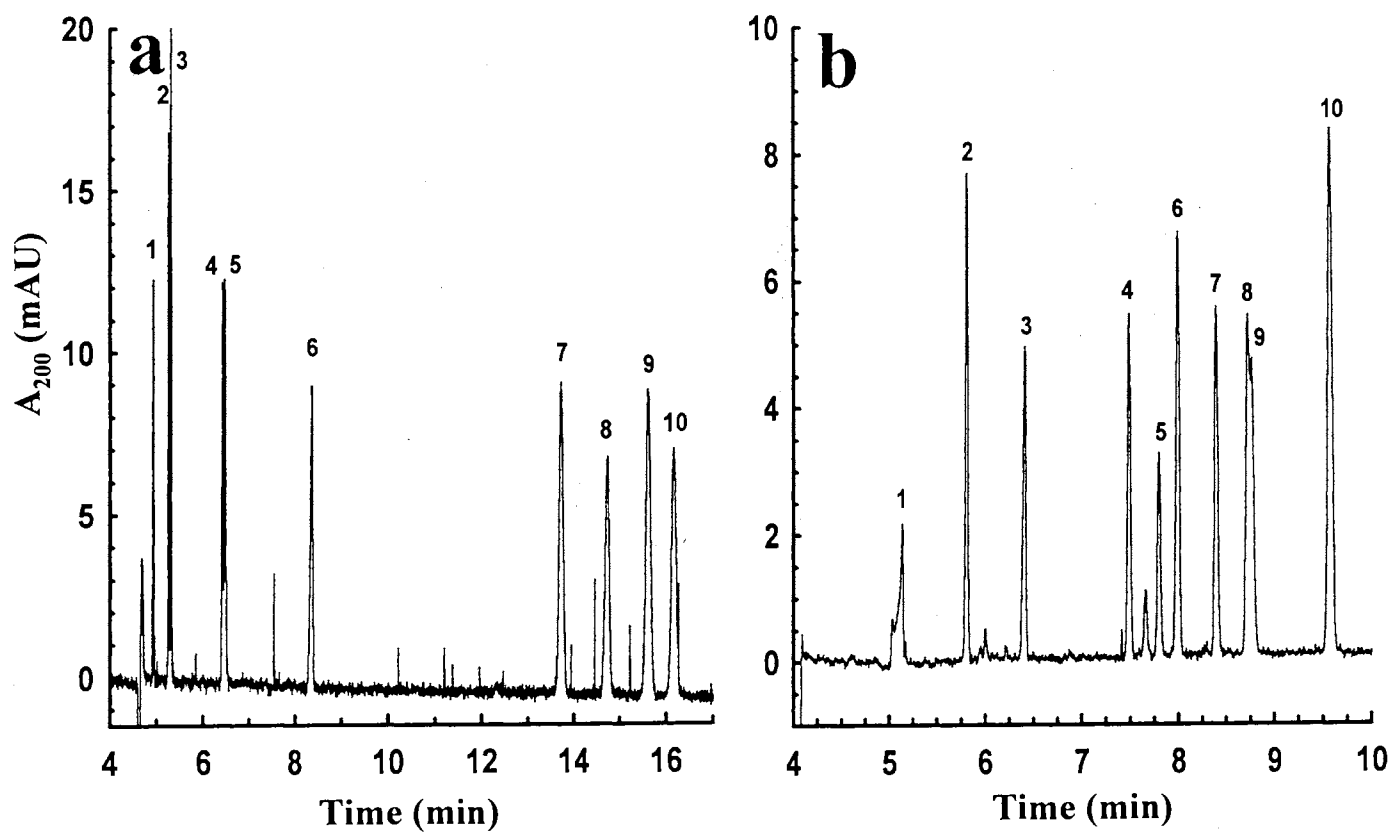
Figure 2. Electropherograms of the underivatized analytes using CZE. Conditions: capillary column, 50 cm / 57 cm x 50 μm; voltage, 25 kV; column temperature, 25 °C. Running electrolyte consists of (a) 85 mM sodium borate, pH 9.5, and (b) 20 mM sodium borate, pH 10.5. Underivatized analytes: 1, 2-Isopropoxyph; 2, Dihydro; 3, Phenol; 4, Naphthol; 5, 4-Clph; 6, 3-Clph; 7, 2-Clph; 8, 2,4-DiClph; 9, 2,4,5-TriClph; 10, PentaClph.

deprotonated species by CZE.[16, 19, 26] In fact, Fig. 2 shows typical electropherograms of underivatized phenols obtained using two simple borate buffer systems at alkaline pH. The separation is based on the differences in charge-to-mass ratio and is easily explained with the most acidic and lower molecular mass phenols being migrated the slowest. The observed migration of phenol ahead of naphthol is also consistent considering the fact the pK_a of phenol is 9.99 as compared to naphthol whose pK_a is 9.30, thus giving naphthol a higher charge-to-mass ratio. This is because the electroosmotic flow (EOF) is counter-directional to the electrophoretic mobility of the solutes. The 85 mM sodium borate (pH 9.5) yielded better separation than the 20 mM sodium borate (pH 10.5) for the phenol compounds with the more chlorinated (more acidic) phenols, which migrated the slowest (Figure 2a). The less acidic phenols (i.e., early migrating solutes) can be separated more easily with an increase in pH, which in turn increases the ionization of the given phenols as shown in Figure 2b.

SM-EKC

Since they are relatively hydrophobic compounds, the native phenols can also be separated using SM-EKC, which uses differences in hydrophobicity as the driving force for selectivity. Figure 3 shows electropherograms of the underivatized phenols incorporating a surfactant electrolyte system consisting of DOSS and ACN buffered with sodium borate. As expected the more hydrophobic phenols are more retained by the DOSS. Although differences in hydrophobicity drive the separation, the charge-to-mass ratio also plays a role in the amount of retention. Figure 3a shows an electropherogram of the 10 compounds using 30 mM DOSS with 8 mM sodium borate, pH 8.5, containing
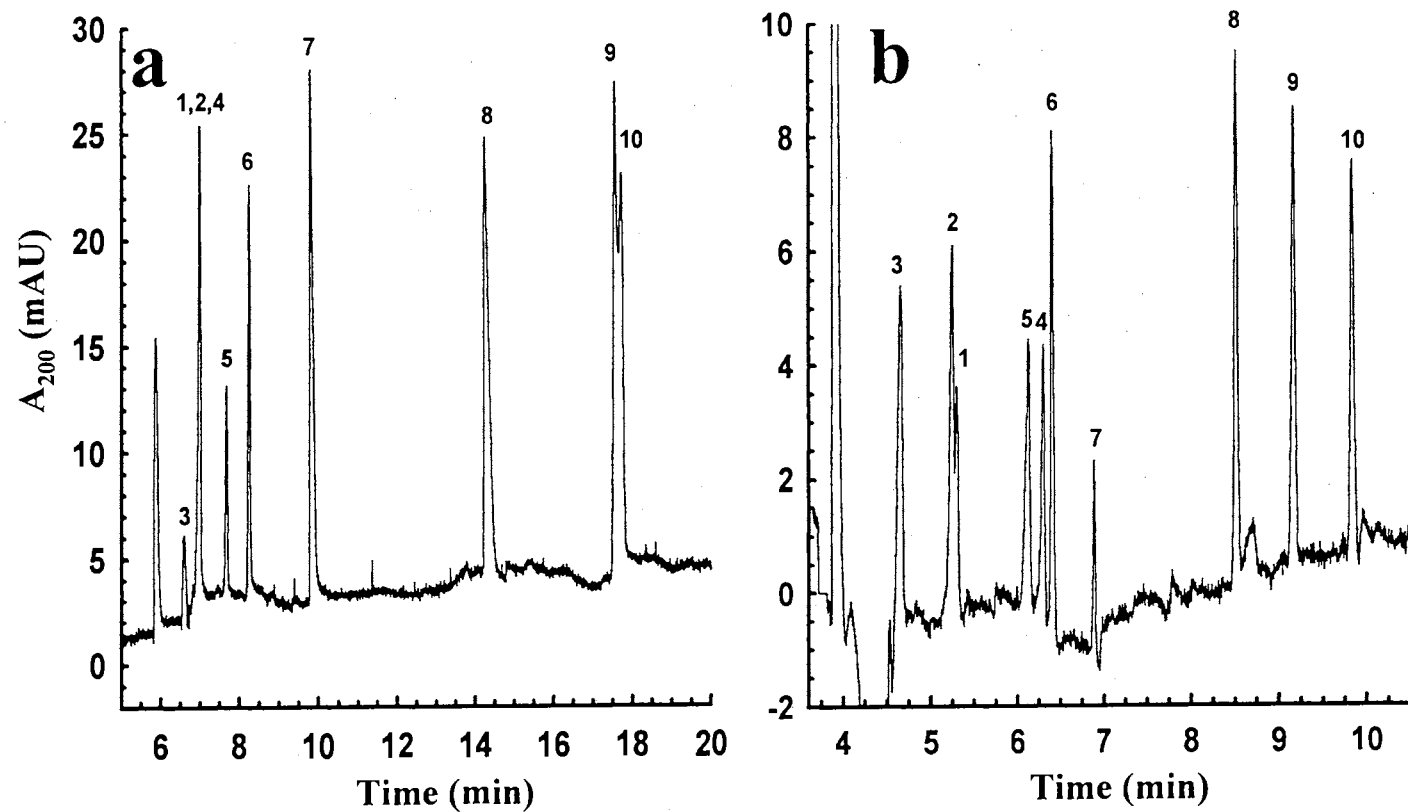
Figure 3. Separation of underivatized analytes using SM-EKC. Running electrolyte consists of (a) 30mM DOSS with 8 mM sodium borate, pH 8.5, in 30 % ACN v/v and (b) 30mM DOSS with 8 mM sodium borate (pH=8.5) in 20 % ACN v/v. Same conditions as in Fig. 2.

30% ACN (v/v). The less acidic phenols, e.g., 2-Isopropoxyph, Dihydro, and Nap, were not resolved under these conditions however the selectivity was easily adjusted by decreasing the organic content by 10% (v/v) as shown in figure 3b. Decreasing the organic content allowed for an increased interaction of the more hydrophobic phenols with the DOSS surfactant, which resolved the three previously co-eluting analytes. PentaClph, which was shouldering TriClph, was also more retained and was totally resolved under these conditions.

Limits of Detection of Underivatized Phenols

The LOD's for the native phenols were determined at 200 and 254 nm using a run buffer of 85 mM borate, pH 9.5, and the results are summarized in Table 2. As can be seen in Table 2, for a few compounds, e.g., 2,4-DiClph, 2,4,5-TriClph, PentaClph and Nap, the LOD is lower at 200 nm than at 254 nm by a factor of 4 to 8, while for the rest of the phenols (except for 4-Clph) the LOD is about the same at both wavelengths. In most cases, it may be more convenient to use 254 nm to avoid baseline noise due to absorbance of running electrolyte components such as organic solvents and surfactants. Although they are well separated, the limit of detection is quite high ($\sim 10^{-5}$ M) using UV absorbance detection at either wavelength. Thus, the initial need for a quick and efficient pre-column derivatization to allow their detection at low levels.

TABLE 2.

LIMITS OF DETECTION OF UNDERIVATIZED PHENOLS IN THE UV

Phenols	LOD (M) of Underivatized Phenols		
	UV at 200 nm	UV at 254 nm	UV "Stacking" 214 nm
ph	4.8×10^{-5}	3.6×10^{-4}	2.3×10^{-8}
2-Clph	1.2×10^{-5}	1.1×10^{-5}	2.8×10^{-8}
3-Clph	1.9×10^{-5}	1.9×10^{-5}	5.4×10^{-8}
4-Clph	6.0×10^{-5}	3.8×10^{-5}	4.1×10^{-8}
2,4-DiClph	1.2×10^{-5}	4.7×10^{-5}	3.3×10^{-9}
2,4,5-TriClph	2.1×10^{-5}	3.5×10^{-5}	7.7×10^{-9}
PentaClph	1.3×10^{-5}	4.7×10^{-5}	2.2×10^{-8}
Nap	1.0×10^{-5}	8.1×10^{-5}	5.0×10^{-8}
2-Isopropoxyph	2.0×10^{-5}	2.1×10^{-5}	1.4×10^{-7}
Dihydro	1.3×10^{-5}	1.2×10^{-5}	6.5×10^{-8}

CE of Derivatized Phenols

CRA Derivatization - Percent Conversion and Limits of Detection

Figure 1b illustrates the reaction scheme for the CRA derivatization of phenols, which involves the formation of an ester bond between the carboxyl group of the CRA and the hydroxyl group of the phenol analyte. The CRA derivatization was performed at a 5:1 mole ratio of tag to analyte, see experimental section. The percent conversion was found to be anywhere from 27.3 % for the more chlorinated phenols (e.g., 2,4,5-TriClph) up to 95.1% for the nonchlorinated phenols such as Dihydro. Higher mole ratios of CRA

to analyte (e.g., 50:1) were tried to help increase the percent conversion of the derivatization, however, this only seemed to produce more interfering side products with no significant increase in the amount of derivatized phenols. The percent conversion of a given phenol solute to its CRA derivative was determined by CZE analysis according to our previous procedure with other precolumn derivatizations,[27, 28] see Chapters 2 and 3. Briefly, it involves the CZE analysis of two aliquots of the given phenol at the same solute concentration where one aliquot consisted of the underivatized solute while the other aliquot was derivatized with CRA. The comparison of the peak area of the analyte obtained on the electropherogram of the derivatized aliquot permitted the determination of the percent of remaining underivatized analyte and in turn the percent conversion.

The measurement of percent conversion was necessary for the determination of the exact LOD of the CRA-phenol derivatives. The LOD values were measured from successive dilution of a derivatization reaction involving the 5:1 mole ratio of tag to analyte with an overnight reaction time. The LOD was approximated when a signal-to-noise ratio of 3 to 1 was achieved. As can be seen in Table 3, the CRA derivatization allowed a slightly more sensitive UV absorbance detection of phenols and yielded LOD's in the low 10^{-6} M to mid 10^{-5} M level. For the majority of CRA-phenols, this was approximately 1 order of magnitude increase in sensitivity. However, 2,4-DiClph showed no improvement in sensitivity and the LOD for CRA derivatives of the more chlorinated phenols could not be determined due to the large amount of interfering side product peaks, and the relatively low percent conversion.

The LOD achieved by LIF varied from 1.9×10^{-5} M for CRA-2,4-DiClph to as low as 7.7×10^{-9} M for CRA-Dihydro. The LIF improved the sensitivity about 100 fold

for most of the CRA phenols, but the polychlorinated CRA derivatives such as 2,4-DiClph gained very minute improvement. Again, the CRA-2,4,5-TriClph and CRA-PentaClph could not be determined due to their relatively low percent conversion to CRA derivatives and to the large amount of CRA side products which were also fluorescent and caused much interference at higher concentrations of analyte. In addition, the apparent reason for the higher or unattainable LOD's of these polychlorinated phenol derivatives is the fact that halogen substitution on aromatic ring leads, in general, to a decrease in fluorescence intensity.[29] Halogen substitution is thought to increase the probability for intersystem crossing to the triplet state.[29]

SM-EKC of CRA derivatives

Since the CRA-phenols are neutral derivatives, it was necessary to analyze them by SM-EKC. Figure 4 is an electropherogram of 8 of the 10 CRA-phenol derivatives obtained by LIF detection with an electrolyte system composed of 35 mM DOSS, 8 mM sodium borate, pH 8.5, containing 35% ACN (v/v). In this mode of separation, i.e., SM-EKC, the neutral CRA-derivatized phenols eluted in the order of increasing hydrophobic character as opposed to the mixed order of elution (i.e., according to solute hydrophobic character and its and charge-to-mass ratio) when underivatized, compare Fig. 4 to Fig. 3. As expected, CRA-ph was the first derivative to elute since it is less hydrophobic and interacts the least with the very hydrophobic DOSS surfactant. CRA-2-Isopropoxyph, CRA-Dihydro, and CRA-2-Clph all co-eluted under a variety of surfactant concentrations and percent organic in the mobile phase while keeping the amount of electrolyte at 8 mM sodium borate and the pH at 8.5 throughout all experiments. For instance, using the most

95
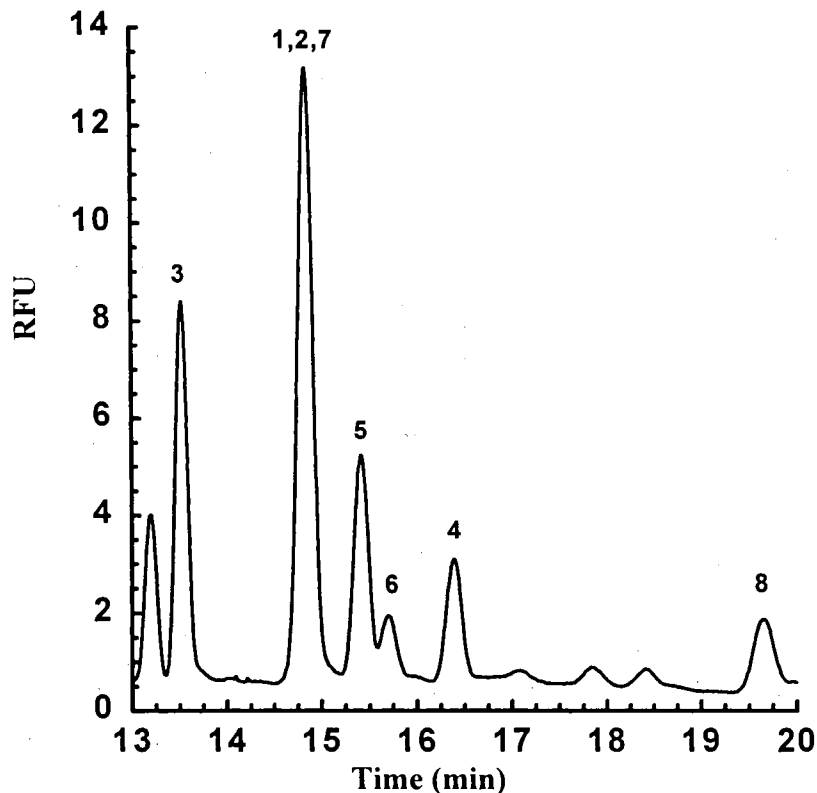
Figure 4. Separation of 6 of the CRA-phenol derivatives. Running electrolyte consists of 35 mM DOSS with 8 mM sodium borate, pH 8.5, in 35% ACN v/v. Same conditions as in Fig. 2.

hydrophobic conditions, which consisted of an electrolyte system of 40 mM DOSS with 30% ACN, resulted simply in increasing the overall retention as expected due to the increased amount of analyte-surfactant interaction without improving the resolution among the three analytes CRA-2-Isopropoxyph, CRA-Dihydro, and CRA-2-Clph. Also, using an electrolyte system of 35 mM DOSS consisting of a binary mixture of organic solvents composed of 25% (v/v) ACN and 5% (v/v) methanol in the aim of inducing more interaction without decreasing the solubility of the 35 mM DOSS yielded a slightly longer analysis time but still provided no selectivity for the three unresolved phenol derivatives. An electrolyte composition of 35 mM DOSS, 8 mM sodium borate, pH 8.5,

TABLE 3.

LIMITS OF DETECTION AND PERCENT CONVERSION OF DERIVATIZED
CRA-PHENOLS IN THE UV AND LIF

| Phenols | % Conversion | LOD (M) of Derivatized Phenols | |
		UV at 254 nm	LIF
ph	52.3	3.8×10^{-6}	1.8×10^{-8}
2-Clph	59.4	8.3×10^{-6}	3.8×10^{-8}
3-Clph	53.2	5.6×10^{-6}	6.9×10^{-8}
4-Clph	66.3	9.9×10^{-6}	6.6×10^{-8}
2,4-DiClph	44.2	4.6×10^{-5}	1.9×10^{-5}
2,4,5-TriClph	27.3	*	*
PentaClph	28.5	*	*
Nap	81.5	3.0×10^{-5}	1.1×10^{-7}
2-Isopropoxyph	88.9	4.9×10^{-6}	2.0×10^{-8}
Dihydro	95.1	2.3×10^{-6}	7.7×10^{-9}

* See discussion in text

with 35% ACN (v/v) showed the best overall separation and was used for the LOD

determinations using LIF, and the results are listed in Table 3. As expected, the order of

elution of the mono-chlorinated phenols was CRA-2-Clph, CRA-4-Clph and CRA-3-

Clph, respectively, which corroborate that obtained in RPC for positional isomers,[30] a

fact that indicates that the mechanism of retention of neutral solutes in SM-EKC is based

primarily on nonpolar interactions. CRA-Nap was the next to elute and CRA-2,4-DiClph

97

was the last detectable derivative under these conditions. CRA-TriClph and CRA-PentaClph were not able to be determined due to the large amount of interfering side products as mentioned earlier and due to the decreased LIF properties, which correlate to the chloride substituents. Thus, the need for a better method for detection of these polychlorinated compounds under UV absorbance conditions.

On-column Pre-concentration of Underivatized Phenols by FASS. Detection of Trace Amounts of Phenols in Real Waters

Field-amplified sample stacking was incorporated for its ability to pre-concentrate anionic analytes.[31-34] The analytes were hydrodynamically introduced into the column up to the detection window (50-cm) at a concentration several orders of magnitude lower than the measured analytical LOD. The analyte's solvent buffer consisted of 0.1 mM sodium borate, pH 10.5. A running electrolyte consisting of 20 mM sodium borate, pH 10.5, was then introduced at the inlet and outlet positions of the capillary. A negative polarity of 25 kV was applied and was discontinued when approximately 97% of the normal running electrolyte current was achieved. A positive polarity of 30 kV was then applied for the purpose of the separation. Figure 5 shows typical electropherograms of 6 of the FASS stacked phenols using deionized water as the sample matrix. Figure 5a incorporated a stacking solvent of deionized water with no background electrolyte (BGE) and a separation electrolyte of 20 mM sodium borate, pH 10.5. However, the peaks were slightly broader than in Fig. 5b, which used a BGE of deionized water buffered with 0.1 mM sodium borate, pH 10.5, and the same separation electrolyte as that in Fig. 5a. This is most probably accounted for by the more basic stacking electrolyte ionizing the analytes to a much larger extent, thus focusing the analytes into narrower zones. The
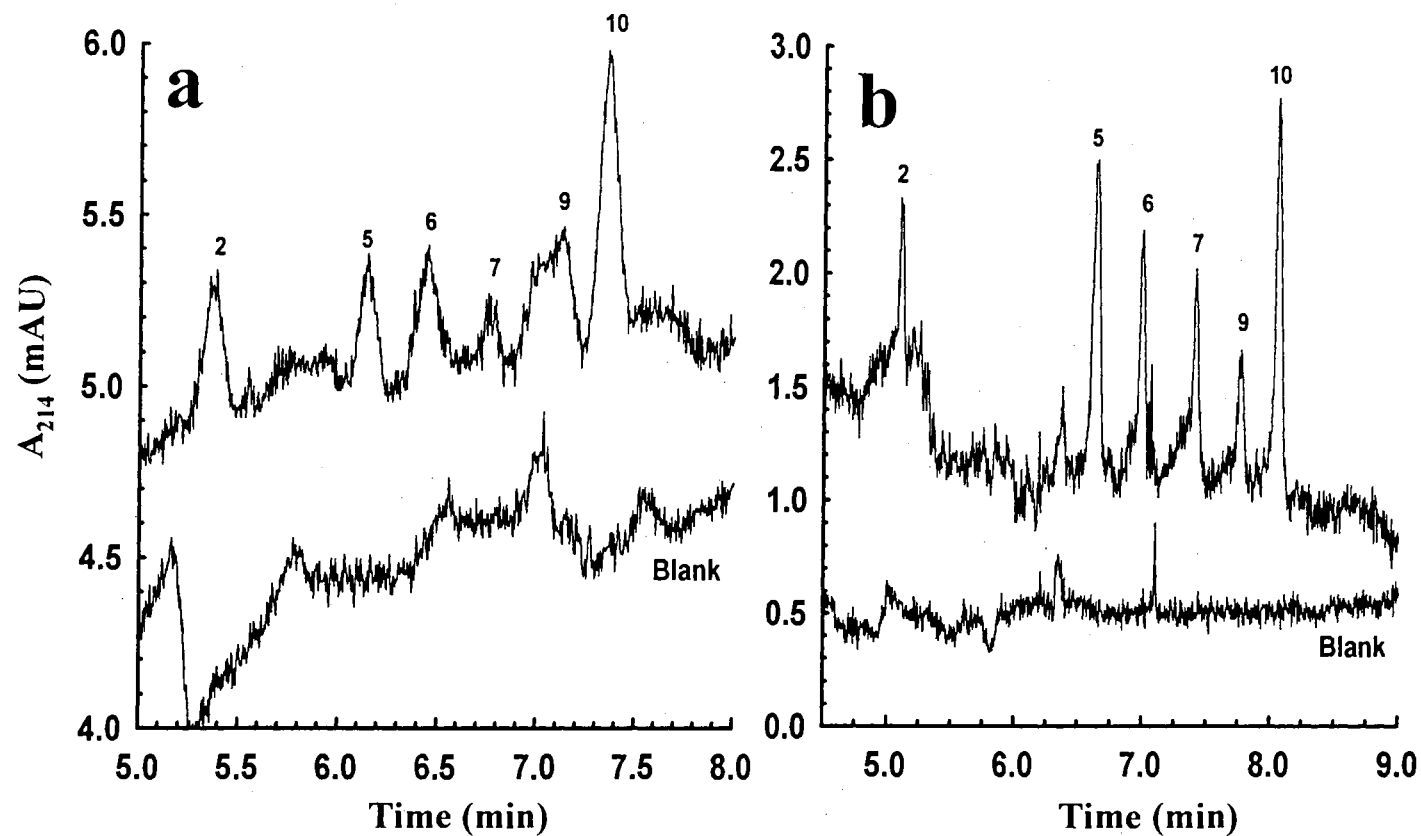
Figure 5. Electropherograms of the separation of 6 of the underivatized analytes using FASS as an on-column preconcentration method. Running electrolyte consists of (a) 20 mM sodium borate, pH=10.5, with a stacking BGE of deionized water only and (b) 20 mM sodium borate, pH=10.5, with a stacking BGE of 0.1 mM sodium borate, pH 10.5, in deionized water. A voltage of 30 kV was used for the separation. Other conditions are the same as in Fig. 2. Concentrations of loaded analytes: Dihydro, 4×10^{-8} M; 4-Clph, 7.5×10^{-8} M; 3-Clph, 7.5×10^{-8} M; 2-Clph 7.5×10^{-8} M; 2,4,5-TriClph, 7.5×10^{-8} M; PentaClph, 5×10^{-8} M.

order of elution correlated to the analytical separation run under the same conditions (see Fig. 2b). Most of the extra peaks in the sample run were accounted for after running the blank, however, there were a few peaks that were not present in the blank. According to the literature on this topic,[35] it is apparent that "ghost" peaks are common with this process along with baseline shifts usually due to slight differences in the BGE stacking electrolyte and the running electrolyte of higher ionic strength.

The hydrodynamically loaded analyte concentration varied from 4×10^{-8} M to 7.5×10^{-8} M (see Fig. 5). The overall "LOD" obtained using this preconcentration method was improved by approximately 1000 fold ($\sim 10^{-8}$ M) from the normal analytically determined LOD's. This is approximately the same magnitude as determining these compounds with LIF, however very good LOD values for the polychlorinated phenols are now able to be determined.

Figure 6 shows a typical electropherogram of the same 6 compounds using tap water buffered with 0.1 mM sodium borate, pH 10.5, as the BGE. The running electrolyte was altered to 30 mM sodium borate to incorporate a larger difference in ionic strength, and thus a larger difference in conductivity of the running electrolyte to sample BGE. The concentrations of 4-Clph, 3-Clph, and 2-Clph were lowered from 7.5×10^{-8} M to 4×10^{-8} M to see if the LOD could be achieved using a more realistic sample matrix (i.e., tap water). The peaks were broader than in the case of stacking in buffered deionized water, most likely due to more ion competition in the tap water matrix. The three peaks were approximately the LOD (3 to 1 signal-to-noise ratio) as determined using deionized water and definitely correlated to the same elution pattern. The overall

migration times were a fraction longer most probably due to a coating effect of any heavy

metal cations in the tap water on the walls of the capillary.
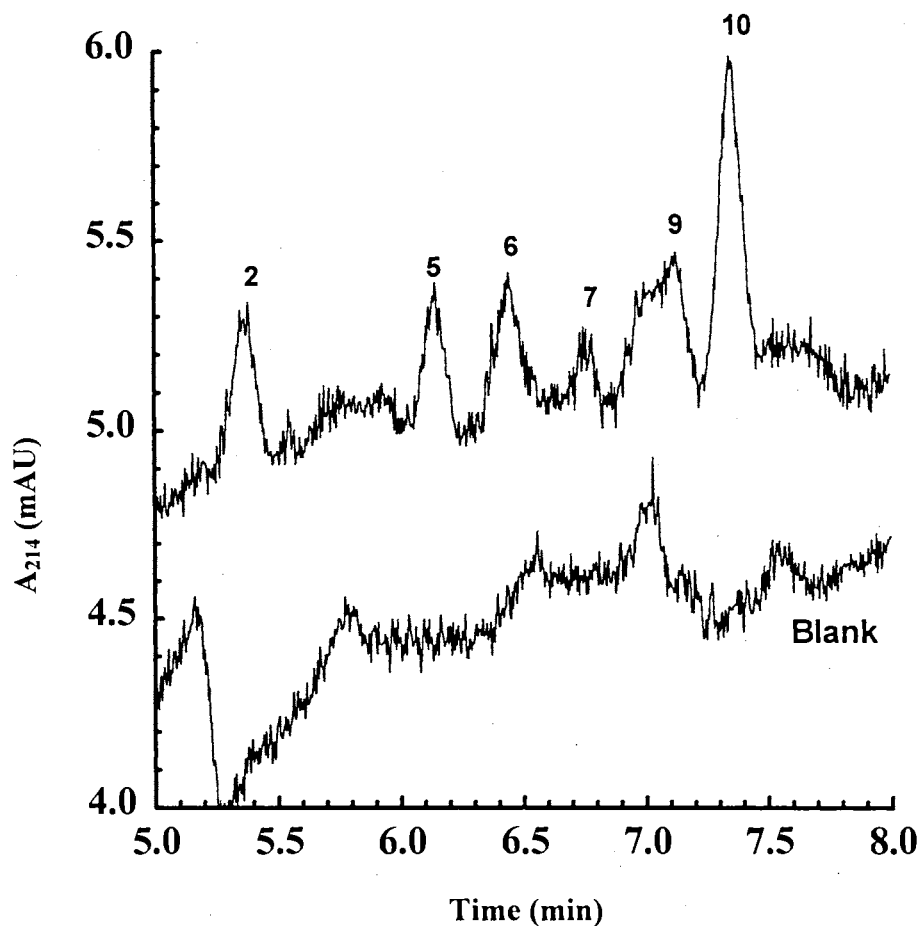
Figure 6. Electropherogram of the same 6 analytes using tap water. Running electrolyte consists of 30 mM sodium borate (pH=10.5) with a stacking BGE of 0.1 mM sodium borate, pH 10.5, in tap water. A voltage of 30 kV was used for the separation. Other conditions are the same as in Fig. 2. Molarity of loaded analytes: Dihydro, 4.0×10^{-8} M; 4-Clph, 4.0×10^{-8} M; 3-Clph, 4.0×10^{-8} M; 2-Clph 4.0×10^{-8} M; 2,4,5-TriClph, 7.5×10^{-8} M; PentaClph, 5×10^{-8} M.

Conclusions

We have shown that CE is a powerful microcolumn separation approach for the analysis of pesticidic phenol metabolites at low levels. With the exception of polychlorinated phenols derivatized with a fluorescent tag, LIF detection provides the sensitivity required for the direct analysis of dilute samples of substituted phenols. UV absorbance detection combined with FASS of dilute samples of phenols helped to overcome the shortcoming of LIF as far as the detection of polychlorinated phenols is concerned. Furthermore, both CZE at alkaline pH and SM-EKC provided the selectivity required for the separation of closely related phenols while SM-EKC proved useful for the separation of CRA derivatized phenols.

References

1. Ong, C.P.; Ng, C.L.; Chong, N.C.; Lee, H.K.; Li, S.F.Y., *J. Chromatogr.* **1990**, *516*, 263-270.

2. Renberg, L.; Lindstrom, K., *J. Chromatogr.* **1981**, *214*, 327.

3. Abrahamsson, K.; Ekdahl, A.J., *J. Chromatogr.* **1993**, *643*, 239.

4. Tesarova, E.; Pacakova, V., *Chromatographia* **1983**, *17*, 269-284.

5. Fiehn, O.; Jekel, M., *J. Chromatogr. A* **1997**, *769*, 189-200.

6. Klampfl, C.W.; Spanos, E., *J. Chromatogr. A* **1995**, *715*, 213-218

7. Thomson, C.A.; Chesney, D.J., *Anal. Chem.* **1992**, *64*, 848-853.

8. Terabe, S.; Otsuka, K.; Ichikawa, K.; Tsuchiya, A.; Ando, T., *Anal. Chem.* **1984**, *56*, 111-113.

9. Harino, H.; Tsunoi, S.; Sato, T.; Tanaka, M., *Anal. Sci.* **2000**, *16*, 1349-1351.

10. Harino, H.; Tsunoi, S.; Yoshioka, J.; Araki, T.; Masuyama, A.; Nakatsuji, Y.; Ikeda, I.; Tanaka, M., *Anal. Sci.* **1998**, *14*, 719-724.

11. Gaitonade, C.D.; Pathak, P.V., *J. Chromatogr.* **1990**, *514*, 389-393.

12. Otsuka, K.; Terabe, S.; Ando, T., *J. Chromatogr.* **1987**, *396*, 350-354.

13. Masselter, S.M.; Zemann, A.J., *Anal. Chem.* **1995**, *67*, 1047-1053.

14. Khaledi, M.G.; Smith, S.C.; Strasters, J.K., *Anal. Chem.* **1991**, *63*, 1820-1830.

15. Zhang, S.S.; Yuan, Z.B.; Liu, H.X.; Zou, H.; Wu, Y.J., *J. Chromatogr. A* **2000**, *872*, 259-268.

16. Crego, A.L. Marina, M.L., *J. Liq. Chrom. & Rel. Technol.* **1997**, *20*, 1-20.

17. Otsuka, K.; Terabe, S.; Ando, T., *J. Chromatogr.* **1985**, *348*, 39-47.

18. Smith, S.C.; Khaledi, M.G., *Anal. Chem.* **1993**, *65*, 193-198.

19. Chao, Y.-C.; Whang, C.-W., *J. Chromatogr. A* **1994**, *663*, 229-237.

20. Baldwin, R.P., *Electrophoresis* **2000**, *21*, 4017-4028.

21. Swinney, K.; Bornhop, D.J., *Electrophoresis* **2000**, *21*, 1239-1250.

22. Yang, C.; El Rassi, Z., *Electrophoresis* 1999, *20*, 2337-2342.

23. Li, J.; *Approches for the Determination of Phenolic Compounds by High Performance Liquid Chromatography and Electrochromatography.* **2001**, Oklahoma State University: Stillwater. p. 44-64.

24. Fan, X.; You, J.; Kang, J.; Ou, Q.; Zhu, Q., *Anal. Chim. Acta* **1998**, *367*, 81-91.

25. You, J.; Zhang, B.; Zhang, W.; Yang, P.; Zhang, Y., *J. Chromatogr. A* **2001**, *909*, 171-182.

26. Li, G.; Locke, D.C., *J. Chromatogr. B* **1995**, *669*, 93-102.

27. Wall, W.; Chan, K.; El Rassi, Z., *Electrophoresis* **2001**, *22*, 2320-2326.

28. Wall, W.; El Rassi, Z., *Electrophoresis* **2001**, *22*, 2312-2319.

29. Skoog, D.A.; Holler, F.J.; Nieman, T.A., *Principles of Instrumental Analysis.* 5th ed. **1998**, Philadelphia: Saunders College Publishing.

30. Snyder, L.R.; Glajch, J.L.; Kirkland, J.J., *Practical HPLC Method Development.* **1988**, New York: John Wiley & Sons.

31. Burgi, D.S.; Chien, R.L., *Anal. Chem.* **1991**, *63*, 2042-2047.

32. Burgi, D.S.; *Anal. Chem.* **1993**, *65*, 3726-3729.

33. Beckers, J.L.; Bocek, P., *Electrophoresis* **2000**, *21*, 2747-2767.

34. Osbourn, D.M.; Weiss, D.J.; Lunte, C.E., *Electrophoresis* **2000**, *21*, 2768-2779.

35. Quirino, J.P.; Terabe, S., *Science* **1998**, *282*, 465-468.

36. Dean, J.A.; *Lange's Handbook of Chemistry*. 13th ed. **1985**, New York: McGraw-Hill Book Co.

VITA

William Eric Wall

Candidate for the Degree of

Doctor of Philosophy

Thesis: ELECTROKINETIC CAPILLARY CHROMATOGRAPHY: METHODS FOR SEPARATION AND DETECTION OF ANILINES AND PHENOL PESTICIDIC METABOLITES

Major Field: Chemistry

Biographical:

   Personal Data: Born in Dallas, Texas, on June 14, 1974, the son of Johnny Ray and Andrea Doris Wall.

   Education: Graduated from Wapanucka High School, Wapanucka, Oklahoma in May, 1992; received Bachelor of Science degree in Chemistry from Southeastern Oklahoma State University, Durant, Oklahoma in July, 1997. Completed the requirements for the Doctor of Philosophy Degree with a major in Chemistry at Oklahoma State University in Stillwater, Oklahoma in May, 2003

   Experience: Worked as a research assistant in the Minority High School research program from June 1992 – August 1992; employed in the Minority Biomedical Research Student program at Southeastern Oklahoma State University for Dr. Gordon Eggleton from August 1994 - August 1996; employed as a research assistant for Dr. Tim Smith from September 1996 – July 1997 at Southeastern Oklahoma State University; employed by Oklahoma State University, Department of Chemistry as a graduate student from August 1997 to present.

   Professional Memberships: Phi Lambda Upsilon Honorary Chemical Society; Blue Key National Honor Fraternity; Alpha Chi Sigma Professional Chemistry Fraternity; American Chemical Society